Sediment Fingerprinting to Identify Sources of In-Stream Sediment in an Urbanized Watershed

by

Kritika Malhotra

A thesis submitted to the Graduate Faculty of
Auburn University
in partial fulfillment of the
requirements for the Degree of
Master of Science

Auburn, Alabama
August 4, 2018

Approved by

Jasmeet Lamba, Chair, Assistant Professor of Biosystems Engineering
Puneet Srivastava, Professor of Biosystems Engineering
Stephanie Shepherd, Assistant Professor of Department of Geosciences

ABSTRACT

Excessive delivery of fine-grained sediment and sediment-bound nutrients to surface waters results in water quality impairment. Information on the relative contribution of different sources contributing sediment to river systems is a prerequisite to target management practices. Sediment fingerprinting technique can help to estimate sediment contributions from various sediment sources to fluvial sediment load. The overall goal of this study was to determine the sources of in-stream sediment (stream bed and suspended) at a subwatershed scale using sediment fingerprinting approach in an urbanized, 31 km^2 Moore's Mill Creek watershed in Southern Piedmont region in Alabama. The relative source contribution from construction sites and stream banks to in-stream sediment was quantified for two different particle size fractions, 63-212μm (fine sand) and <63μm (silt and clay). Results of this study showed that both construction sites and stream banks were important sources of stream bed sediment. The stream bed sediment in the upstream reaches originated largely from channel bank sources, and in the lower reach (watershed outlet), construction sites were the dominant sources of stream bed sediment. Also, this study showed that the construction sites were the dominant sources of suspended sediment in the watershed with contribution ranging from 0 to 100%, varying temporally. The relative source contribution from different sources is dependent on the particle size of the sediment, time and location of sampling within a watershed, riparian buffers, and areas of construction activities in proximity to the sampling sites. Also, it was observed that different source contributions could be obtained with different fingerprinting procedures as apportionments are sensitive to the statistical

procedures employed. Soil and Water Assessment Tool (SWAT) was used in parallel to assess valuable information of watershed-level hydrological processes that affect sediment erosion and transport within a watershed. SWAT identified areas that generate high surface runoff and water yield and have the potential to contribute disproportionately high amount of sediment to streams. Targeting best management practices (BMPs) in these areas can significantly reduce the sediment loadings to the streams. Overall, this study underscores the importance of considering the spatial and temporal variability of sediment sources as a function of sediment particle size for targeting BMPs. The combined use of sediment fingerprinting technique and watershed-level modeling can provide valuable information of sediment transport processes and dynamics within a watershed.

ACKNOWLEDGMENTS

I express my sincere gratitude to my Major Professor Dr. Jasmeet Lamba for providing me a wonderful opportunity to work under his able guidance. The encouragement by Dr. Lamba has been the greatest asset to my pursuit of an interesting project. I thank him for nurturing my interest, guiding me, motivating me, and showing faith in me throughout my study.

The constructive comments and critical suggestions provided by members of my advisory committee helped to improve the manuscripts. My sincere thanks are due to my committee members for their time and effort. I am grateful to people who helped me during field and lab work at various stages of my research. I am also thankful to my colleagues and friends, Palki Arora, Sandeep Patil, Hemendra Kumar, Divya Sadana, Sarthak Behera, Amrit Mundi, Gurpreet Singh, Laljeet Sangha, Sanjiv K C, and Vivek Patil for their support and encouragement. I would also like to thank the staff of City of Auburn for their help in providing me the data required for analysis in my research. I am really grateful to Ms. Mary Black, Division Director at UGA-Extension, who allowed me to work towards the completion of the thesis during the course of my internship.

Most importantly, I would like to thank my parents, Mr. Janak Kumar Malhotra and Mrs. Neelam Malhotra for their unconditional love, guidance and support throughout my life, as it would not be possible without them. I would also like to thank my younger brother Rishab Malhotra for his love, and support in my life.

Thank you to all for helping make my MS journey an enjoyable one!

Table of Contents

List of Tables

List of Figures

CHAPTER 1

INTRODUCTION

1.1 BACKGROUND

Sediment is a natural component of a river and a stream, however excessive quantities of fine sediment in surface waters degrade aquatic ecosystems (Burt and Allison, 2010). Elevated concentrations of sediment in surface waters increase water turbidity, restricting light penetration to underwater plants and thereby lowering the rates of photosynthesis and dissolved oxygen concentrations. Furthermore, excessive levels of sediment in streams smothers stream beds, reduce oxygen circulation through the stream bed, and increase the concentration of sediment-bound nutrients. In order to mitigate the impacts of sediment and sediment-associated contaminants on aquatic ecosystems, reliable quantitative information on the sources of in-stream sediment is required. The information on the sources of sediment can help to target best management practices (BMPs) and control sediment mobilization and subsequent siltation of the streams.

Sediment fingerprinting and watershed-scale modeling can help to prioritize areas/sources of sediment for targeting BMPs. Sediment fingerprinting techniques can be used to determine in-stream sediment sources and therefore help quantify the temporal and spatial variability of in-stream sediment sources. These techniques typically involve combination of field data collection, laboratory analysis and statistical modeling to allocate the amount of in-stream sediment (suspended and stream bed) contributed by each source (e.g., stream banks, construction sites)

(Davis and Fox, 2009). The two primary components involved in the sediment fingerprinting approach are: (1) identification of a set of fingerprinting properties that can be used to discriminate among the sediment sources, and (2) quantification of the relative proportion of the sediment sources to in-stream sediment. The latter is accomplished by comparing the concentrations of fingerprinting properties in the source sediment and in-stream sediment. Watershed models can help to understand hydrology, sediment, and nutrient transport processes within a watershed. The conjunctive use of Soil and Water Assessment Tool (SWAT) modeling and sediment fingerprinting approach could facilitate effective targeting of BMPs. For example, the dominant sources of in-stream sediment can be identified using sediment fingerprinting technique. Then SWAT model can be used to identify subwatersheds contributing disproportionately high amounts of surface runoff per unit area to streams. The subwatersheds generating significant amount of surface runoff have potential to contribute disproportionately high amount of sediment to streams. Therefore, the dominant sources of sediment (identified using sediment fingerprinting) in subwatersheds prioritized based on the amount of surface runoff generated per unit area should be targeted for BMPs.

1.2 RESEARCH OBJECTIVES

The major goal of this study was to identify sources contributing disproportionately high amounts of in-stream sediment (stream bed and suspended). A combination of sediment fingerprinting technique and watershed-level modeling approach was used. The major objectives of this study are listed below:

1. Sediment fingerprinting to identify the sources of stream bed sediment in an urbanized watershed.
2. Apportionment of suspended sediment sources in an urbanized watershed using sediment

fingerprinting.

3. Fingerprinting the dominant sources of in-stream sediment using distances from Discriminant Function Analysis (DFA).

1.3 THESIS OUTLINE

Each objective mentioned is the focus of a separate chapter in this thesis and each chapter is written as a separate manuscript.

Chapter 2 focusses on the use of geochemical properties to identify sources of sediment deposited on the stream bed at the subwatershed scale as a function of sediment particle size. The subwatersheds based on the amount water yield per unit area were identified using SWAT model. Furthermore, a land use change scenario to evaluate the effect of increase in urbanization on the amount of subwatershed level water yield was performed.

In chapter 3, geochemical fingerprinting properties were used to identify sources of suspended sediment at a subwatershed scale as a function of sediment particle size. The subwatersheds generating disproportionately high amount of surface runoff were also prioritized for BMP implementation using SWAT model.

In chapter 4, distances from discriminant function analysis (DFA) were used to quantify sediment source contributions and the results were compared with the mixing model results.

In chapter 5, conclusions of this study and recommendations for the future work are discussed.

REFERENCES

Burt, T., & Allison, R. J. (2010). Sediment Cascades: An Integrated Approach. John Wiley & Sons.

Davis, C. M., & Fox, J. F. (2009). Sediment Fingerprinting: Review of the Method and Future Improvements for Allocating Nonpoint Source Pollution. Journal of Environmental Engineering, 135(7), 490–504.

CHAPTER 2

SEDIMENT FINGEPRINTING TO IDENTIFY SOURCES OF STREAM BED SEDIMENT IN AN URBANIZED WATERSHED

2.1 INTRODUCTION

Excessive loading of sediment to streams adversely affects the biodiversity and water quality of streams. For example, loss of sediment from uplands and stream banks to surface waters reduces light penetration in the water column, changes the stream channel morphology, leads to increase in the operational costs of water treatment plants, results in siltation of reservoirs, and delivers sediment-bound nutrients such as phosphorus (P) to surface waters (Koiter et al., 2013; Mukundan et al., 2012; Stewart et al., 2015). In the United States (U.S.), for approximately 24% of the impaired rivers and streams, sedimentation has been considered as the potential cause of impairment (USEPA, 2017). Approximately one of every six river and stream miles in U.S. has excessive stream bed sediment (USEPA, 2008). Thousands of miles of the rivers and streams in the southern Piedmont region of U.S. are impaired because of excessive sedimentation, which can be attributed to some extent to historic disturbances during the mid-20th century (McCarney-Castle et al., 2017; Mukundan et al., 2010). Furthermore, recent urbanization in the southern region of the U.S. has increased the potential for channel alterations (O'Driscoll et al., 2010). O'Driscoll et al. (2009) have documented how streams respond to urbanization induced land-cover change. For example, streams in urban watersheds have lower sinuosity, greater width, and higher channel incision ratios as compared to streams in rural watersheds Also, urban streams have disconnected

floodplains, and reduced floodplain sediment retention. Furthermore, streams in urban watersheds experience large sediment loads from construction sites because the clearing of land during the process of building results in high erosion rates particularly during storm events (Pitt et al., 2007). Because of inputs of large quantities of sediment, a stream channel undergoes a variety of physical and biological changes, such as, deposition of channel bars, shifting configuration of the channel bottom, and smothering of bottom dwelling flora and fauna (Wolman and Schick, 1967; Harbor, 1999).

Information on the sources of sediment can help target best management practices (BMPs) at areas contributing disproportionately high amounts of sediment to streams (Collins et al., 2017). Targeted implementation of BMPs would enable effective use of federal and state funds (Ferreira et al., 2017; Liu et al., 2016). However, the task of understanding the sediment transport processes at a watershed level is complicated owing to high spatial and temporal variability of sediment erosion and deposition processes within a watershed (Koiter et al., 2013). Different approaches (e.g., aerial photography, modeling, and traditional monitoring techniques based on erosion pins and erosion plots) are available to identify sources of sediment delivered to stream. However, these techniques are time consuming, labor intensive, expensive and lack accuracy (Haddadchi et al., 2013). Sediment fingerprinting techniques are commonly used to determine relative contribution from different sources to in-stream sediment (Mukundan et al., 2012; Walling, 2013; Collins et al., 2017). These techniques involve collection of soil samples from different input sources (e.g., banks, croplands) and sampling in-stream sediment (e.g., suspended sediment or fine sediment deposited on the stream bed), laboratory analysis of the collected samples for fingerprinting properties and then using statistical methods to quantify the relative contribution from different sources to in-stream sediment (Collins et al., 2010; Gellis and Noe, 2013; Huisman

et al., 2013; Koiter et al., 2013; Walling, 2005). Recently, sediment fingerprinting has turned into a key technique to determine the significance of suspended (e.g., Huisman et al., 2013; Smith & Blake, 2014) and stream bed (e.g., Collins et al., 2013; Koiter et al., 2013) sediment sources in a catchment (Pulley et al., 2017). Different types of fingerprinting properties, such as fallout radionuclides (Huisman et al., 2013; Nagle et al., 2007; Walling, 2013; Wilson et al., 2008; Pulley et al., 2015), trace elements (Devereux et al., 2010; Gholami et al., 2017), mineral magnetic properties (Hatfield and Maher, 2009; Manjoro et al., 2017; Pulley et al, 2018), and stable isotopes (Fox and Papanicolaou, 2007) have been used to identify in-stream sediment sources. Generally, multivariate approaches are used, which consist of analyzing samples for large number of fingerprinting properties and then employing statistical analysis to select optimum number of fingerprinting properties based on their ability to successfully discriminate among different sources (Collins et al., 2010; Davis and Fox, 2009; Koiter et al., 2013).

Depending on watershed characteristics (e.g., land use type, soil type, and slope), some areas (referred to as "critical source areas") in a watershed can contribute a large proportion of storm flow to streams, which can cause accelerated bank erosion. Additionally, critical source areas can contribute significant amounts of sediment and nutrients to streams from uplands. Management practices implemented in critical source areas have potential to be more effective at treating larger quantities of storm water flow (White et al., 2009). Watershed models are commonly used to identify critical source areas in a watershed. For example, the Soil and Water Assessment Tool (SWAT) model has been successfully used in various studies to simulate watershed level hydrologic processes (Niraula et al., 2011; White et al., 2009; Xu et al., 2009). Use of sediment fingerprinting techniques in conjunction with watershed models offers a great

potential to improve our knowledge on sediment transport processes within a watershed and targeting BMPs.

While previous studies have focused on identification of sediment sources in agricultural catchments (Gruszowski et al., 2003; Collins et al., 2012; Smith and Blake, 2014; Russell et al., 2001), limited work has been done to identify sources of in-stream sediment in urban watersheds using sediment fingerprinting techniques (Carter et al., 2003; Devereux et al., 2010; Franz et al., 2014; Poleto et al., 2009). Typically, sediment fingerprinting studies focus on single sediment particle size fraction (Franz et al. 2014; Nosrati et al. 2014), such as, <63 μm (Smith et al., 2011; Owens et al., 2012), <10 μm (Olley et al., 2013), however sources of in-stream sediment can change as a function of sediment particle size (Laceby et al., 2017; Collins et al., 2017). Therefore, understanding the variability in sediment sources as a function of sediment particle size fraction will improve our knowledge on sediment transport processes within a watershed. The objectives of this study were to: (a) identify sources of fine sediment deposited on the stream bed in a rapidly urbanizing watershed, (b) quantify the effect of sediment particle size (63-212 μm and <63 μm) on relative contributions from different sources to fine sediment deposited on the stream bed and (c) prioritize the areas for implementing best management practices based on the amount of water yield (total amount of water leaving the subwatershed and entering the main stream) to the stream using SWAT model. The overall goal of this study was to quantify how the relative contribution of different sources to fine sediment deposited on the stream bed varies temporally and spatially within this watershed as a function of sediment particle size.

2.2 METHODS AND MATERIALS

2.2.1 Study Site

The study was conducted in the Moore's Mill creek watershed (Fig. 2.1.a), a sub-watershed of the lower Tallapoosa River Basin. The watershed area is 31 km^2 with sandy loam and sandy clay as the dominant soil textures. The land use within the Moore's Mill creek watershed is 66% developed, 23% forest, 5% pasture, and 4% shrubland based on the Cropland Data Layer (2017) developed by USDA-NASS (https://www.nass.usda.gov/Research_and_Science/Cropland /SARS1a.php). The climate is characterized by hot summers and mild winters with average annual high and low temperatures of 23º C and 12º C, respectively (1997-2017). The watershed receives approximately 1430 mm of precipitation annually (1997-2017). The underlying geology consists of formations of Schist, Gneiss, Mylonite, Quartzite, and Sandstone with rock units belonging to geologic era of Cretaceous and Precambrian to Paleozoic. Moore's Mill Creek is listed on the Alabama Department of Environmental Management's 303(d) list of impaired water bodies because of excessive sedimentation (ADEM, 2016). Urbanization, historic channel modifications, reduction in riparian buffers, and agriculture are all major contributors to this degradation (City of Auburn, 2011).

2.2.2 Collection of Source and Stream Bed Sediment Samples

The potential sources of sediment considered in this study included: (1) construction sites (surface) and (2) stream banks (sub-surface). The source samples were collected from 30 different sites (13 construction sites and 17 eroding streambanks) within this watershed (Fig. 2.1.b; Appendix A Fig. A1 and A2). Soil samples from construction sites were collected from the top 2.5 cm of the soil, to correspond with the layer susceptible to detachment and mobilization by surface runoff. To obtain representative samples from each construction site, 10 surface soil samples per site were collected and combined for analysis. Stream bank samples were collected from 5 different locations laterally along the bank of the reach at each site. Three cores (~5 cm

deep) were collected vertically from top to bottom of the bank face at each of those 5 sampling points and were combined into one sample at each site. Presence of exposed actively eroding banks and accessibility were the governing factors in deciding the sampling locations for the stream banks within a reach following Pulley et al., 2017. Also, this sampling protocol was followed because banks erode across the entire bank height, either by bank mass failure or asynchronous lower and upper bank retreat through a combination of erosion by flow scour and sub-aerial processes (which includes wetting and drying of soil that weakens the surface of stream bank) (Smith & Blake, 2014).

To determine temporal and spatial variability of stream bed sediment sources, we collected stream bed sediment samples from December, 2016 to September, 2017 at three different reaches within this watershed (Fig. 2.1.b; Appendix A Fig. A3). The stream bed sediment sample collection dates are included in Table 2.1. With the exception of the first month of the sampling period (December, 2016), stream bed sediment samples were collected from the top 10 cm. For the first month of the sampling period, stream bed sediment samples were collected from the top 20 cm, top 15 cm, and top 10 cm at site 1, site 2, and site 3, respectively, because of variation in the amount of sediment deposited at each site. Stream bed sediment cores were collected using a 5 cm diameter acrylic tube. Cores were collected from 3-5 representative locations within each reach and composited for analysis. Sampling points for stream bed sediment samples (i.e., mid channel or near banks) were based on where the sediment deposits were located. Each core of stream bed sediment collected in the first month of our sampling period was sectioned into the following depth intervals: 0-5 cm, 5-10 cm, 10-15 cm, and 15-20 cm, then combined for analysis.

2.2.3 Laboratory Analysis

All soil samples collected (construction sites, stream banks, and stream beds) were oven dried at 60º C and manually disaggregated using a mortar and pestle, then dry-sieved through 212 µm and 63 µm sieves. The samples were divided into two particle size fractions, 63-212 µm (fine sand) and <63 µm (silt and clay). Based on the U.S. Environmental Protection Agency (USEPA) method 3052 (USEPA, 1996), samples were analyzed for 59 geochemical elements including Li, Be, B, Mg, Na, Al, P, S, K, Ca, Sc, Ti, V, Cr, Mn, Fe, Co, Ni, Cu, Zn, Ga, As, Se, Rb, Sr, Y, Zr, Nb, Rh, Pd, Ag, Mo, Cd, Sn, Sb, Cs, Ba, La, Ce, Pr, Nd, Sm, Eu, Gd, Dy, Ho, Yb, Lu, Hf, Ta, W, Ir, Pt, Hg, Tl, Pb, Bi, Th, and U at the Wisconsin State Laboratory of Hygiene, Madison, Wisconsin, USA. The particle size analysis was performed using a Malvern Mastersizer 3000 (Malvern Instruments, Worcestershire, UK) in the Geomorphology Laboratory, Auburn University, Auburn, Alabama, USA following a chemical dispersion with sodium hexametaphosphate (50 g L^{-1}) (Appendix A Fig. A5). The specific surface area (SSA) of the sediment particles was determined from the particle size analysis assuming particle sphericity (Collins et al. 2010; Lamba et al., 2015).

2.2.4 Statistical Analysis

Since sediment fingerprinting techniques require the critical sediment properties to behave conservatively during transport from source to in-stream sampling point, a range test was performed. This test determines whether the fingerprinting property concentrations in the stream bed sediment samples fall within the range of equivalent values of the fingerprinting property concentrations in the source samples (Franz et al., 2014; Gellis and Noe, 2013; Lamba et al., 2015; Smith and Blake, 2014; Wilkinson et al., 2013). All non-conservative properties, which did not satisfy this criterion were not considered for further analysis as these properties may have been subjected to transformation during erosion or transport processes.

A composite of fingerprinting properties, which provided the best discrimination between the sources was generated using a two-step statistical procedure (Yu and Rhoads, 2018; Collins et al., 1997). In step 1, a non-parametric Kruskal-Wallis H-test (α= 0.05) was used to select the fingerprinting properties which can successfully discriminate between the source categories namely, construction sites and stream banks. A non-parametric test was utilized because the fingerprinting property data sets for soils and sediment rarely satisfy normal distribution and often have unequal variances (Collins and Walling, 2002).

All the fingerprinting properties that passed the Kruskal-Wallis H-test were subjected to a stepwise discriminant function analysis (DFA) to provide maximum discrimination between the sources. This analysis is based on the stepwise selection algorithm of minimization of the Wilks' lambda (λ) to select the smallest set of fingerprinting properties for discriminating the source samples. A λ close to 0 indicates a small within group variability as compared to variability between the source groups. Statistical Analysis Software 9.2 (SAS 9.2) and R statistical software were used to conduct this analysis.

2.2.5 Apportioning Stream Bed Sediment Sources

A multivariate mixing model was used to quantify the relative source contributions from construction sites and stream banks to stream bed sediment at each site. The mixing model involves solving a set of linear equations by minimizing the objective function i.e. sum of squares of the weighted relative errors (Collins et al., 2012):

$$\sum_{j=1}^{p}\left(\frac{C_{ssj}-\sum_{i=1}^{m}C_{sj}P_i}{C_{ssj}}\right)^2 W_i$$

where p is the number of fingerprinting properties in the composite fingerprint; m is the number of source groups; C_{ssj} is the concentration of the fingerprinting property (j) in the stream bed sediment sample; Cs_j is the mean concentration of the fingerprinting property (j) in the source group; P_i is the relative contribution from source group (i); and W_i is the tracer discriminatory weighting factor. The mixing model solves the equations by comparing the concentration of each of the fingerprinting property in the stream bed sediment with the property concentration in each of the source groups.

Two linear boundary conditions must be satisfied by the multivariate mixing model to ensure that the relative source contributions from each source group to stream bed sediment must lie between 0 and 1, and the sum of the relative source contributions from all the source groups is unity:

$$\sum_{i=1}^{m} P_i = 1$$

$$0 \leq P_i \leq 1$$

The fingerprinting property discriminatory weighting factor (W_i) was used in the mixing model to ensure that the fingerprinting property with the greatest discriminatory power exerts the greatest influence on the solutions of the mixing model (Collins et al., 2010). These weightings were calculated using

$$W_i = \frac{d_1}{d_2}$$

where d_1 is the individual property discrimination percentage and d_2 is the lowest individual property discrimination percentage. No particle sizes or organic matter correction factors were used in this study (Martínez-Carreras et al., 2010; Liu et al. 2016).

2.2.6 Goodness-of-Fit and Uncertainty Analysis

The goodness-of-fit was assessed by comparing the actual fingerprinting property concentration in the stream bed sediment samples with the values predicted by the optimized

mixing model. We used the average value of RME determined at each site to assess the goodness-of-fit. The average RME values were determined by taking the mean of the RME of all the fingerprinting properties within the composite signature (Collins et al., 2010). To assess the uncertainty in the results produced by the mixing model with the use of average fingerprinting property concentration of each source category, a Monte-Carlo simulation approach was used (Gellis and Noe, 2013). This is important to check the extent to which the average of the fingerprinting property concentrations for a source group actually represent the true value of the source group. This technique removes one sample from each of the source groups and the mixing model is run without these samples. The simulation was run 1000 times and the mean relative source contributions were determined for each site (Gellis and Noe, 2013; Liu et al., 2016).

2.2.7 Mass of Stream Bed Sediment Deposited

Mass of sediment deposited per stream length was estimated to prioritize stream reaches with sedimentation issues. To estimate mass of sediment deposited within a stream reach, we measured thickness of sediment using a meter stick along three transects perpendicular to the direction of flow (Lamba et al., 2015). The three transects were considered within the reach length of 60 feet for all sites. The average thickness of sediment deposited was calculated along each transect and then was averaged for the three transects considered. The average thickness of sediment deposited was multiplied with the average width of the reach and the reach length to quantify the volume of sediment deposited. Consequently, the volume of sediment deposited was multiplied with bulk density of the sediment to estimate the mass of sediment deposited within a reach (Lamba et al., 2015).

2.2.8 SWAT Modeling

SWAT model was used in this study to prioritize subwatersheds with high amount of water yields. Subwatersheds with high water yield values have potential to cause accelerated stream bank erosion (due to high stream flows) and contribute significant amount of surface runoff to streams, and therefore deliver excessive amount of sediment to streams. SWAT is a process based, daily time-step and long-term simulation model developed by the U.S. Department of Agriculture (USDA) (Douglas-Mankin et al., 2010; Neitsch et al., 2005).Major components of SWAT model include hydrology, weather, crop growth, nutrients, pesticides, sedimentation, and land management. A 10-m resolution digital elevation model (DEM) was used to delineate the watershed and sub-watershed boundaries in Arcmap, obtained from available from the Geospatial Data Gate- way (http://datagateway.nrcs.usda.gov/).

Land use/cover data was obtained from Cropland Data Layer (CDL) for the year 2011 (https://www.nass.usda.gov/Research_and_Science/Cropland/SARS1a.php) and Soil Survey Geographic database (SSURGO) was used to derive soil parameters (USDA-NRCS). Weather data (daily precipitation and temperature (maximum and minimum)) was obtained from the National Oceanic and Atmospheric Administration (NOAA) weather station located near the watershed and from the Parameter-elevation Relationships on Independent Slopes Model (PRISM) climate dataset (http: //www.prism.oregonstate.edu/). Surface Runoff was calculated using modified Soil Conservation Service Curve Number (SCS-CN) method (Mishra and Singh, 2003; Neitsch et al., 2005). For this study, the temperature-based Hargreaves method (Hargreaves and Samani, 1985) was used to estimate potential evapotranspiration (PET).

The Moore's Mill Creek watershed is a part of the larger Chewacla Creek watershed (119 km^2). The SWAT model was setup, calibrated and validated for the Chewacla Creek watershed because observed streamflow data (USGS gage # 02418760) is available at the outlet of the

Chewacla Creek watershed. Whereas, Moore's Mill Creek watershed does not have observed streamflow data available required for model calibration and validation. A manual calibration approach was adopted to calibrate the SWAT model. For calibration, the streamflow was separated into baseflow and surface runoff components using the web-based hydrograph separation program (WHAT) (Lim et al., 2005). The model was calibrated (January 2011 to December 2014) and validated (January 2015 to December 2017) for surface runoff and baseflow at a monthly time scale by changing one parameter at a time and comparing the simulated surface runoff and baseflow against the observed surface runoff and baseflow data. The model was not calibrated and validated for sediment, because observed sediment data at the watershed outlet was not available. The first six years (January 2005 to December 2010) of the simulation were used as the warm-up period to minimize uncertainties due to initial unknown conditions, such as antecedent soil moisture conditions. The Nash-Sutcliffe model efficiency (NSE) coefficient (equation 1), the regression correlation coefficient (R^2) (equation 2), and percent bias (PBIAS) (equation 3), along with graphical evaluations, were used to assess the model accuracy (Moriasi et al., 2007) :

$$\mathrm{NSE} = 1 - \frac{\sum_{i=1}^{n}(O_i - P_i)^2}{\sum_{i=1}^{n}(O_i - O)^2} \quad (1)$$

$$\mathrm{PBIAS} = \frac{\sum_{i=1}^{n}(O_i - P_i) * 100}{\sum_{i=1}^{n} Oi} \quad (2)$$

$$R^2 = \frac{\sum_{i=1}^{n}(O_i - O)(P_i - P)}{\sqrt{\sum_{i=1}^{n}(O_i - O)^2}\sqrt{\sum_{i=1}^{n}(P_i - P)^2}} \quad (3)$$

where O_i is the i^{th} observation for the constituent being evaluated; P_i is the i^{th} simulated value for the constituent being evaluated; O is the mean of observed data for the constituent being evaluated; P is the mean of simulated data for the constituent being evaluated and n is the total number of observations.

Curve number (CN2), available soil water capacity (Soil_AWC), threshold depth of water (GWQMN), groundwater revap coefficient (GWREVAP), and potential evapotranspiration were the parameters that were adjusted during the flow calibration (Table 2.2).

2.2.9 Land Use Scenario

The Moore's Mill Creek watershed is rapidly undergoing urbanization, with increase of urbanized area from 44 % to 65 % and decrease of forested area from 41 % to 23 % from 2008 to 2017 (CDL, 2008-2017). Therefore, to quantify the change in water yield values as a result of land use change we performed a land use change scenario. In this scenario, forested area was changed to urbanized area to evaluate the effect of increase in urbanization on the water yields for the Moore's Mill Creek watershed.

2.3 RESULTS AND DISCUSSIONS

2.3.1 Optimum Fingerprinting Properties

The sediment properties that passed the range test and Kruskal Wallis H-Test (p=0.05) for 63-212 μm and <63 μm at each site are included in Tables 2.3 and 2.4, respectively. Out of 59 possible fingerprinting properties, the majority of the fingerprinting properties passed the range test, indicating that these properties possessed conservative behavior. The number of fingerprinting properties that successfully discriminated between the construction sites and stream banks for the two particle sizes after passing Kruskal Wallis-H test ranged from 5 to 24 (Tables 2.3 and 2.4).

The results of the stepwise DFA on the fingerprinting properties that passed the Kruskal-Wallis H test for 63-212 μm and <63 μm particle size fractions at each site are shown in Tables 2.5 and 2.6, respectively. The optimum set of fingerprinting properties selected by the stepwise DFA classified 100% of the sources correctly at each site, indicating that the selected fingerprinting properties provided strong discrimination between construction sites and stream banks. The number and combination of the fingerprinting properties used in the mixing model varied among different subwatersheds. Different factors, such as the number of source samples collected within each subwatershed, parent material, and anthropogenic activities (Lamba et al., 2015; Smith and Blake, 2014) can affect the type and number of fingerprinting properties that successfully discriminate between different sources. The variability in fingerprinting properties that successfully discriminate between different sources at a subwatershed level has been reported in previous studies (Collins et al., 2013; Smith and Blake, 2014).

The fingerprinting properties that were selected as a part of the composite fingerprint that have association with anthropogenic sources, were found to have greater concentrations in soils collected from construction sites compared to soils sampled from stream banks. For example, Ni, Ga, Ag, As, and V had greater concentration in samples collected from construction sites compared to stream bank samples. Bini et al., 2011 has well documented that heavy metals have less concentration in sub-soils than the surface soils. Different factors can contribute to the elevated concentration of the heavy metals in construction site samples. For example, the use of heavy metal V for making steel alloys for tools and construction purposes (Hooda, 2010) could cause higher concentration of V in the samples collected from the construction sites. Similarly, higher concentration of Ni (considered as a heavy metal of environmental concern in urban areas (Iyaka, 2011) in surface soil (construction sites) also indicated the effect of anthropogenic

activities (combustion of fuel or increased acid rain in industrialized areas) on deposition of Ni in the surface soils (Iyaka, 2011; Cempel and Nikel, 2006). In contrast, the concentrations of rare earth elements, such as Sm, Ho, and La were greater in the soils collected from the stream banks than those from construction sites. Tyler (2004) has reported that typically the concentrations of the rare earth elements is greater in sub-soils and parent material as compared to surface soils. Since stream banks are composed of less weathered sub-surface material, concentrations of rare earth elements in the samples collected from stream banks were greater than those in surface soils (Smith and Blake, 2014). It should be noted that additional factors, such as, parent material, geomorphic landform, and hydrology can also affect the concentrations of elements within different sources (Horowitz, 1991).

2.3.2 Sediment Source Ascription

The relative source contributions of stream banks and construction sites to stream bed sediment (for both particle sizes) are shown in Fig 2.2 (a-c) - 2.3 (a-c). It should be noted that core 1, 2, 3 and 4 for the month of December, 2016 represent the soil cores sectioned into 0-5, 5-10, 10-15 and 15-20 cm, respectively. With the exception of the first month of our sampling period, all stream bed cores were collected from top 10 cm.

At site 1 for particle size 63-212 μm, stream banks were the dominant source of the stream bed sediment. The relative contribution from stream banks and construction sites to stream bed sediment ranged from 88% to 100% and 0 to 12%, respectively. For <63μm particle size, the relative contribution from stream banks and construction sites to stream bed sediment ranged from 0% to 100% and 0 to 100%, respectively. Historic changes in the southern Piedmont region at watershed level (increase in impervious areas) and/or reach level (stream channel straightening, loss of riparian areas, abrupt changes in stream course) might be responsible for accelerated

stream bank erosion (Mukundan et al. 2010). For example, this subwatershed has experienced an increase in urban land cover from 63 % to 81 % and a decrease in forested land cover from 29 % to 15% from 2008 to 2017 (Cropland Data Layer, 2008 and 2017). Urbanization of a watershed results in the increase of stormwater runoff, which in turn alter the river channels. The observed channel changes include increase in channel width or depth which leads to accelerated bank failures and channel incision due to increased levels of hydraulic stress on stream banks (Booth 1990). Furthermore, the expansion of imperviousness surfaces within a watershed increases the risk of stream instability owing to increased specific stream power (Bledsoe and Watson, 2001). The temporal variability in the stream bed sediment sources during the sampling period was likely affected by the phase of construction activity from the commencement to completion of construction sites located within this watershed. A construction project begins with the site work which involves land clearing and excavation of soils and ends with grading and landscaping (Harbor, 1999). Construction practices which are identified to contribute high sediment yields include land clearance exposing the bare soil, stripping topsoil, piling the excavated soil near or on the streets, and tracking of mud in the streets by construction vehicles (Pitt et al., 2007). Furthermore, it should be noted that the 'lag time' between the erosion of sediment from construction sites and delivery of the sediment to the streams will also affect the temporal variability in stream bed sediment sources.

At site 2, stream banks were the dominant sources of the stream bed sediment for both the particle size fractions. For 63-212 μm particle size, the contribution from stream banks and construction sites ranged from 97 to 100% and 0 to 3%, respectively. Whereas, the relative source contributions from stream banks and construction sites ranged from 72 to 100% and from 0 to 28%, respectively for <63 μm particle size. The land-use under developed category in this

subwatershed increased from 42 % to 61% with the decrease of forested cover from 42 % to 24% from 2008 to 2017 based on the Cropland Data Layer 2008 and 2017. As indicated earlier, an increase in impervious surfaces leads to an increase in specific stream power and a greater risk of stream instability (Bledsoe and Watson, 2001), which likely increased relative contribution from stream banks to stream bed sediment in this subwatershed. Also, for <63μm particle size, site 2 showed the lesser contribution from construction sites to stream bed sediment as compared to site 1.

Compared to site 1 and site 2, relative source contributions from construction sites to stream bed sediment at site 3 were greater. For the 63-212 μm particle size fraction, the contributions from stream banks and construction sites ranged from 9 to 90 % and 10 to 91 %, respectively. The source contributions for the <63 μm particle size fraction, varied from 0 to 47 % and 53 % to 100 % for stream banks and construction sites, respectively. High contributions from construction sites at site 3 were likely because active construction was occurring in close proximity to the stream without enough riparian buffer (Fig. 2.4). Riparian buffers can help to reduce excessive delivery of sediment from upland areas to streams (Zhang et al., 2017). For example, Lee et al. (2000) reported that riparian buffers can help to retain up to 93% of sand and silt particles and 52 % of clay particles entering the stream depending upon the vegetation type (Lee et al., 2000). The percentage of forested land use within the riparian buffer (30 feet on each of the stream, (NCDEHNR, 1997)) of the reach at site 1 and reach at site 2 was 40% and 55%, respectively. However, the reach at site 3 had more developed areas (60%) within the vicinity of the stream, which negatively impacts sediment trapping efficiency at this site. Although a small portion (3%) of the watershed is occupied by active construction sites, but the rates of erosion from construction sites (which can approach up to 500 T ha $^{-1}$ yr^{-1}) are considerably higher than

those from areas occupied by undisturbed vegetation (<1 T ha^{-1} yr^{-1}) (Mukundan et al., 2010). The increased contribution from stream banks for the months of June and July at this site indicates greater stream bank erosion likely because of high flow rates between the sampling period (Fig. 2.5). This is because increase in stream flow rate can increase the stream bank erosion (Gellis and Noe, 2013). Stream bank sediment gets directly delivered to the stream during a storm event as compared to the sediment eroded from uplands due to its storage before reaching the channel (Gellis and Noe, 2013). Therefore, we observed a relationship between the high flows and increased contribution of stream bank sediment to the stream bed sediment. The flow rate values were obtained from the SWAT model.

Also, the stream bank stability is reduced with the increase of stream bed width and stream bank height. The process of lateral erosion leads to increase of stream bank width and the bed lowering of stream bed increases the bank height which results in stream bank instability (Osman and Thorne, 1988). The average shear stress on the banks of site 1 and site 2 watersheds was more than those on the banks of site 3 watershed (Table 2.7). Therefore, the shear stress on streambanks caused by high velocities of water at site 1 and site 2 watersheds likely increased the relative contribution from stream banks to stream bed sediment in these watersheds.

2.3.3 Effect of Particle Size on Stream Bed Sediment Sources

During stream bed sediment sampling period, contributions from constructions sites were greater for particle size <63 μm compared to 63-212 μm particle size. The SSA values of soil samples collected from construction sites and stream banks are included in table 2.8. As indicated by the SSA values, the soils samples collected from construction sites were finer (i.e., greater SSA) compared to soil samples collected from stream banks (Table 2.8). For example, for particle size <63μm, the mean SSA of soil samples collected from construction sites and stream banks

was 291.26 ± 24.5 $m^2 kg^{-1}$ and 212.7 ± 9.5 $m^2 kg^{-1}$, respectively. The construction sites had greater contribution for fine sediment (<63 μm) than for 63-212 μm particle size because soils at construction sites were finer relative to stream bank soils. Therefore, the results show that the sediment particle size affected the relative contributions from construction sites and stream banks to stream bed sediment.

2.3.4 Mass of Stream Bed Sediment Deposited

The estimated mass of sediment deposited within reaches of site 1, site 2 and site 3 is shown in Table 2.7. The results show that the mass of sediment deposited per unit length of reach was greater at the watershed outlet compared to upstream sites. Channel slope and transport capacity of the stream can affect the mass of sediment deposited within the reaches (FISRWG, 1998). The reaches in the upper part of the watershed were steep and velocity of water was greater in the upstream reaches compared to the downstream reaches (Table 2.7). Therefore, lesser velocity of water and flatter slopes in the downstream reaches compared to upstream reaches likely facilitated sediment deposition on the stream bed. There was a direct relationship between the drainage area (stream size) and the mass of sediment deposited on the stream bed per unit length of a reach. This could be because of proximity of construction sites to reach 3 without enough riparian buffer likely resulted in greater sediment loading from construction sites than the transport capacity of the stream, which resulted in greater sediment deposition at site 3. The results of source apportionment along with the mass of sediment deposited within the stream reaches can be used to prioritize subwatersheds for targeting BMPs.

2.3.5 Goodness-of-fit and Uncertainty Analysis

The RME values calculated to assess the goodness-of-fit of the mixing model indicated that mixing model provided satisfactory agreement between predicted and actual stream bed

sediment fingerprinting properties concentration. The RME values ranged from 11 to 31 %, 4 to 38%, and 17 to 33% at site 1, 2, and 3, respectively (Table 2.9). The majority of RME values were less than 25%, indicating that the mixing model satisfactorily predicted the concentration of fingerprinting property in stream bed sediment (Lamba, Karthikeyan, and Thompson 2015). The relative source contribution differences obtained from the average of Monte Carlo results and the corresponding values obtained from the mixing model using the mean source fingerprinting property concentration ranged from 0 to 2 %, 0 to 1%, and 0 to 7% at site 1, 2, and 3, respectively. The results show that the use of mean fingerprinting property concentrations of the source samples in the mixing model was not a significant source of uncertainty (Lamba et al., 2015).

2.3.6 SWAT Model Calibration and Validation

Fig. 2.6 (a–c) shows calibrated and validated monthly surface runoff, base flows, and total stream flow, respectively. The statistical values calculated for calibration and validation time periods for surface runoff, baseflow and total streamflow are presented in Table 2.10. Very good model calibration and validation results were obtained, as shown by NSE and R^2 values. As indicated by PBIAS, model performed satisfactorily for calibrated period and very good validation results were obtained (Moriasi et al., 2007). Overall, the model performance statistics showed that model was able to represent the surface runoff, baseflow and total flow successfully.

2.3.7 Prioritizing Subwatersheds for BMPs

Average annual values of water yield (mm/hac/yr) were obtained for the 2011-2017 period. The values of average annual water yield varied from 3.58 mm/hac/yr to 17511.30 mm/hac/yr. The total amount of water which leaves the subwatershed and enters the main stream will cause accelerated bank erosion. Since the stream banks were the dominant source of the

stream bed sediment in this watershed, therefore the BMPs should be targeted in the subwatersheds generating disproportionate amount of water yield.

2.3.8 Land-Use Change Scenario

The impacts of land-use change were assessed by running the calibrated models for the same time period and keeping the DEM and soil maps constant while just changing the land use. A comparison of before and after the land use scenario revealed some noteworthy changes in the watershed. The results showed that the subbasins (Fig. 2.7) which had a higher percentage of forested area (threshold of 50%) before the land use change scenario, showed an increase in the water yield which ranged from 24 % to 152 % after running the scenario (Table 2.11). Therefore, these subbasins contributing greater amount of flow to the stream will cause accelerated bank erosion. As a result, the implementation of management strategies, such as, riparian zones, vegetation strips, infiltration ponds or trenches in these areas can help in reducing the delivery of stormwater to the streams.

2.4 CONCLUSIONS

The results of this study show that the relative source contributions from construction sites and stream banks varied spatially and temporally within this watershed. Extent of an impervious area and riparian land use within a subwatershed affected the relative contributions from construction sites and stream banks to stream bed sediment at each site. The relative contributions to stream bed sediment from construction sites were greater in the subwatershed with active construction activities in proximity to the stream. The sediment particle size affected the relative contribution from construction sites and stream banks to stream bed sediment. The construction sites were the dominant sources of the stream bed sediment for particle size <63 μm, whereas for 63-212 μm, stream banks were the dominant sources of stream bed sediment. The relative

contribution from eroding stream banks to the stream bed sediment decreased with increase in the drainage area. Targeting effective and efficient conservation measures at construction sites would help to reduce excessive delivery of sediment to streams. The riparian areas should be restored and managed as they perform an important function of trapping sediment. Soil and Water Assessment Tool (SWAT) model was used in conjunction with the sediment fingerprinting approach to gain insight on hydrological and sediment transport processes within a watershed. Broadly, the study showed that with the combination of sediment fingerprinting and watershed modeling, BMPs could be targeted on the critical source areas effectively.

Table 2.1 Individual depth intervals at each site and the dates of sample collection throughout the sampling period

Sites	Depth Intervals of the soil cores for the first month of sampling period	Stream Bed Sample Collection Dates
Site 1	0-5 cm, 5-10 cm, 10-15 cm, and 15-20 cm	December 2, 2016, February 5, 2017, March 10, 2017,April 14, 2017,May 18, 2017,June 28, 2017, July 28, 2017, September 22, 2017.
Site 2	0-5 cm, 5-10 cm, 10-15 cm	_*
Site 3	0-5 cm, 5-10 cm	_*

*Sampling dates were same for all sites

Table 2.2 SWAT parameters used for calibration

SWAT Calibration Parameter	Default Value	Final Calibrated Value
Soil _AWC (mm/mm)	Varies	15 % increase
GWREVAP (dimensionless)	0.02	0.2
CN2 (dimensionless)	Varies	10 % decrease
GWQMN (mm)	1000	3907

Table 2.3 Fingerprinting properties that satisfied the range test and the Kruskal-Wallis H-test (p=0.05) criteria at each site for particle size 63-212μm

Range test

Sites	Fingerprinting Properties														
1	Li	Be	Na	P	K	Ca	V	Cr	Mn	Co	Ni	Cu	Zn	Rb	Nb
	Ag	Cd	Cs	Ba	Nd	Sm	Eu	Gd	Dy	Ho	Yb	Lu	Tl	Pb	Th
	U														
2	Be	B	Na	P	K	Ca	Mn	Co	As	Rb	Y	Zr	Rh	Ag	Sr
	Sb	Cs	Ba	Pr	Nd	Sm	Eu	Gd	Dy	Ho	Yb	Lu	Hg	Tl	Pb
3	Li	Be	Na	P	K	Ca	Sc	Ti	V	Cr	Mn	Fe	Co	Ni	Zn
	Ga	As	Rb	Y	Zr	Nb	Mo	Ag	Sr	Sb	Cs	Ba	La	Ce	Pr
	Nd	Sm	Eu	Gd	Dy	Ho	Yb	Lu	Hf	Ta	Tl	Pb	U		

Kruskal-Wallis H-test

Sites	Fingerprinting Properties														
1	Be	V	Cr	Nb	Ag	Pb	Th								
2	Be	B	Zr	Ag	Pb										
3	Li	Be	Sc	V	Cr	Fe	Ni	Ga	As	Y	Zr	Nb	Mo	Ag	Pr
	Nd	Sm	Ho	Hf	Ta	Pb	U								

Table 2.4 Fingerprinting properties that satisfied the range test and the Kruskal- Wallis H-test (p=0.05) criteria at each site for particle size <63μm

Range test

Sites	Fingerprinting Properties														
1	Li	Be	B	Na	Al	S	Ca	Sc	Cr	Mn	Co	Ni	Ga	As	Rb
	Sr	Zr	Mo	Cd	Cs	Ba	Pr	Nd	Sm	Eu	Gd	Dy	Ho	Yb	Lu
	Hf	Pt	Tl	Pb											
2	Li	Be	B	Al	P	S	Ca	Sc	V	Cr	Mn	Fe	Co	Ni	Zn
	Ga	As	Y	Zr	Mo	Pd	Cd	Sn	Sb	Cs	La	Pr	Nd	Sm	Eu
	Gd	Dy	Ho	Yb	Lu	Hf	W	Hg	Tl	Pb	U				
3	Li	Be	B	Na	Al	P	S	Ca	Sc	V	Cr	Fe	Co	Ni	Zn
	Ga	As	Rb	Sr	Y	Zr	Mo	Pd	Cd	Sb	Cs	La	Pr	Eu	Gd
	Dy	Yb	Lu	Hf	Hg	Tl	Pb	U							

Kruskal-Wallis H-test

Sites	Fingerprinting Properties														
1	Be	Sc	Mn	Co	Ga	As	Rb	Cd	Ba	Pr	Nd	Sm	Eu	Gd	Dy
	Ho	Yb	Lu	Pt	Pb										
2	Be	B	V	Cr	Fe	Ni	Ga	Zr	Cd	Hf	U				
3	Be	B	V	Cr	Fe	Co	Ni	Ga	Rb	Sr	Y	Zr	Pd	Cd	La
	Pr	Eu	Gd	Dy	Yb	Lu	Hf	Pb	U						

Table 2.5 Results of stepwise DFA at each site for particle size 63-212 μm

Site	Fingerprinting property	Wilks' lambda	Percentage source samples classified correctly	Cumulative percentage source samples classified correctly	Fingerprinting property discriminatory weighting
1	V	0.258	100	100	1.08
	Nb	0.134	92.3	100	1
2	Ag	0.078	100	100	1.25
	Be	0.057	80	100	1
3	V	0.286	96.7	96.7	1.53
	Sm	0.262	70	93.33	1.1
	Y	0.162	73.33	96.7	1.16
	Fe	0.113	86.7	96.7	1.37
	Zr	0.099	80	96.7	1.26
	Ta	0.087	76.7	96.7	1.21
	Ho	0.077	63.33	100	1

Table 2.6 Results of stepwise DFA at each site for particle size <63 μm

Site	Fingerprinting property	Wilks' lambda	Percentage source samples classified correctly	Cumulative percentage source samples classified correctly	Tracer discriminatory weighting
1	Mn	0.218	100	100	1.3
	Be	0.116	76.9	100	1
	Co	0.035	100	100	1.3
	Rb	0.023	76.9	100	1
	Ba	0.005	76.9	100	1
	As	0.002	92.3	100	1.2
	Sc	0.0006	84.6	100	1.1
	Pt	0.0002	76.9	100	1
2	Ga	0.198	100	100	1.25
	Ni	0.152	80	100	1
3	Cd	0.468	90	90	1.23
	Rb	0.313	76.7	86.7	1.04
	Ga	0.181	93.3	96.7	1.27
	Sr	0.108	73.3	100	1
	La	0.092	80	100	1.09

Table 2.7 Reach dimensions (m), velocity of water (m s^{-1}) and the mass of sediment deposited within each reach (kg m^{-1})

			Bank Height (m)				
Reach	**Width (m)**	**Slope (%)**	**Left**	**Right**	****Velocity of water (ms^{-1})**	**Mass of sediment deposited (kg m^{-1})**	**Average Shear Stress (kg m^{-2})***
1	5.55	0.87	1.37	1.43	0.96	1800	4.73
2	6.8	0.50	1.3	1.61	0.55	3800	4.97
3	10	0.4	1.7	2	0.42	5300	1.80

*τ(Shear Stress) = γRs (kg.m-2), where τ is the fluid shear stress, γ is the specific weight of water ,R is the hydraulic radius, s is the slope of the channel (Osman and Thorne 1988).

**These average daily values (from 2011-2017) of velocity of water for each reach included in table 7 were obtained from the Soil and Water Assessment Tool (SWAT) model.

Table 2.8 SSA values of soil samples collected from construction sites and stream banks

	Mean specific surface area ($m^2 kg^{-1}$)	
Particle size fractions (μm)	**Construction sites samples**	**Stream bank samples**
63-212	129.91 ± 9.6	114.35 ± 6.4
<63	291.26 ± 24.5	212.7 ± 9.5

Table 2.9 Relative mean error between actual and optimized mixing model predicted stream bed fingerprinting property concentration

Relative Mean Error (%)			Relative Mean Error (%)			Relative Mean Error (%)		
Site 1			Site 2			Site 3		
Month	63-212 μm	<63μm	Month	63-212 μm	<63μm	Month	63-212 μm	<63μm
2 Dec (core 1)	12	22	Dec (core 1)	15	16	Dec (core 1)	31	25
2 Dec (core 2)	27	19	Dec (core 2)	26	15	Dec (core 2)	32	28
2 Dec (core 3)	14	17	Dec (core 3)	28	16	-*	-*	-*
2 Dec (core 4)	11	23	-*	-*	-*	-*	-*	-*
2 Dec-5 Feb	28	15	2 Dec-5 Feb	31	13	2 Dec-5 Feb	33	29
5Feb-10 March	23	12	5 Feb-10 March	29	9	5Feb-10 March	18	29
10 March-14 April	24	13	10 March-14 April	32	4	10 March-14 April	25	26
14 April-18 May	24	14	14 April-18 May	30	4	14 April-18 May	24	33
18 May-28 June	15	19	18 May-28 June	27	20	18 May-28 June	17	24
28 June-28 July	19	31	28 June-28 July	30	27	28 June-28 July	25	20
28 July-22 Sept	19	23	28 July-22 Sept	30	24	28 July-22 Sept	23	19

*Deeper soil cores were not collected for site 2 and site 3 because sampling depth was dependent on the amount of sediment deposited at each site

Table 2.10 Calibration and Validation metrics for monthly surface runoff (m^3/sec), base flow (m^3/sec) and total flow (m^3/sec)

	Calibration (January 2011-December 2014)			Validation (January 2015-December 2017)		
	R^2	**NSE**	**PBIAS**	**R^2**	**NSE**	**PBIAS**
Surface Runoff (m^3/sec)	0.84	0.77	18.5	0.83	0.82	-6.5
Baseflow (m^3/sec)	0.85	0.75	18.8	0.90	0.88	-9.3
Total Flow (m^3/sec)	0.86	0.77	18.6	0.84	0.83	-7.5

Table 2.11 Change in the water yield from subbasins with the land use change scenario

	Before Land Use Change			After Land Use Change		
Subbasin	Forested %	Urban %	Water Yield (mm/yr)	Forested %	Urban %	Water Yield (mm/yr)
1	50.6	18.3	326.6	0.0	68.9	486.5
2	62.2	7.3	359.7	0.0	69.5	528.9
3	84.3	8.6	294.9	0.0	92.9	546.9
4	91.4	7.2	269.9	0.0	98.7	541.5
5	74.7	15.3	333.6	0.0	90.0	541.1
6	70.2	13.7	338.1	0.0	83.9	541.2
7	67.6	11.0	273.4	0.0	78.6	488.9
8	75.1	23.5	245.4	0.0	98.6	487.4
9	76.2	15.9	252.7	0.0	92.1	490.3
10	96.0	0.7	204.4	0.0	96.6	515.5
11	68.3	11.2	305.3	0.0	79.5	511.9
12	87.2	5.2	203.7	0.0	92.4	489.2
13	89.4	3.9	326.1	0.0	93.2	562.1
14	82.9	11.8	299.2	0.0	94.8	541.0

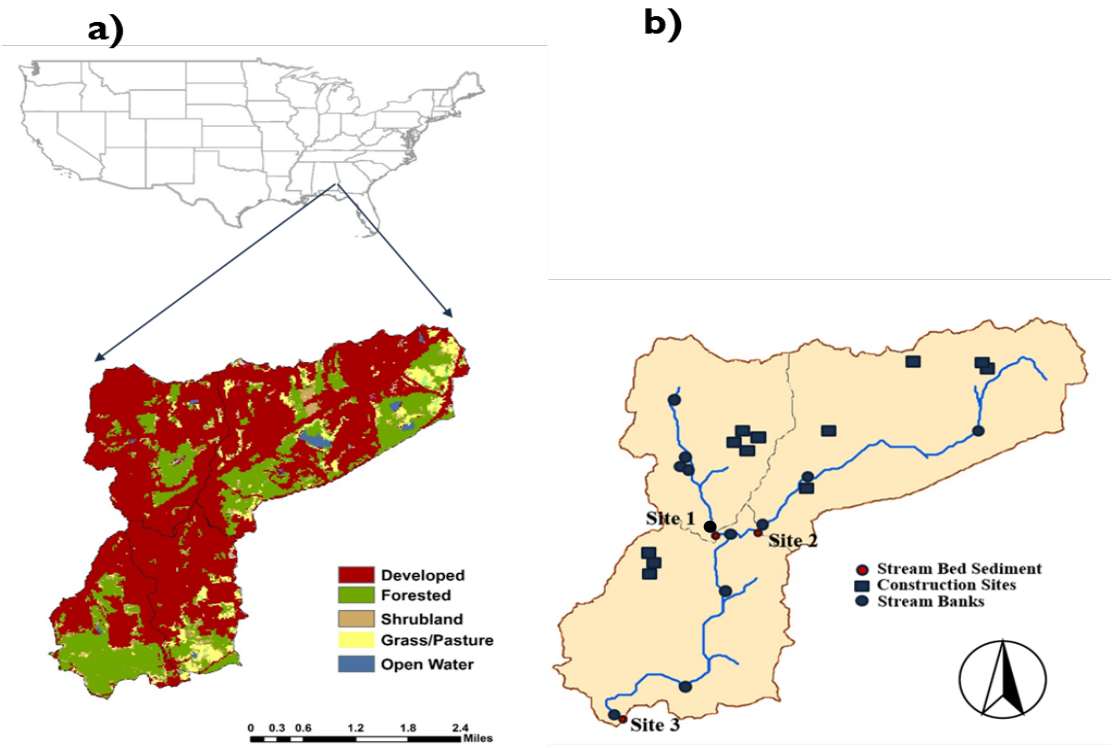

Figure 2.1 Land use distribution in the Moore's Mill Creek watershed and b. Location of stream bed sediment, stream banks and construction sampling sites.

a)

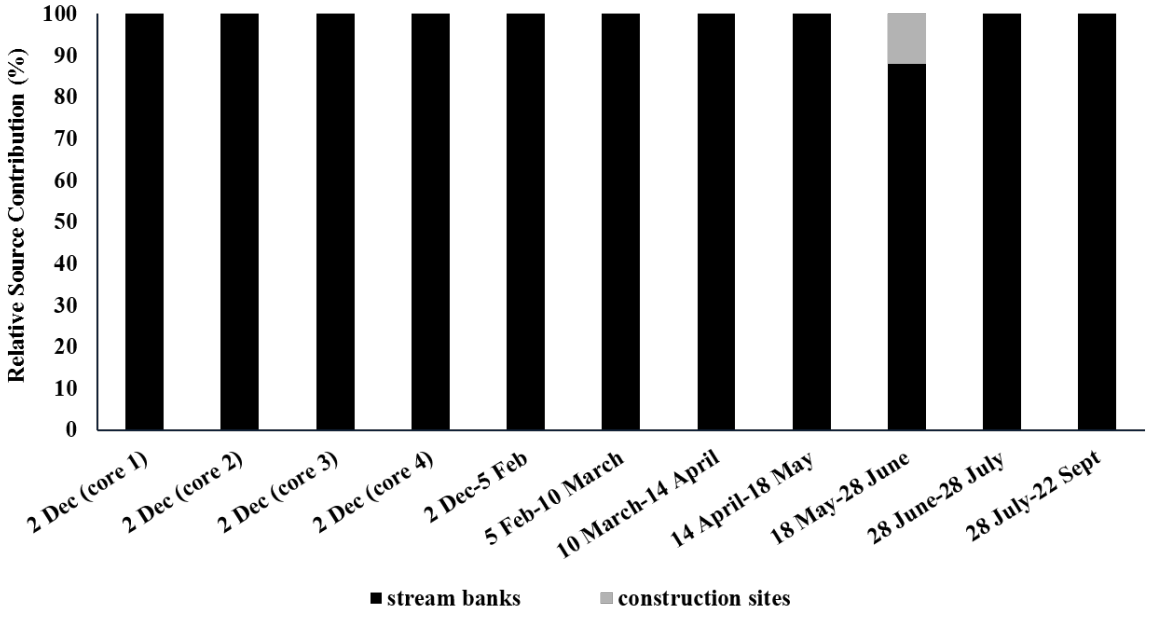
Relative Source Contribution (%)
100
90
80
70
60
50
40
30
20
10
0
2 Dec (core 1)
2 Dec (core 2)
2 Dec (core 3)
2 Dec (core 4)
2 Dec-5 Feb
5 Feb-10 March
10 March-14 April
14 April-18 May
18 May-28 June
28 June-28 July
28 July-22 Sept
stream banks
construction sites

b)

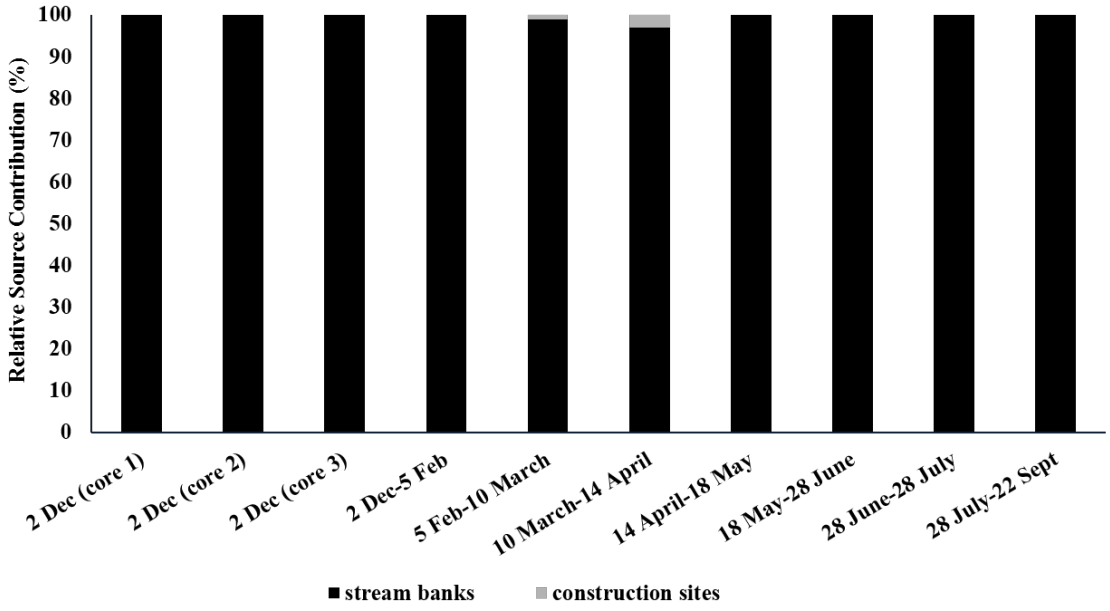
Relative Source Contribution (%)
100
90
80
70
60
50
40
30
20
10
0
2 Dec (core 1)
2 Dec (core 2)
2 Dec (core 3)
2 Dec-5 Feb
5 Feb-10 March
10 March-14 April
14 April-18 May
18 May-28 June
28 June-28 July
28 July-22 Sept
stream banks
construction sites

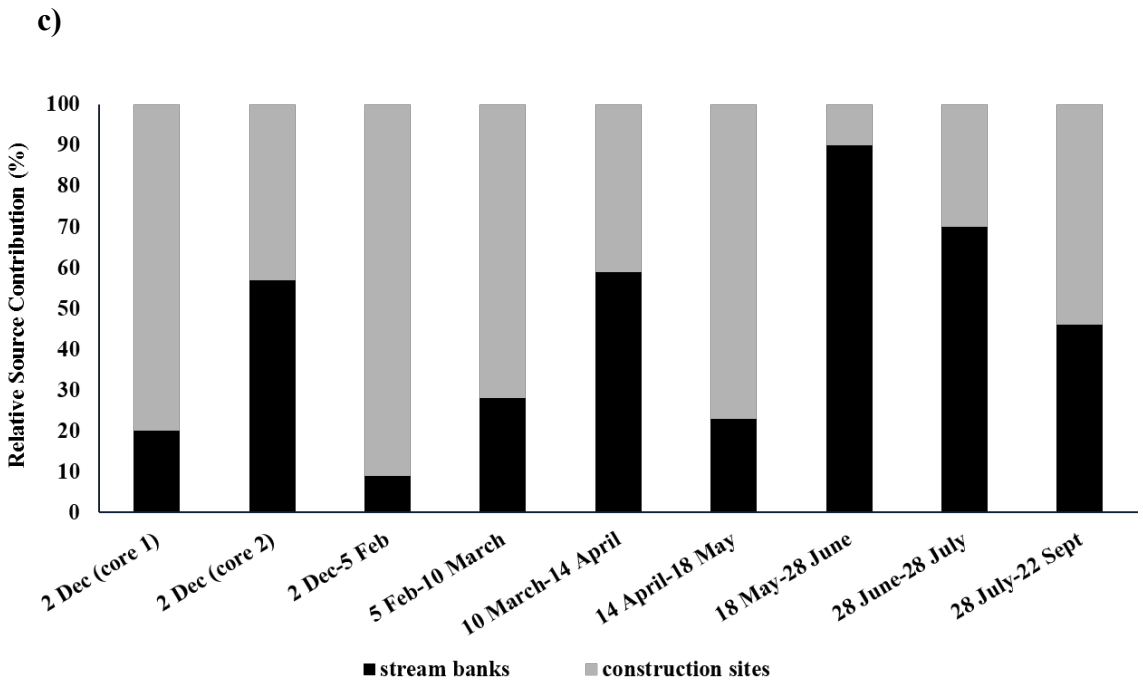

Figure 2.2 Relative source contribution (%) to stream bed sediment (for particle size 63-212 μm) from stream banks and construction sites at: (a) site 1, (b) site 2, and (c) site 3

a)

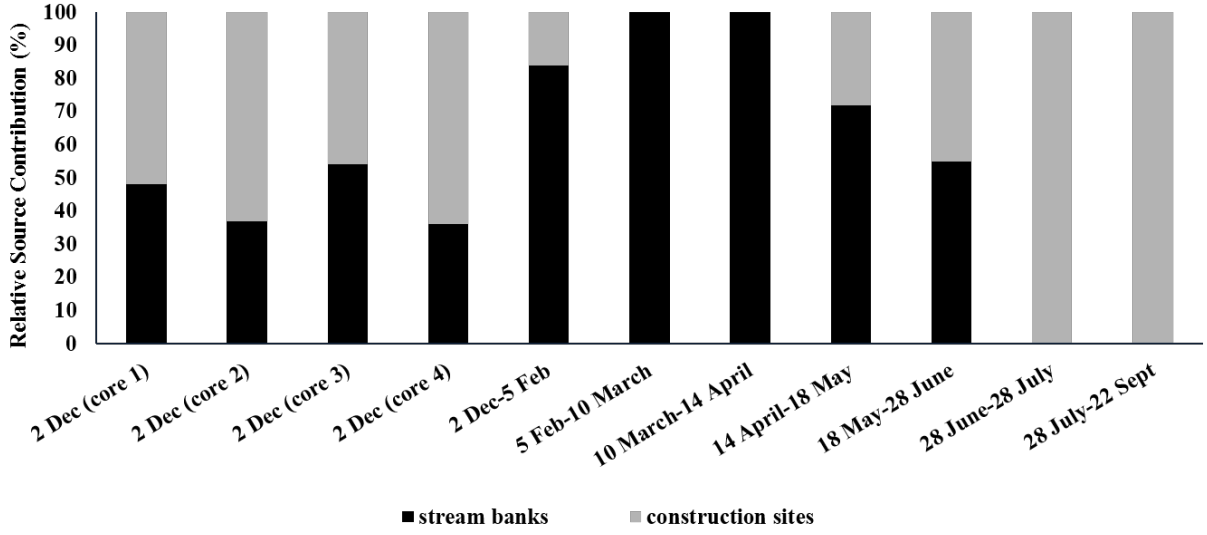
Relative Source Contribution (%)
100
90
80
70
60
50
40
30
20
10
0
2 Dec (core 1)
2 Dec (core 2)
2 Dec (core 3)
2 Dec (core 4)
2 Dec-5 Feb
5 Feb-10 March
10 March-14 April
14 April-18 May
18 May-28 June
28 June-28 July
28 July-22 Sept
stream banks
construction sites

b)

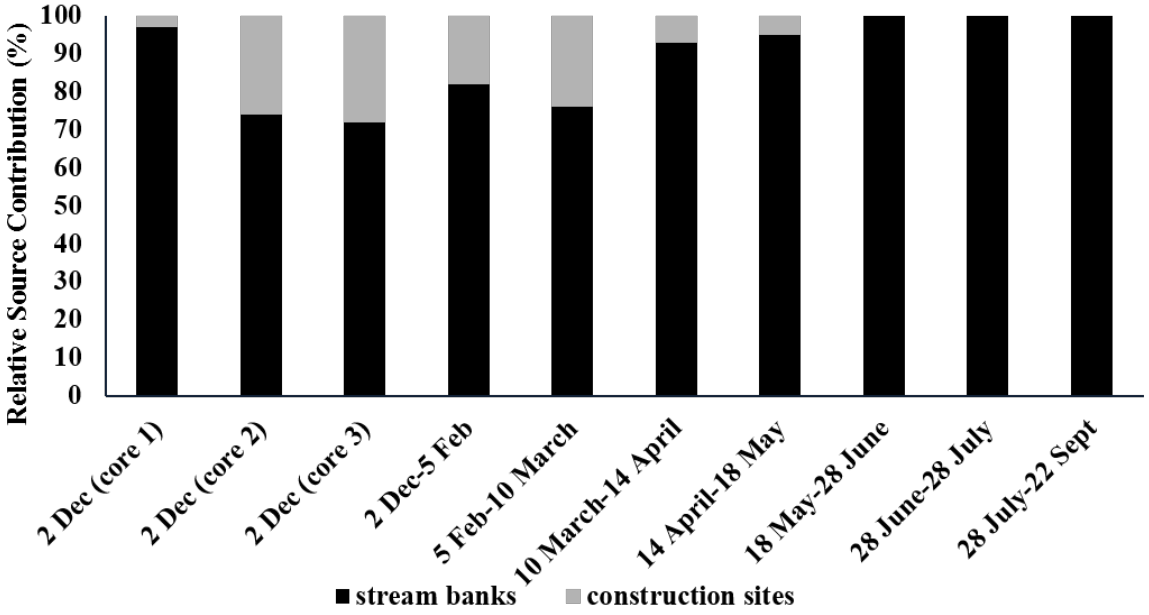
Relative Source Contribution (%)
100
90
80
70
60
50
40
30
20
10
0
2 Dec (core 1)
2 Dec (core 2)
2 Dec (core 3)
2 Dec-5 Feb
5 Feb-10 March
10 March-14 April
14 April-18 May
18 May-28 June
28 June-28 July
28 July-22 Sept
stream banks
construction sites

c)

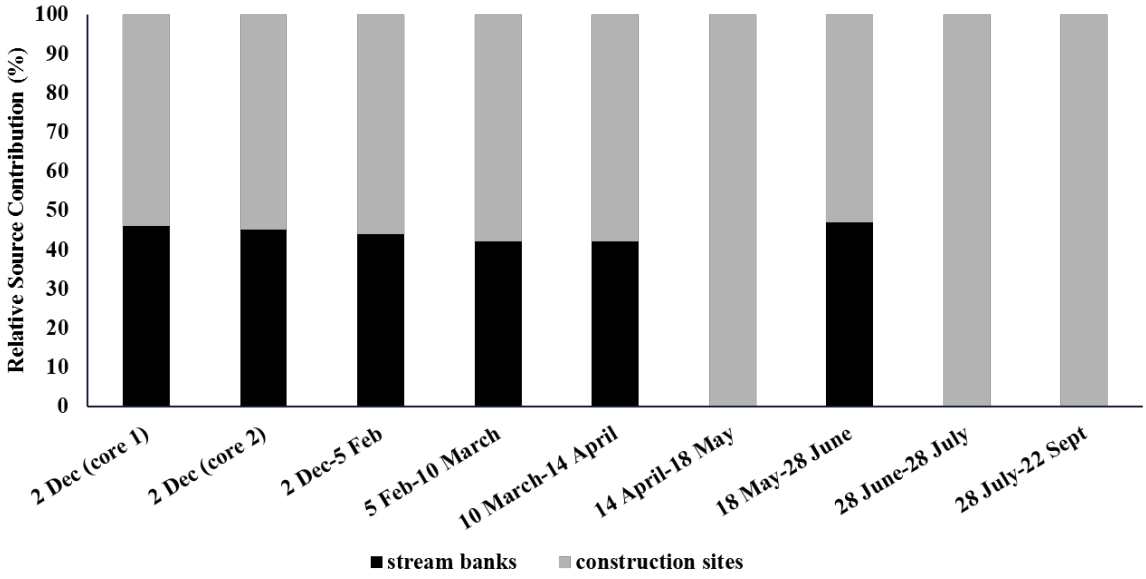

Figure 2.3 Relative source contribution (%) to stream bed sediment (for particle size <63μm) from stream banks and construction sites at: (a) site 1, (b) site 2, and (c) site 3

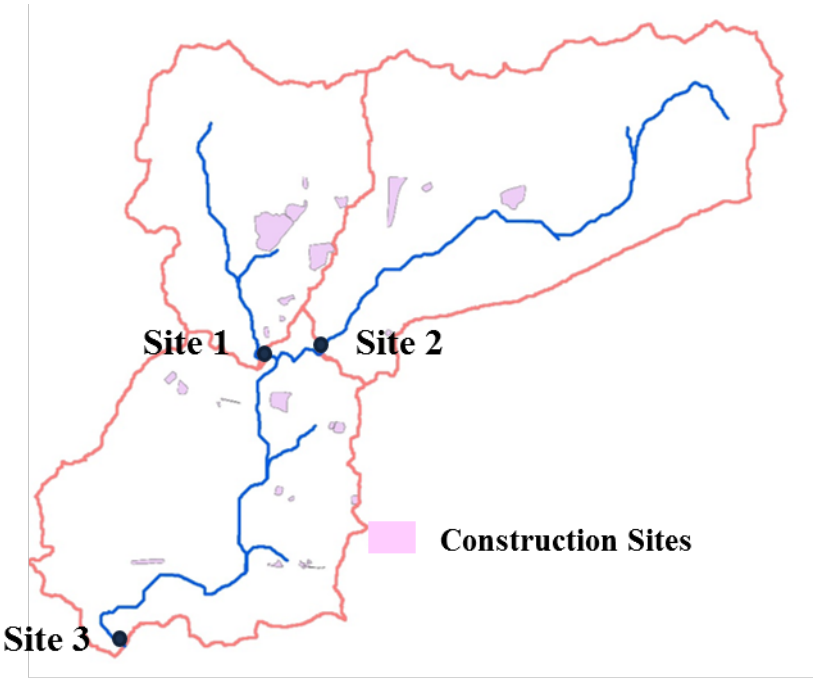

Figure 2.4 Active construction sites in the watershed during stream bed sediment sampling

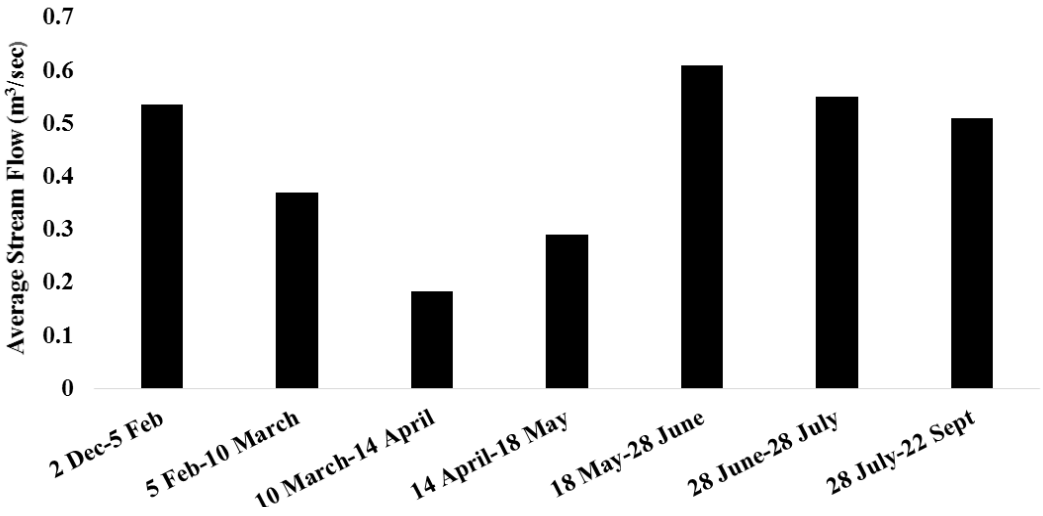

Figure 2.5 Temporal distribution in monthly stream flow (m^3/sec) at site 3 (watershed outlet) during the sampling period.

a.

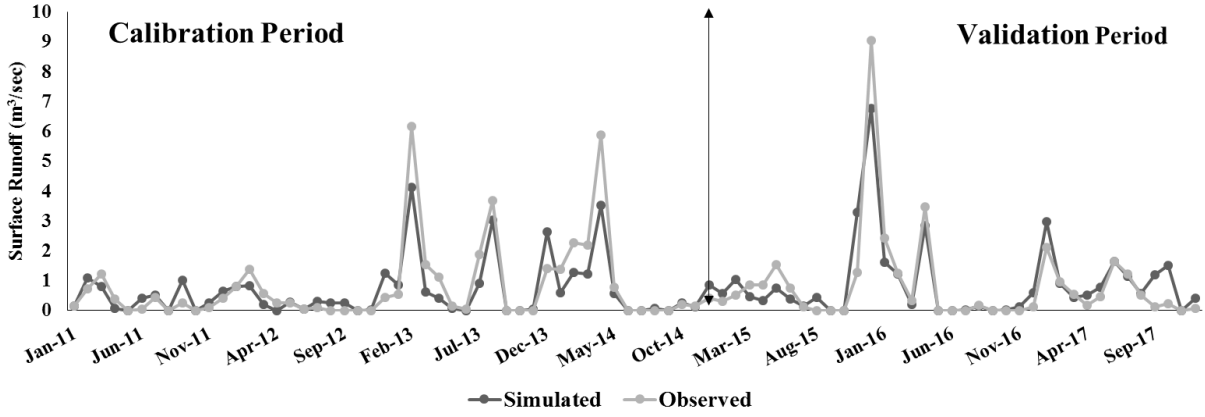
Calibration Period
Validation Period
Surface Runoff (m³/sec)
10
9
8
7
6
5
4
3
2
1
0
Jan-11
Jun-11
Nov-11
Apr-12
Sep-12
Feb-13
Jul-13
Dec-13
May-14
Oct-14
Mar-15
Aug-15
Jan-16
Jun-16
Nov-16
Apr-17
Sep-17
Simulated
Observed

b.

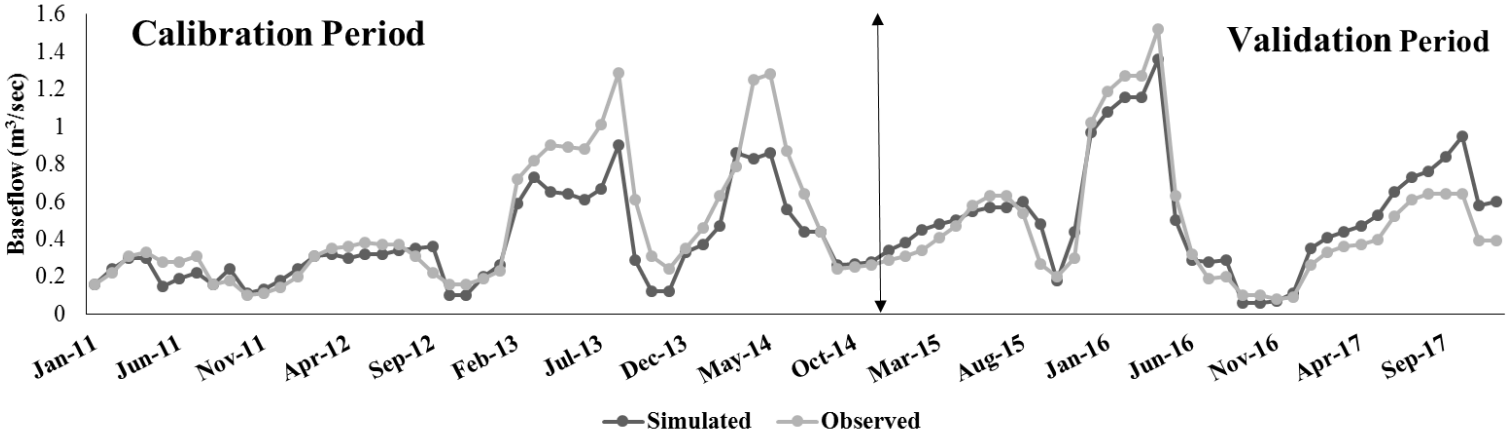
Calibration Period
Validation Period
Baseflow (m³/sec)
1.6
1.4
1.2
1
0.8
0.6
0.4
0.2
0
Jan-11
Jun-11
Nov-11
Apr-12
Sep-12
Feb-13
Jul-13
Dec-13
May-14
Oct-14
Mar-15
Aug-15
Jan-16
Jun-16
Nov-16
Apr-17
Sep-17
Simulated
Observed

c.

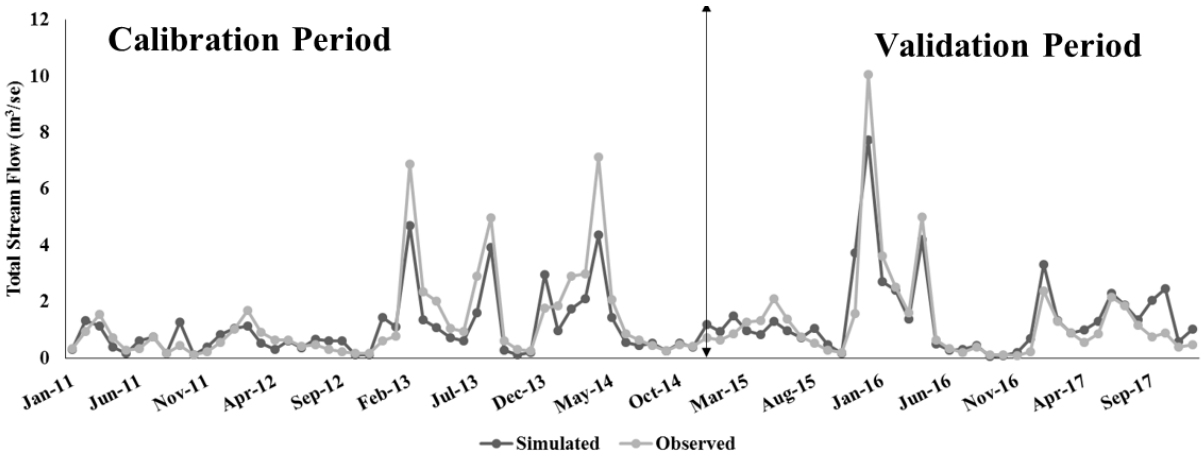

Figure 2.6 Observed and SWAT-simulated average monthly: (a) surface runoff (m^3/sec); (b) baseflows (m^3/sec); and (c) total flow (m^3/sec) rates for the calibration and validation periods (January 2011–December 2017)

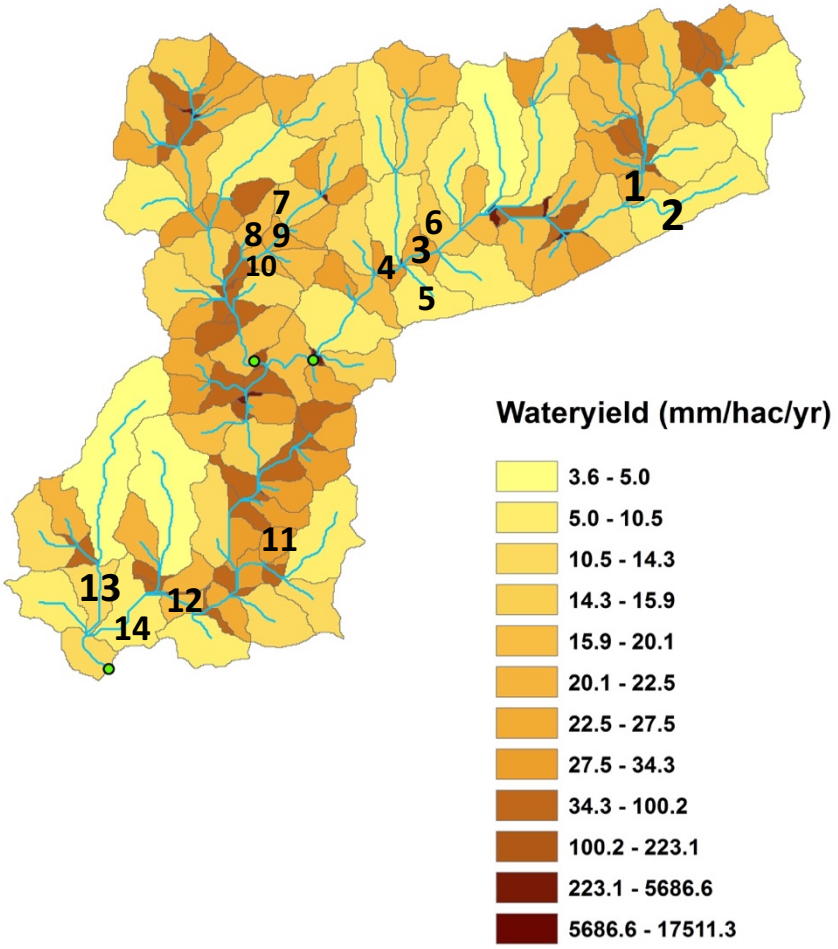

Figure 2.7 Average annual water yield from each subbasin as obtained from SWAT model

REFERENCES

Alabama Department of Environmental Management 303 (d) list, 2016 ADEM 303 (d) (http://www.adem.state.al.us/programs/water/wquality/2016AL303dList.pdf (accessed 17 June, 2017)).

Bini, Claudio, Giacomo Sartori, Mohammad Wahsha, and Silvia Fontana. (2011). Background Levels of Trace Elements and Soil Geochemistry at Regional Level in NE Italy. Journal of Geochemical Exploration 109(1). Pedogeochemical Mapping of Potentially Toxic Elements: 125–133.

Bledsoe, Brian P., and Chester C. Watson. (2001). Effects of Urbanization on Channel Instability1. JAWRA Journal of the American Water Resources Association 37(2): 255–270.

Booth, Derek B. (1990). Stream-Channel Incision Following Drainage-Basin Urbanization1. JAWRA Journal of the American Water Resources Association 26(3): 407–417.

Burt, Tim, and R. J. Allison. (2010). Sediment Cascades: An Integrated Approach. John Wiley & Sons.

Carter, Julie, Philip N Owens, Desmond E Walling, and Graham J. L Leeks. (2003). Fingerprinting Suspended Sediment Sources in a Large Urban River System. Science of The Total Environment 314–316. Land Ocean Interaction: Processes, Functioning and Environmental Management:A UK Perspective: 513–534.

Cempel, M, and G Nikel. (2006). Nickel: A Review of Its Sources and Environmental Toxicology: 8. Polish J. of Environ. Stud. 15(3): 375-382

City of Auburn (2011). Natural Systems. https://www.auburnalabama.org/CompPlan2030/4.0%20Natural%20Systems.pdf. Accessed June 17, 2017.

Collins, A. L., S. Pulley, I. D. L. Foster, et al. (2017). Sediment Source Fingerprinting as an Aid to Catchment Management: A Review of the Current State of Knowledge and a Methodological Decision-Tree for End-Users. Journal of Environmental Management 194(Supplement C). Sediment Source Fingerprinting for Informing Catchment Management: Methodological Approaches, Problems and Uncertainty: 86–108.

Collins, A. L., D. E. Walling, and G. J. L. Leeks. (1997). Source Type Ascription for Fluvial Suspended Sediment Based on a Quantitative Composite Fingerprinting Technique. CATENA 29(1): 1–27.

Collins, A. L., D. E. Walling, L. Webb, and P. King. (2010). Apportioning Catchment Scale Sediment Sources Using a Modified Composite Fingerprinting Technique Incorporating Property Weightings and Prior Information. Geoderma 155(3): 249–261.

Collins, A. L., D. E. Walling. (2002). Selecting fingerprint properties for discriminating potential suspended sediment sources in river basins. Journal of Hydrology 261(1-4): 218-244.

Collins, A. L., Y. Zhang, D. McChesney, et al. (2012). Sediment Source Tracing in a Lowland Agricultural Catchment in Southern England Using a Modified Procedure Combining Statistical Analysis and Numerical Modelling. Science of The Total Environment 414(Supplement C): 301–317.

Collins, A. L., Y. Zhang, D. E. Walling, S. E. Grenfell, and P. Smith. (2010). Tracing Sediment Loss from Eroding Farm Tracks Using a Geochemical Fingerprinting Procedure

Combining Local and Genetic Algorithm Optimisation. Science of The Total Environment 408(22): 5461–5471.

Collins, A.l., Y.s. Zhang, D. Duethmann, D.e. Walling, and K.s. Black. (2013). Using a Novel Tracing-Tracking Framework to Source Fine-Grained Sediment Loss to Watercourses at Sub-Catchment Scale. Hydrological Processes 27(6): 959–974.

Davis, C M, and J F Fox. (2009). Sediment Fingerprinting: Review of the Method and Future Improvements for Allocating Nonpoint Source Pollution. Journal of Environmental Engineering 135(7): 490–504.

Devereux, Olivia H., Karen L. Prestegaard, Brian A. Needelman, and Allen C. Gellis. (2010). Suspended-Sediment Sources in an Urban Watershed, Northeast Branch Anacostia River, Maryland. Hydrological Processes 24(11): 1391–1403.

Ferreira, Carla S.S., Rory P.D. Walsh, William H. Blake, Ryunosuke Kikuchi, and António J.D. Ferreira. (2017). Temporal Dynamics of Sediment Sources in an Urbanizing Mediterranean Catchment. Land Degradation & Development 28(8): 2354–2369.

FISRWG, Federal interagency stream restoration working group. (1998). Stream corridor restoration: principles, processes, and practices.

Fox, James F., and Athanasios N. Papanicolaou. (2007). The Use of Carbon and Nitrogen Isotopes to Study Watershed Erosion Processes1. JAWRA Journal of the American Water Resources Association 43(4): 1047–1064.

Franz, C., F. Makeschin, H. Weiß, and C. Lorz. (2014). Sediments in Urban River Basins: Identification of Sediment Sources within the Lago Paranoá Catchment, Brasilia DF, Brazil - Using the Fingerprint Approach. The Science of the Total Environment 466–467: 513–523.

Gellis, Allen C., and Gregory B. Noe. (2013). Sediment Source Analysis in the Linganore Creek Watershed, Maryland, USA, Using the Sediment Fingerprinting Approach: 2008 to 2010. Journal of Soils and Sediments 13(10): 1735–1753.

George H. Hargreaves, and Zohrab A. Samani. (1985). Reference Crop Evapotranspiration from Temperature. Applied Engineering in Agriculture 1(2): 96–99.

Gholami, Hamid, Nick Middleton, Ali Akbar Nazari Samani, and Robert Wasson. (2017). Determining Contribution of Sand Dune Potential Sources Using Radionuclides, Trace and Major Elements in Central Iran. Arabian Journal of Geosciences 10(7): 163.

Gruszowski, K. E., I. D. L. Foster, J. A. Lees, and S. M. Charlesworth. (2003). Sediment Sources and Transport Pathways in a Rural Catchment, Herefordshire, UK. Hydrological Processes 17(13): 2665–2681.

Haddadchi, Arman, Darren S. Ryder, Olivier Evrard, and Jon Olley. (2013). Sediment Fingerprinting in Fluvial Systems: Review of Tracers, Sediment Sources and Mixing Models. International Journal of Sediment Research 28(4): 560–578.

Harbor, Jon. (1999). Engineering Geomorphology at the Cutting Edge of Land Disturbance: Erosion and Sediment Control on Construction Sites. Geomorphology 31(1): 247–263.

Hatfield, Robert G., and Barbara A. Maher. (2009). Fingerprinting Upland Sediment Sources: Particle Size-Specific Magnetic Linkages between Soils, Lake Sediments and Suspended Sediments. Earth Surface Processes and Landforms 34(10): 1359–1373.

Hooda, Peter. (2010). Trace Elements in Soils. John Wiley & Sons.

Horowitz, A.J. (1991). A Primer on Sediment-Trace Element Chemistry. USGS Numbered Series, 91–76. Open-File Report. U.S. Geological Survey ; Books and Open-File Reports Section [distributor],. http://pubs.er.usgs.gov/publication/ofr9176.

Huisman, Natalie L. H., K. G. Karthikeyan, Jasmeet Lamba, Anita M. Thompson, and Graham Peaslee. (2013). Quantification of Seasonal Sediment and Phosphorus Transport Dynamics in an Agricultural Watershed Using Radiometric Fingerprinting Techniques. Journal of Soils and Sediments 13(10): 1724–1734.

K. R. Douglas-Mankin, R. Srinivasan, and J. G. Arnold. (2010). Soil and Water Assessment Tool (SWAT) Model: Current Developments and Applications. Transactions of the ASABE 53(5): 1423–1431.

Koiter, A. J., P. N. Owens, E. L. Petticrew, and D. A. Lobb. (2013). The Behavioural Characteristics of Sediment Properties and Their Implications for Sediment Fingerprinting as an Approach for Identifying Sediment Sources in River Basins. Earth-Science Reviews 125(Supplement C): 24–42.

Koiter, Alexander J., David A. Lobb, Philip N. Owens, et al. (2013). Investigating the Role of Connectivity and Scale in Assessing the Sources of Sediment in an Agricultural Watershed in the Canadian Prairies Using Sediment Source Fingerprinting. Journal of Soils and Sediments 13(10): 1676–1691.

Laceby, J. Patrick, Olivier Evrard, Hugh G. Smith, et al. (2017). The Challenges and Opportunities of Addressing Particle Size Effects in Sediment Source Fingerprinting: A Review. Earth-Science Reviews 169: 85–103.

Lamba, Jasmeet, K. G. Karthikeyan, and A. M. Thompson. (2015). Apportionment of Suspended Sediment Sources in an Agricultural Watershed Using Sediment Fingerprinting. Geoderma 239–240: 25–33.

Lamba, Jasmeet, A.M. Thompson, K.G. Karthikeyan, and Faith A. Fitzpatrick. (2015). Sources of Fine Sediment Stored in Agricultural Lowland Streams, Midwest, USA. Geomorphology 236: 44–53.

Lee, K.-H., Isenhart, T.M., Schultz, R.C., Mickelson, S.K. (2000). Multispecies riparian buffers trap sediment and nutrients during rainfall simulations. Journal of environmental quality 29, 1200–1205.

Lim, Kyoung Jae, Bernard A. Engel, Joongdae Choi, et al. N.d. AUTOMATED WEB GIS BASED HYDROGRAPH ANALYSIS TOOL, WHAT1 - Lim - 2005 - JAWRA Journal of the American Water Resources Association - Wiley Online Library. https://onlinelibrary.wiley.com/doi/full/10.1111/j.1752-1688.2005.tb03808.x, accessed May 8, 2018.

Liu, Bing, Daniel E. Storm, Xunchang J. Zhang, Wenhong Cao, and Xingwu Duan. (2016). A New Method for Fingerprinting Sediment Source Contributions Using Distances from Discriminant Function Analysis. CATENA 147: 32–39.

Manjoro, Munyaradzi, Kate Rowntree, Vincent Kakembo, Ian Foster, and Adrian L. Collins (2017). Use of Sediment Source Fingerprinting to Assess the Role of Subsurface Erosion in the Supply of Fine Sediment in a Degraded Catchment in the Eastern Cape, South Africa. Journal of Environmental Management 194. Sediment Source Fingerprinting for Informing Catchment Management: Methodological Approaches, Problems and Uncertainty: 27–41.

Martínez-Carreras, Núria, Thomas Udelhoven, Andreas Krein, et al. (2010). The Use of Sediment Colour Measured by Diffuse Reflectance Spectrometry to Determine Sediment

Sources: Application to the Attert River Catchment (Luxembourg). Journal of Hydrology 382(1): 49–63.

McCarney-Castle, Kerry, Tristan M. Childress, and Christian R. Heaton. (2017). Sediment Source Identification and Load Prediction in a Mixed-Use Piedmont Watershed, South Carolina. Journal of Environmental Management 185(Supplement C): 60–69.

Mishra, Surendra Kumar, and Vijay P. Singh. (2003). SCS-CN Method. *In* Soil Conservation Service Curve Number (SCS-CN) Methodology Pp. 84–146. Water Science and Technology Library. Springer, Dordrecht. https://link.springer.com/chapter/10.1007/978-94-017-0147-1_2, accessed May 16, 2018.

Moriasi, D. N., J. G. Arnold, M. W. Van Liew, et al. (2007). Model Evaluation Guidelines for Systematic Quantification of Accuracy in Watershed Simulations.

Mukundan, R., D. E. Radcliffe, J. C. Ritchie, L. M. Risse, and R. A. McKinley. (2010). Sediment Fingerprinting to Determine the Source of Suspended Sediment in a Southern Piedmont Stream. Journal of Environmental Quality 39(4): 1328–1337.

Mukundan, Rajith, Des Walling, Allen Gellis, Michael Slattery, and David E Radcliffe. (2012). Sediment Source Fingerprinting: Transforming From a Research Tool to a Management Tool. JAWRA Journal of the American Water Resources Association 48: 1241–1257.

Nagle, Gregory N., Timothy J. Fahey, Jerry C. Ritchie, and Peter B. Woodbury. (2007). Variations in Sediment Sources and Yields in the Finger Lakes and Catskills Regions of New York. Hydrological Processes 21(6): 828–838.

NCDEHNR. (1997). Report of Proceedings on the Proposed Neuse River Basin Nutrient Sensitive Waters (NSW) Management Strategy. Environmental Management

Commission Meeting, June 12, 1997, State of North Carolina, Department of Environment, Health and Natural Resources, Raleigh, NC.

Neitsch, S L, J G Arnold, J R Kiniry, And J R Williams. (2005). Soil And Water Assessment Tool Theoretical Documentation: 494.

Nosrati, Kazem, Gerard Govers, Brice X. Semmens, and Eric J. Ward. (2014). A Mixing Model to Incorporate Uncertainty in Sediment Fingerprinting. Geoderma 217–218: 173–180.

O'Driscoll, Michael A., Jason R. Soban, and Scott A. Lecce. (2009). Stream Channel Enlargement Response to Urban Land Cover in Small Coastal Plain Watersheds, North Carolina. Physical Geography 30(6): 528–555.

O'Driscoll, Michael, Sandra Clinton, Anne Jefferson, Alex Manda, and Sara McMillan. (2010). Urbanization Effects on Watershed Hydrology and In-Stream Processes in the Southern United States. Water 2(3): 605–648.

Olley, Jon, Kate Smolders, Francis Pantus, and Timothy Pietsch. (2012). The Application of Fallout Radionuclides to Determine the Dominant Erosion Process in Water Supply Catchments of Subtropical South-east Queensland, Australia - Olley - 2013 - Hydrological Processes - Wiley Online Library.

Osman, Akode M., and Colin R. Thorne. (1988). Riverbank Stability Analysis. I: Theory. Journal of Hydraulic Engineering 114(2): 134–150.

Owens, Philip N., William H. Blake, Tim R. Giles, and Neil D. Williams. (2012). Determining the Effects of Wildfire on Sediment Sources Using ^{137}Cs and unsupported ^{210}Pb: The Role of Landscape Disturbances and Driving Forces. Journal of Soils and Sediments 12(6): 982–994.

Pitt, Robert, Shirley E. Clark, and Donald W. Lake. (2007). Construction Site Erosion and Sediment Controls: Planning, Design and Performance. DEStech Publications, Inc.

Poleto, Cristiano, Gustavo H. Merten, and Jean P. Minella. (2009). The Identification of Sediment Sources in a Small Urban Watershed in Southern Brazil: An Application of Sediment Fingerprinting. Environmental Technology 30(11): 1145–1153.

Pulley, S., A. L. Collins, and B. Van der Waal. (2018) . Variability in the Mineral Magnetic Properties of Soils and Sediments within a Single Field in the Cape Fold Mountains, South Africa: Implications for Sediment Source Tracing. CATENA 163: 172–183.

Pulley, Simon, Ian Foster, and Paula Antunes. (2015). The Application of Sediment Fingerprinting to Floodplain and Lake Sediment Cores: Assumptions and Uncertainties Evaluated through Case Studies in the Nene Basin, UK. Journal of Soils and Sediments 15(10): 2132–2154.

Pulley, Simon, Ian Foster, and Adrian L. Collins. (2017). The Impact of Catchment Source Group Classification on the Accuracy of Sediment Fingerprinting Outputs. Journal of Environmental Management 194(Supplement C). Sediment Source Fingerprinting for Informing Catchment Management: Methodological Approaches, Problems and Uncertainty: 16–26.

National Oceanic and Atmospheric Administration (NOAA). National Climatic Data Center (https://www.ncdc.noaa.gov/cdo-web/).

Niraula, R., L. Kalin, R. Wang, and P. Srivastava. (2011). Determining Nutrient and Sediment Critical Source Areas with SWAT: Effect of Lumped Calibration. Transactions of the ASABE 55(1): 137–147.

Russell, M. A, D. E Walling, and R. A Hodgkinson. (2001). Suspended Sediment Sources in Two Small Lowland Agricultural Catchments in the UK. Journal of Hydrology 252(1): 1–24.

Smith, Hugh G., and William H. Blake. (2014). Sediment Fingerprinting in Agricultural Catchments: A Critical Re-Examination of Source Discrimination and Data Corrections. Geomorphology 204(Supplement C): 177–191.

Smith, Hugh G., Gary J. Sheridan, Patrick J. Lane, Philip J. Noske, and Henk Heijnis. (2011). Changes to Sediment Sources Following Wildfire in a Forested Upland Catchment, Southeastern Australia - Smith - 2011 - Hydrological Processes - Wiley Online Library.

Stewart, Heather A., Arash Massoudieh, and Allen Gellis. (2015). Sediment Source Apportionment in Laurel Hill Creek, PA, Using Bayesian Chemical Mass Balance and Isotope Fingerprinting. Hydrological Processes 29(11): 2545–2560.

Tyler, Germund. (2004). Rare Earth Elements in Soil and Plant Systems - A Review. Plant and Soil 267(1–2): 191–206.

USDA-NRCS.Soil Survey Geographic (SSURGO) database for Lee County, Alabama.

USEPA. (1996). Microwave assisted acid digestion of siliceous and organically based matrices. OHW, Method, 3052.

USEPA. (2008). The National Rivers and Streams Assessment 2008/2009. https://www.epa.gov/sites/production/files/2016-03/documents/fact_sheet_draft_variation_march_2016_revision.pdf. Accessed 9 December 2017.

USEPA, 2017. National Summary of State Information. https://ofmpub.epa.gov/waters10/attains_nation_cy.control#STREAM/CREEK/RIVER. Accessed 9 December 2017.

Walling, D. E. (2005). Tracing Suspended Sediment Sources in Catchments and River Systems. Science of The Total Environment 344(1–3). Linking Landscape Sources of Phosphorus and Sediment to Ecological Impacts in Surface WatersHaygarth S.I.: 159–184.

Walling, Desmond E. (2013). The Evolution of Sediment Source Fingerprinting Investigations in Fluvial Systems. Journal of Soils and Sediments; Dordrecht 13(10): 1658–1675.

White, Michael J., Daniel E. Storm, Philip R. Busteed, Scott H. Stoodley, and Shannon J. Phillips. (2009). Evaluating Nonpoint Source Critical Source Area Contributions at the Watershed Scale. Journal of Environmental Quality 38(4): 1654–1663. https://dl.sciencesocieties.org/publications/jeq/abstracts/38/4/1654, accessed April 20, 2017.

Wilkinson, Scott N., Gary J. Hancock, Rebecca Bartley, Aaron A. Hawdon, and Rex J. Keen. (2013). Using Sediment Tracing to Assess Processes and Spatial Patterns of Erosion in Grazed Rangelands, Burdekin River Basin, Australia. Agriculture, Ecosystems & Environment 180(Supplement C). Catchments to Reef Continuum: Minimising Impacts of Agriculture on the Great Barrier Reef: 90–102.

Wilson, C. G., R. A. Kuhnle, D. D. Bosch, et al. (2008). Quantifying Relative Contributions from Sediment Sources in Conservation Effects Assessment Project Watersheds. Journal of Soil and Water Conservation 63(6): 523–532.

Wolman M. Gordon, and Schick Asher P. (2010). Effects of Construction on Fluvial Sediment, Urban and Suburban Areas of Maryland. Water Resources Research 3(2): 451–464.

Xu, Z. X., J. P. Pang, C. M. Liu, and J. Y. Li. (2009). Assessment of Runoff and Sediment Yield in the Miyun Reservoir Catchment by Using SWAT Model. Hydrological Processes 23(25): 3619–3630.

Yahaya Ahmed Iyaka. (2011). Nickel in Soils: A Review of Its Distribution and Impacts. Scientific Research and Essays 6(33).

Yu, Mingjing, and Bruce L. Rhoads. (2018). Floodplains as a Source of Fine Sediment in Grazed Landscapes: Tracing the Source of Suspended Sediment in the Headwaters of an Intensively Managed Agricultural Landscape. Geomorphology.

Zhang, Chengfu, Sheng Li, Junyu Qi, Zisheng Xing, and Fanrui Meng. (2017). Assessing Impacts of Riparian Buffer Zones on Sediment and Nutrient Loadings into Streams at Watershed Scale Using an Integrated REMM-SWAT Model. Hydrological Processes 31(4): 916–924.

CHAPTER 3

APPORTIONMENT OF SUSPENDED SEDIMENT SOURCES IN AN URBANIZED WATERSHED USING SEDIMENT FINGERPRINTING

3.1 INTRODUCTION

Nonpoint Source (NPS) pollution has been identified as the leading cause of surface water impairment in the U.S. and sediment has been considered as the most common NPS pollutant (Harbor, 1999; Davis and Fox 2009). Elevated supplies of suspended sediment from terrestrial and aquatic sources to surface waters as a result of anthropogenic activities negatively impacts aquatic ecosystems (Kemp Paul et al., 2011; Vercruysse, et al., 2017). For example, excessive sediment delivery to surface waters can increase turbidity, deliver sediment-bound nutrients to streams and lakes, and result in sedimentation of the river bed (Koiter et al., 2013). In the state of Alabama (AL), U.S. for approximately 34% of the impaired streams and rivers, sedimentation has been considered as the potential cause of impairment (USEPA, 2017). Thousands of miles of the rivers and streams in the southern Piedmont region of U.S. are impaired because of excessive sedimentation, which can be attributed to some extent to historic disturbances during mid-20th century (McCarney-Castle et al., 2017; Mukundan et al., 2010). With the urban populations increasing at a rate of 2.1 % per year and, with more than half of the world's population living in urban areas (The World Bank, 2014), the degradation of streams because of urbanization is significant (Russell et al., 2017). The streams in urban

areas are often subjected to severe impacts from human activities and land use changes, a problem recognized as 'the urban stream syndrome'(Russell et al., 2017; Walsh et al., 2005). Because of the presence of large impervious surfaces, urban areas have the potential to generate higher volumes of overland flow, which results in increased transport of sediment to rivers and artificial drainage networks (Rossi et al. 2013; Vercruysse et al., 2017). In urbanized watersheds, even small rainfall events can result in generation of surface runoff which is sufficient enough to cause frequent disturbance to streams because of connectivity between impervious surfaces and streams (Walsh et al., 2005).

The sediment delivered to streams via construction-site storm water runoff has been considered as the leading cause of impairment of streams and rivers in the U.S. and over the world (Fang et al., 2015). Implementation of best management practices (BMPs) can help to reduce loss of sediment to streams. However, there would be a wastage of resources, if control measures in a watershed are focused on reducing stream bank erosion, when most of the sediment transported through a stream was contributed by surface erosion in upland areas (Walling, 2005). Therefore, quantitative information on the sources of suspended sediment delivered to stream can help to target management strategies at the most important sources of suspended sediment in a watershed (Collins et al., 2017).

Sediment fingerprinting techniques have been widely used to provide information on the sources of suspended sediment in a watershed (Barthod et al., 2015; Collins et al., 2017; Liu et al., 2017; Nosrati et al., 2014). This technique is based on two major assumptions: firstly, potential sources of suspended sediment are distinguishable on the basis of selected fingerprinting properties (e.g., physical or geochemical properties) and secondly, the relative source contributions of different sources to suspended sediment can be determined with the comparison of fingerprinting

properties in the suspended sediment and the source material samples (Collins and Walling, 2002). The procedure employs statistical analysis to select a combination of fingerprinting properties that discriminate among the sources (Smith and Blake, 2014). By comparing the fingerprint properties in suspended sediment and potential sources of suspended sediment using statistical testing, it is possible to obtain quantitative information on relative contributions from different sources to suspended sediment (Koiter et al., 2015; Davis and Fox, 2009). Different types of fingerprinting properties, such as fallout radionuclides (Huisman et al., 2013; Wilson et al., 2008), major and trace elemental composition (Miller et al., 2005), mineral magnetic properties (Mzuza et al., 2017; Walling et al., 1999), color (Barthod et al. 2015; Martínez-Carreras et al., 2010) and stable isotopes (Rhoton et al., 2008; Fox and Papanicolaou, 2007) have been successfully used in the past to identify suspended sediment sources. However, the use of a single fingerprinting property can result in erroneous sediment source ascriptions. Therefore, typically multiple fingerprinting properties and multivariate statistical techniques are used to determine relative source contribution of different sources to suspended sediment. Geochemical element fingerprinting properties are most commonly used sediment fingerprinting properties (Pulley et al., 2015; Fu et al., 2006) due to their ability to successfully discriminate among different sources and determination of in-stream sediment sources with less uncertainty (Davis and Fox, 2009).

Sediment delivered to streams can originate from different sources (e.g., construction sites, cropland areas, stream banks) and contribution from different sources to suspended sediment can vary depending on the susceptibility of a soil to erosion (Vercruysse et al., 2017). Previous researchers have successfully used sediment fingerprinting techniques to determine relative source contributions to suspended sediment on the basis of land use types, contrasting geological zones, heterogeneous soil types, tributary sub-basins, and surficial vs subsurface sources (Pulley et al.,

2017; Collins and Walling, 2002; Nosrati et al., 2014; Wilkinson et al., 2013; Smith and Blake, 2014; Palazón et al., 2015).

Typically, previous sediment fingerprinting studies have focused on identification of suspended sediment sources in agricultural watersheds (e.g., Collins et al., 2010; Huisman et al., 2013; Smith and Blake, 2014; Foucher et al., 2015). Whereas, limited work has been done in urban settings (e.g., Devereux et al., 2010; Franz et al., 2014). Furthermore, particle size exerts an important influence on relative contributions from different sources to suspended sediment (Smith and Blake, 2014). However, limited work (Laceby et al., 2017; Koiter et al., 2015; Owens et al., 2015) has been done to quantify the effect of particle size on suspended sediment sources. Use of sediment fingerprinting in combination with watershed-level modeling can provide valuable information of watershed-level hydrological processes that affect sediment erosion and transport within a watershed. Typically, areas generating significant amount of surface runoff have potential to contribute disproportionately high amount of sediment to streams (Russell et al., 2017; Walsh, 2005; Deasy et al., 2009). Watershed-level modeling can help to prioritize areas based on the amount of surface runoff generated and the dominant sources of suspended sediment (determined using sediment fingerprinting) in those prioritized areas can be targeted for BMPs. Several researchers have successfully used Soil and Water Assessment Tool (SWAT) model to identify areas contributing significant amount of surface runoff to streams (Rostamian et al., 2008; Chanasyk et al., 2003; Easton et al., 2008). However, limited work (Palazón et al., 2014; Palazón et al., 2016) has been done to use sediment fingerprinting technique in conjunction with SWAT modeling to identify areas for targeting BMPs. The objectives of this study were to: (a) identify sources of suspended sediment in a rapidly urbanizing watershed in southern Piedmont region of AL, (b) quantify the effect of sediment particle size (63-212 μm and <63 μm) on relative

contributions from different sources to suspended sediment at a subwatershed level, and (c) Use to SWAT model to prioritize the subwatersheds for targeting BMPs based on the amount of surface runoff generated. The overall goal of this study was to better understand the sediment transport processes within an urbanizing watershed.

3.2 METHODS AND MATERIALS

3.2.1 Study Site

Sampling was conducted in the 31 km^2 watershed of the Moore's Mill Creek, located in eastern part of AL, USA (Fig. 3.1.a). Lying within the southern Piedmont physiographic province, this watershed is a part of the lower Tallapoosa River Basin. The main land uses in the study watershed are developed (66%), forested (23%), pasture (5%), and shrubland (4%) based on the Cropland Data Layer (CDL, 2017) (https://www.nass.usda.gov/Research_and_Science/Cropland/SARS1a.php). This watershed receives an average annual precipitation of 1337 mm and with average annual high and low temperatures of 23º C and 12º C, respectively. Bedrock lithology ranges from schist and gneiss to saprolite and granite. The Moore's Mill Creek is listed on the Alabama Department of Environmental Management's 303(d) list of impaired water bodies because of excessive sedimentation (ADEM, 2016). Urbanization, historic channel modifications, reduction in riparian buffers, and agriculture have been recognized as the major contributors to this degradation (City of Auburn, 2011).

3.2.2 Collection of Representative Source and Suspended Sediment Samples

The fieldwork for this study involved collection of samples from potential sources of suspended sediment and suspended sediment sampling. The potential sources of suspended sediment considered in this study included: (1) stream banks (sub-surface) and (2) construction

sites (surface). The source samples were collected from 30 different sites (13 samples from construction sites and 17 samples from stream banks sites) (Fig. 3.1.b). The source sample collection procedure is discussed in detail in the section 2.2.2 of chapter 2.The suspended sediment samples were collected using the time-integrated suspended sediment sampler developed by Phillips et al. (2000).The time-integrated trap samplers have been successfully used in previous studies for suspended sediment sampling (Walling et al., 2008; Lamba et al., 2015; Martínez-Carreras, et al., 2010). These samplers were installed at 3 sites within the watershed (Fig. 3.1b). At each site (i.e. subwatershed or overall watershed outlet), four time-integrated trap samplers were installed to ensure that sufficient sediment mass was collected for subsequent analyses. To determine temporal variability of suspended sediment sources, we collected suspended sediment samples from December, 2016 to September, 2017. The suspended sediment sample collection dates are included in Table 3.1.

3.2.3 Sample Preparation and Analytical Procedures

Laboratory analysis included oven drying of both the soil and suspended sediment samples at 60° C and disaggregation using pestle and mortar and then dry-sieving to two particle size fractions, namely, 63-212 μm (fine sand) and <63 μm (silt and clay). The samples were then analyzed for 59 geochemical elements which included, Li, Be, B, Mg, Na, Al, P, S, K, Ca, Sc, Ti, V, Cr, Mn, Fe, Co, Ni, Cu, Zn, Ga, As, Se, Rb, Sr, Y, Zr, Nb, Rh, Pd, Ag, Mo, Cd, Sn, Sb, Cs, Ba, La, Ce, Pr, Nd, Sm, Eu, Gd, Dy, Ho, Yb, Lu, Hf, Ta, W, Ir, Pt, Hg, Tl, Pb, Bi, Th, and U using ICP-MS microwave-aided digestion (EPA Method 3052) at the Wisconsin State Laboratory of Hygiene, Madison, Wisconsin, USA (USEPA, 1996). Particle size analyses of suspended sediment and source samples was performed using a Malvern Mastersizer 3000 (Malvern Instruments, Worcestershire, UK) at the Geosciences Laboratory, Auburn University, Auburn, AL, USA after

a chemical dispersion with sodium hexametaphosphate (50 g L^{-1}) (Foucher et al. 2015b) (Appendix A Fig. A5). The specific surface area of the sediment particles was determined from the particle size analysis assuming particle sphericity (Collins et al., 2010; Lamba et al, 2015).

3.2.4 Statistical Discrimination and Sediment Source Ascription

Range test was conducted to evaluate the conservative behavior of fingerprinting properties during sediment erosion and transport processes within a watershed. This test determines whether the suspended sediment sample fingerprinting property concentrations fall within the range of source samples fingerprinting property concentrations (Wilkinson et al., 2013; Kraushaar et al., 2015; Franz et al., 2014; Gellis and Noe, 2013). All the non-conservative fingerprinting properties, which did not satisfy this criterion were not considered for further statistical analysis. Subsequently, to select the optimum number of fingerprinting properties that discriminated between the sources successfully, a two-step statistical procedure was used (Yu and Rhoads, 2018; Lamba et al, 2015; Collins et al., 1997). In step 1, a non-parametric Kruskal-Wallis H-test (α= 0.05) was used to select the fingerprinting properties which can discriminate between the source categories namely, construction sites and stream banks. All the fingerprinting properties that passed the Kruskal-Wallis H-test were subjected to a stepwise discriminant function analysis (DFA) to select the composite of fingerprinting properties which can provide maximum discrimination between the sources. This analysis is based on the stepwise selection algorithm of minimization of the Wilks' lambda (λ) to select the smallest set of fingerprinting properties for discriminating between suspended sediment sources. A λ close to 0 indicates a small within group variability as compared to variability between the source groups.

A multivariate mixing model was used to quantify the relative proportions from the source groups to suspended sediment. The mixing model involves solving a set of linear equations defined

by a conservative mass balance. The concentrations of fingerprinting properties within each source were multiplied by their unknown source apportionments and summed to be equal to the concentrations of the same equivalent fingerprinting properties from the suspended sediment samples (Palazón et al. 2016). The equations were solved by minimizing the sum of squares of the weighted relative errors (Collins et al. 2012):

$$\sum_{j=1}^{p}\left(\frac{C_{sj}-\sum_{i=1}^{m}C_{ij}P_i}{C_{sj}}\right)^2 W_i$$

where p is the number of fingerprinting properties in the composite fingerprint; m is the number of source groups; C_{sj} is the concentration of fingerprinting property (j) in the suspended sediment sample; C_{ij} is the mean concentration of fingerprinting property (j) in the source group; P_i is the relative contribution from source group (i) in the suspended sediment sample; and W_i is the tracer discriminatory weighting factor.

Two linear boundary conditions must be satisfied by the multivariate mixing model to ensure that the relative source contributions from each source group to suspended sediment must lie between 0 and 1; and the sum of the relative contributions from all the source groups is unity:

$$\sum_{i=1}^{m} P_i = 1$$

$$0 \leq P_i \leq 1$$

It should be noted that the relative contribution from construction sites and stream banks was determined at a subwatershed level as a function of sediment particle size. The fingerprinting property discriminatory weighting factor (W_i) was used to ensure that the fingerprinting property with the greatest discriminatory power exerts the greatest influence on the solutions of the mixing model (Collins et al., 2010).

3.2.5 Goodness-of-Fit and Uncertainty Analysis

The goodness-of-fit of the optimized model was assessed using the mean relative error (RME) between the actual fingerprinting properties concentrations in the suspended sediment sample and those predicted by the mixing model (Franz et al., 2014). To assess the uncertainty in the extent to which the average fingerprinting properties concentration of each source category in the mixing model reflects the true value, a Monte-Carlo simulation approach was used. Details of goodness-of-fit and Monte-Carlo analysis are discussed in detail in chapter 2 section 2.2.6.

3.2.6 SWAT Modeling

To identify areas contributing disproportionately high amount of surface runoff to streams, we used the Soil and Water Assessment Tool (SWAT) model. The SWAT model is a physically based, deterministic, continuous, watershed-scale simulation model developed by the United States Department of Agriculture-Agricultural Research Service (USDA-ARS) (Douglas-Mankin et al., 2010; Neitsch et al., 2005). In SWAT model, a watershed is divided into subwatersheds and each subwatershed is further divided into hydrological response units (HRU). The HRUs are the portions of subwatersheds that possess unique landuse/management/soil attributes.

Surface runoff in each HRU was estimated using modified Soil Conservation Service Curve Number (SCS-CN) method (Mishra and Singh, 2003; Neitsch et al., 2005). For this study, the temperature-based Hargreaves method (Hargreaves and Samani, 1985) was used to estimate potential evapotranspiration (PET). A 1/3 arc second (10-m) resolution digital elevation model (DEM) was used to delineate the watershed and subwatershed boundaries. The Cropland Data Layer (CDL) for the year 2011 (USDA- CDL, 2011) developed by the National Agricultural Statistics Service was used to derive land cover parameters (https://www.nass.usda.gov/Research_and_Science/Cropland/SARS1a.php). The soil data used in

this study was based on the geospatial soil survey SSURGO database developed by the National Resources Conservation Service (USDA-NRCS). Weather data (daily precipitation and temperature (maximum and minimum)) was obtained from the National Oceanic and Atmospheric Administration (NOAA) weather station located near the watershed and from the Parameter-elevation Relationships on Independent Slopes Model (PRISM) climate dataset (http://prism.oregonstate.edu/). SWAT built-in weather generator was used to simulate solar radiation, wind speed, and relative humidity.

The model was calibrated separately for surface runoff and baseflow for four years (January 2011 to December 2014) and validated for three years (January 2015 to December 2017) at a monthly time-step. Using web-based hydrograph separation program (WHAT), streamflow was separated into surface runoff and baseflow components (Lim et al., 2005). The study watershed is a part of the larger Chewacla Creek watershed. The SWAT model was setup for the Chewacla Creek watershed and calibrated and validated using observed stream flow measured by the United States Geological Survey (USGS) (gage # 02418760) at the outlet of this watershed. A literature review was done to identify sensitive parameters. Curve number (CN2), available soil water capacity (Soil_AWC), threshold depth of water (GWQMN), and groundwater revap coefficient (GWREVAP) parameters were used for model calibration (Table 3.2). Due to unavailability of observed sediment data at the watershed outlet, the model was not calibrated and validated for sediment.

Quantitative measurements (Nash-Sutcliffe model efficiency (NSE) coefficient (equation 1), the regression correlation coefficient (R^2) (equation 2), and percent bias (PBIAS) (equation 3)) along with graphical evaluations were used to assess whether the surface runoff and baseflow

simulated by the SWAT model accurately represents the measured surface runoff and baseflow (Moriasi et al., 2007):

$$\text{NSE} = 1 - \frac{\sum_{i=1}^{n}(O_i - P_i)^2}{\sum_{i=1}^{n}(O_i - O)^2} \quad (1)$$

$$\text{PBIAS} = \frac{\sum_{i=1}^{n}(O_i - P_i) * 100}{\sum_{i=1}^{n} Oi} \quad (2)$$

$$R^2 = \frac{\sum_{i=1}^{n}(O_i - O)(P_i - P)}{\sqrt{\sum_{i=1}^{n}(O_i - O)^2}\sqrt{\sum_{i=1}^{n}(P_i - P)^2}} \quad (3)$$

where O_i is the i^{th} observation for the constituent being evaluated; P_i is the i^{th} simulated value for the constituent being evaluated; O is the mean of observed data for the constituent being evaluated; P is the mean of simulated data for the constituent being evaluated and n is the total number of observations.

3.3 Results And Discussions

3.3.1 Optimum Fingerprinting Properties

The fingerprinting properties that passed the range test and Kruskal Wallis H-test (p=0.05) for both the particle sizes, namely 63-212 μm and <63 μm at each site are included in Tables 3.3 and 3.4, respectively. Out of 59 fingerprinting properties, majority of the fingerprinting properties passed the range test, indicating that most of the fingerprinting properties possessed conservative behavior. Based on the results of the Kruskal-Wallis H-test, the number of fingerprinting properties that successfully discriminated between the construction sites and stream banks at all sites for the two particle sizes ranged from 9 to 21 (Table 3.3 and 3.4).

The results of the stepwise DFA on the fingerprinting properties that passed the Kruskal-Wallis H-test for 63-212 μm and <63 μm particle size fractions at each site are shown in Tables 3.5 and 3.6, respectively. The optimum number of fingerprinting properties that provided the greatest discrimination between construction sites and stream banks for the two particle sizes ranged from

3 to 6 among all sites and classified >90% of the sources correctly at each site. The cumulative percentage of source samples classified correctly varied from 96.7 to 100% for 63-212 μm, whereas for < 63 μm, optimum number of fingerprinting properties classified 100% of the source samples correctly at each site. For all the monitoring sites, good source discrimination was achieved based on the values of Wilks' lambda, which ranged from 0.022 to 0.153 and 0.025 to 0.107 for 63-212 μm and <63 μm, respectively.

The concentration of geochemical elements in soils depends on parent material, climate, hydrology, amount and types of vegetation, weathering processes and anthropogenic activities. (Bini et al., 2011; Koiter et al., 2013). Out of all the fingerprinting properties selected as a part of the composite fingerprint for all sites, the fingerprinting properties (e.g., Ni, V, and Pb) that had association with anthropogenic sources were found to have greater concentrations in soils collected from construction sites compared to concentration in samples collected from stream banks. Heavy metals have been observed to have less concentration in sub-soils than the surface soils (Bini et al., 2011). Higher concentration of Ni (considered as a heavy metal of environmental concern in urban areas) in soil collected from construction sites reflected the effect of anthropogenic activities on deposition of Ni in the surface soils (Iyaka, 2011; Cempel and Nikel, 2006). Metal V has been extensively used for making steel alloys for tools and construction purposes (Hooda, 2010). Metal Pb, another toxic heavy metal is widely used in building construction and is known to be source of contaminant in soil as a result of man's action (Cheng and Hu, 2010). Therefore, the concentrations of V and Pb were higher in soils collected from construction sites. The concentration of rare earth elements (e.g., Pr, Eu) was greater in stream banks compared to construction sites. Generally, the concentration of rare earth elements is higher in sub-soils and parent material as compared to surface soils (Tyler, 2004). Because stream banks are composed of

less weathered sub-surface material, the concertation of rare earth elements was greater in stream banks than construction sites (Smith and Blake, 2014; Lamba et al., 2015).

3.3.2 Sediment Source Ascription

The relative source contributions of stream banks and construction sites to suspended sediment (for both particle sizes) at each site are shown in Fig 3.2 (a-c) - 3.3 (a-c) At site 1, generally construction sites were the dominant contributors to suspended sediment, with the relative source contributions ranging from 51 % to 71 % for particle size 63-212 μm (Fig. 3.2.a). For <63 μm, the relative source contributions from construction sites ranged from 28 % to 100%, (Fig. 3.3.a). This subwatershed has experienced an increase in urban land cover from 63 % to 81 % and decrease of forested land cover from 29 % to 15% from 2008 to 2017 based on Cropland Data Layer (CDL 2008 and 2017) (https://www.nass.usda.gov/Research_and_Science/Cropland/SARS1a.php). Urbanization of a watershed results in increase of storm water runoff, which likely increased erosion from the construction sites in this subwatershed. Additionally, increased urbanization is accompanied with increased discharge and stream power which severely destabilizes the streams (Bledsoe and Watson 2001), which could have induced stream bank erosion in this subwatershed.

At site 2, both stream banks and construction sites were the dominant sources of suspended sediment for both the particle sizes. For 63-212 μm, the contribution from stream banks and construction sites ranged from 29 % to 85 % and from 15 % to 71 %, respectively (Fig. 3.2.b). The relative contributions from stream banks and construction sites ranged from 45 % to 100% and from 0 % to 55 %, respectively for <63 μm (Fig. 3.3.b). The land-use under developed category in this subwatershed increased from 42 % to 61% with the decrease of forested cover from 42 % to 24% from 2008 to 2017 based on the Cropland Data Layer (CDL 2008 and 2017) (https://www.nass.usda.gov/Research_and_Science/Cropland/SARS1a.php). It has been found

that the increase in imperviousness leads to increase in specific stream power and hence the risk of stream instability (Bledsoe and Watson, 2001) which could have led to increased contribution from the stream banks to suspended sediment. Furthermore, storm water runoff generated in this subwatershed (developed land use- 61 %) likely caused erosion from construction sites. The dataset at this site was limited compared to other sites because time-integrated suspended sediment samplers were lost for most of the sampling period at this site.

Compared to site 1 and site 2, contributions from construction sites to suspended sediment at site 3 were greater. The contributions from stream banks and construction sites ranged from 0 % to 34 % and from 66 % to 100 %, respectively for 63-212 μm (Fig. 3.2.c). For <63 μm, the relative contribution to suspended sediment from stream banks and constructions sites ranged from 0 % to 46 % and 54 to 100 %, respectively (Fig. 3.3.c). Land disturbance as a result of construction activities exposes large areas of bare soil to erosion by water, increasing soil erosion rates to 2–40,000 times preconstruction and agricultural rates (Harbor, 1999). Although a small portion (3%) of the watershed (Fig. 3.4.) was occupied by the active construction sites in 2017. However, rates of soil erosion from construction sites (which can approach up to 500 T ha^{-1} yr^{-1}) are considerably higher than those from areas occupied by undisturbed vegetation (<1 T ha^{-1} yr^{-1}) (Mukundan et al., 2010), which likely resulted in greater contribution from construction sites to suspended sediment. Therefore, as mentioned earlier in the manuscript, increase in urbanization increases the surface runoff which leads to entrainment of sediment from construction sites (for which the erosion rates are too high) in the storm water runoff and results in increased delivery of sediment into the surface water bodies. The temporal variability in the suspended sediment sources during the sampling period was likely affected by the phase of construction activity from the commencement to completion of construction sites located within this watershed. A construction project begins with

the site work which involves land clearance and excavation of soils and ends with grading and landscaping (Harbor, 1999). Construction practices which are identified to contribute high sediment yields include: land clearance exposing the bare soil, stripping topsoil, piling the excavated soil near or on the streets, and tracking of mud in the streets by construction vehicles (Pitt et al., 2007). Additionally, the temporal variability in suspended sediment sources depends upon the 'lag time' between the erosion of sediment from construction site and the consequent delivery of sediment to the creek, which depends upon the phase of the construction activity and the temporary retention or storage of sediment within the watershed.

3.3.3 Comparison between Suspended and Stream Bed Sediment Sources

The results of this study show that the relative source contributions from different sources to suspended sediment and stream bed sediment might not be always similar. For example, a previous study conducted by authors in this watershed (Chapter 2) showed that the dominant sources of bed sediment (for both the particle sizes, 63-212 μm and <63 μm) at site 1 and 2 were stream banks. However, for suspended sediment, construction sites were the dominant sources of suspended sediment at site 1, whereas both stream banks and construction sites were the important sources of suspended sediment at site 2.

Suspended sediment had greater specific surface area or was finer in size (average specific surface area was 132.3±8.7 $m^2 kg^{-1}$ and 170.6±9.1 $m^2 kg^{-1}$ for particle size 63-212 μm and <63 μm, respectively) compared to stream bed sediment (average specific surface area was 60±4.2 $m^2 kg^{-1}$ and 120.6±5.9 $m^2 kg^{-1}$ for particle size 63-212 μm and <63 μm, respectively). The sediment from construction sites were finer (average specific surface area was 129.91±9.6 m^2 kg^{-1} and 291.26±24.5 m^2 kg^{-1} for the particle size 63-212 μm and <63μm, respectively) compared to sediment from stream banks (average specific surface area was 114.35±6.4 $m^2 kg^{-1}$ and 212.7±9.5

m^2 kg^{-1} for the particle size 63-212 μm and <63μm, respectively). Therefore, as indicated by the specific surface area values, construction sites consisted of finer particles compared to stream banks and therefore were the dominant sources of suspended sediment. Depending upon the hydraulic forces exerted during flow events, sediment eroded from stream banks can be present in the stream as individual particles or aggregates (e.g., due to the stream bank mass failure) (Lamba et al., 2015). Therefore, stream banks were the dominant sources of sediment deposited on the stream bed and construction sites were the dominant sources of suspended sediment.

To identify the dominant sources of sediment in a watershed, the stream bed sediment sampling has been used as an alternative to sample suspended sediment (Lamba et al., 2015). However, as indicated by the results of this study, it is important to recognize that the dominant sources of stream bed sediment and suspended sediment in a watershed might not necessarily be similar. Lamba et al. (2015) also reported that the dominant sources of suspended sediment and stream bed sediment were not same in a study conducted in an agricultural watershed located in Wisconsin, USA. Therefore, identification of sources of both the suspended and stream bed sediment is needed in order to target management practices effectively and efficiently. The results of this study have important implications for the design of effective sediment control strategies. For example, reducing stream bank erosion is unlikely to prove an effective means of significantly reducing suspended sediment loads in site 1 subwatershed, since construction sites were the dominant sources of suspended sediment in this subwatershed.

3.3.4 Goodness-of-Fit and Uncertainty Analysis

The RME values calculated to assess the goodness-of-fit of the mixing model indicated that mixing model provided satisfactory agreement between predicted and actual suspended sediment fingerprinting properties concentration. The RME values ranged from 4 % to 29 %, 8 %

to 21%, and 8 % to 31% at site 1, 2, and 3, respectively for both particle size fractions (Table 3.7). The majority of RME values were less than 25%, indicating that the mixing model satisfactorily predicted the concentration of fingerprinting property in suspended sediment (Lamba et al., 2015). The relative source contribution differences obtained from the average of Monte Carlo results and the corresponding values obtained from the mixing model using the mean source fingerprinting property concentration ranged from 0 % to 3 %, 0 % to 7%, and 0 % to 11% at site 1, 2, and 3, respectively for both particle size fractions. The Monte Carlo results show that the use of mean fingerprinting property concentrations of the source samples in the mixing model was not a significant source of uncertainty.

3.3.5 SWAT Model Calibration and Validation

The time series of observed vs simulated surface runoff, baseflow, and total stream flow show that SWAT model successfully captured changes in surface runoff, baseflow and stream flow on a monthly time-step (Fig. 3.5 (a-c). The statistical values calculated for calibration and validation time periods for surface runoff, baseflow, and total stream flow are presented in Table 3.8.

Very good model calibration and validation results were obtained, as indicated by the NSE and R^2 values for surface runoff, baseflow and stream flow. Based on the values of PBIAS for surface runoff, baseflow and stream flow, model performance rating was “satisfactory” for the calibration time period and “very good” for the validation time period (Moriasi et al., 2007). Overall, SWAT model satisfactorily simulated changes in monthly surface runoff, baseflow and total stream flow.

3.3.6 Prioritizing Subwatersheds for BMPs

Average annual values (2011-2017) of surface runoff (mm/ha/yr) estimated using SWAT model are shown in Fig. 3.6. The values of average annual surface runoff varied from 2.3 mm/ha/yr to 3750 mm/ha/yr. Generally, the subwatersheds (Fig. 3.6) dominated by urban areas generated high surface runoff. As stated earlier in the manuscript, SWAT model was not calibrated for sediment, since no observed data for sediment was available for this watershed. Therefore, sediment yield results available from SWAT model were not considered for this study. However, the relationship between surface runoff and the sediment yield has been well documented (Schmalz et al., 2015). With the increase in surface runoff, sediment yield from upland areas increases (Gholami et al., 2013). Since the uplands (construction sites) were the dominant sources of suspended sediment in this watershed, therefore BMPs should be targeted at construction sites in the subwatersheds generating disproportionately high amount of surface runoff. Overall, results of this study show that combining watershed level modeling and sediment fingerprinting technique can help in targeting BMPs effectively. The quantity of sediment discharged from construction sites can be minimized by using BMPs, such as, silt fences, detention basins, utilization of gravel bags around drainage inlets, vegetative filter strips, bioretention areas, and constructed wetlands. Riparian buffer systems should be properly managed as these systems are effective to reduce sediment delivery to streams.

3.4 CONCLUSIONS

The application of sediment fingerprinting in the Moore's Mill Creek watershed provided important information on the relative contributions from construction sites and stream banks to suspended sediment. The results of this study show that generally construction sites were the dominant sources of suspended sediment for both the particle sizes within this watershed. The rapid urbanization in this watershed has increased the amount of surface runoff generated within

this watershed which has resulted in the greater entrainment of sediment from construction sites in the runoff and hence the sediment delivery into the stream. To minimize the sediment delivery to streams in this watershed, BMPs (e.g., silt fences, detention basins, vegetative filter strips) should be targeted in subwatersheds that contain construction sites and generate disproportionately high amount of surface runoff. The conjunctive use of SWAT model and the sediment fingerprinting procedure provided two different but compatible approaches to understand the sediment erosion processes and developing an approach to target BMPs effectively in this urbanized watershed.

Table 3.1. Suspended sediment sample collection dates throughout the sampling period

Sites	Suspended Sediment Sample Collection Dates
1	December 2, February 5, March 10, April 14, May 18, June 28, July 28, September 22
2*	December 2, April 14, May 18
3	December 2, February 5, March 10, April 14, May 18, June 28, July 28, September 22

*Samplers were lost for most of the sampling period

Table 3.2. Parameters used for model calibration

SWAT Calibration Parameter	Default Value	Final Calibrated Value
Soil _AWC (mm/mm)	Varies	15 % increase
GWREVAP (dimensionless)	0.02	0.2
CN2 (dimensionless)	Varies	10 % decrease
GWQMN (mm)	1000	3907

Table 3.3. Fingerprinting properties that satisfied the range test and the Kruskal-Wallis H-test (p=0.05) criteria at each site for particle size 63-212 μm

Range test															
Sites	**Fingerprinting properties**														
1	B	Na	K	Ti	V	Cr	Ga	Rb	Y	Zr	Nb	Sr	Cs	Ba	Sm
	Dy	Lu	Hf	Ta	W	Ir	Pt	Tl	Pb	Bi	U				
2	Li	Be	B	Na	Mg	Al	P	K	Ca	Sc	Ti	V	Fe	Co	Cu
	Zn	Ga	Rb	Y	Zr	Nb	Ag	Cs	Ba	Sm	Eu	Gd	Dy	Ho	Yb
	Lu	Hf	Ta	Tl	Pb	Bi	Th	U							
3	Li	Be	B	Na	K	Al	Sc	Ti	V	Fe	Co	Ni	Ga	Se	Rb
	Zr	Nb	Ag	Cs	Ba	Eu	Lu	Hf	Ta	W	Ir	Pt	Hg	Tl	Pb
	Bi	U													
Kruskal-Wallis H-test															
Sites	**Fingerprinting properties**														
Site 1	V	Cr	Ga	Zr	Nb	Ta	W	Pb	Bi						
Site 2	Be	B	Al	Sc	V	Fe	Ga	Zr	Nb	Ag	Hf	Ta	Pb	Bi	Th
Site 3	Li	Be	B	Al	Sc	V	Fe	Ga	Ni	Se	Zr	Nb	Hf	Ag	Ta
	W	Pb	Bi	U											

Table 3.4. Fingerprinting properties that satisfied the range test and the Kruskal-Wallis H-test (p=0.05) criteria at each site for particle size <63 μm

Range test

Sites	Fingerprinting properties														
1	Li	Be	B	Na	P	K	Sc	Ti	V	Cr	Fe	Co	Ni	Ga	As
	Rb	Zr	Nb	Mo	Cd	Cs	Ba	Pr	Eu	Gd	Ta	W	Ir	Pt	Hg
	Tl	Pb	Bi	U											
2	Li	Be	Mg	Al	K	Sc	V	Cr	Fe	Co	Ni	Zn	Ga	As	Zr
	Nb	Cd	Cs	Ba	Nd	Lu	Hf	Ta	W	Ir	Pt	Tl	Pb	Bi	U
3	Li	Be	B	Na	Al	K	Sc	V	Cr	Fe	Co	Ni	Ga	As	Rb
	Zr	Nb	Cd	Sb	Cs	Ba	Pr	Eu	Hf	Ta	W	Ir	Pt	Hg	Tl
	Pb	Bi	U												

Kruskal-Wallis H-test

Sites	Fingerprinting properties														
1	Be	Sc	V	Co	Ga	As	Rb	Nb	Cd	Ba	Pr	Eu	Gd	Ta	Ir
	Pt	Pb	Bi												
2	Be	V	Cr	Fe	Ni	Ga	Zr	Cd	Hf	Ir	Pt	Bi	U		
3	Be	B	V	Cr	Fe	Co	Ni	Ga	Rb	Zr	Cd	Ba	Pr	Eu	Hf
	Ta	Ir	Pt	Pb	Bi	U									

Table 3.5. Results of stepwise DFA at each site for particle size 63-212 μm

Site	Fingerprinting property	Wilks' lambda	Percentage source samples classified correctly	Cumulative percentage source samples classified correctly	Tracer discriminatory weighting
1	Bi	0.151	100	100	1.18
	Ga	0.101	84.6	100	1.00
	Pb	0.074	84.6	100	1.00
	Ta	0.040	84.6	100	1.00
2	V	0.055	100	100	1.10
	Pb	0.037	100	100	1.10
	Bi	0.022	90	100	1.00
3	V	0.286	96.7	96.7	1.38
	Ag	0.259	86.67	93.3	1.24
	Pb	0.229	80.00	93.3	1.14
	Se	0.181	70.00	96.7	1.00
	Nb	0.153	80.00	96.7	1.14

Table 3.6. Results of stepwise DFA at each site for particle size <63 μm

Site	Fingerprinting property	Wilks' lambda	Percentage source samples classified correctly	Cumulative percentage source samples classified correctly	Tracer discriminatory weighting
1	Bi	0.049	100	100	1.3
	Ir	0.032	84.6	100	1.1
	Ba	0.025	76.9	100	1.0
2	Ga	0.198	100	100	1.25
	Ni	0.152	80	100	1
	Bi	0.107	80	100	1
3	Rb	0.152	76.67	76.67	1.04
	U	0.122	73.33	86.7	1.00
	Zr	0.091	86.67	100	1.18
	Pr	0.070	80	100	1.09
	Eu	0.064	76.67	100	1.04
	Ni	0.038	80	100	1.09

Table 3.7. Relative mean error (%) between actual and optimized mixing model predicted suspended sediment fingerprinting property concentration

Relative Mean Error (%)			Relative Mean Error (%)			Relative Mean Error (%)		
Site 1			Site 2			Site 3		
Month	63-212 μm	<63 μm	Month	63-212 μm	<63μm	Month	63-212 μm	<63μm
20 October-2 Dec	20	6	20 October-2 Dec	21	17	20 October-2 Dec	24	25
2 Dec-5 Feb	9	10	2 Dec-5 Feb	-*	-*	2 Dec-5 Feb	22	29
5 Feb- 10 March	4	14	5 Feb- 10 March	-*	-*	5 Feb- 10 March	25	25
10 March-14 April	22	12	10 March-14 April	11	14	10 March-14 April	31	15
14 April- 18 May	18	11	14 April- 18 May	15	8	14 April- 18 May	30	14
18 May-28 June	17	9	18 May-28 June	-*	-*	18 May-28 June	10	8
28 June-28 July	10	29	28 June-28 July	-*	-*	28 June-28 July	27	13
28 July- 22 Sept	12	22	28 July- 22 Sept	-*	-*	28 July- 22 Sept	18	25

*Data not available because suspended sediment samplers were lost.

Table 3.8. Calibration and Validation metrics for monthly surface runoff (m^3/sec), base flow (m^3/sec) and total flow (m^3/sec)

Calibration (January 2011- December2014)				Validation (January 2015- December 2017)		
Variable	R^2	NSE	PBIAS	R^2	NSE	PBIAS
Surface Runoff (m^3/sec)	0.84	0.77	18.5	0.83	0.82	-6.5
Baseflow (m^3/sec)	0.85	0.75	18.8	0.90	0.88	-9.3
Total Stream Flow (m^3/sec)	0.86	0.77	18.6	0.84	0.83	-7.5

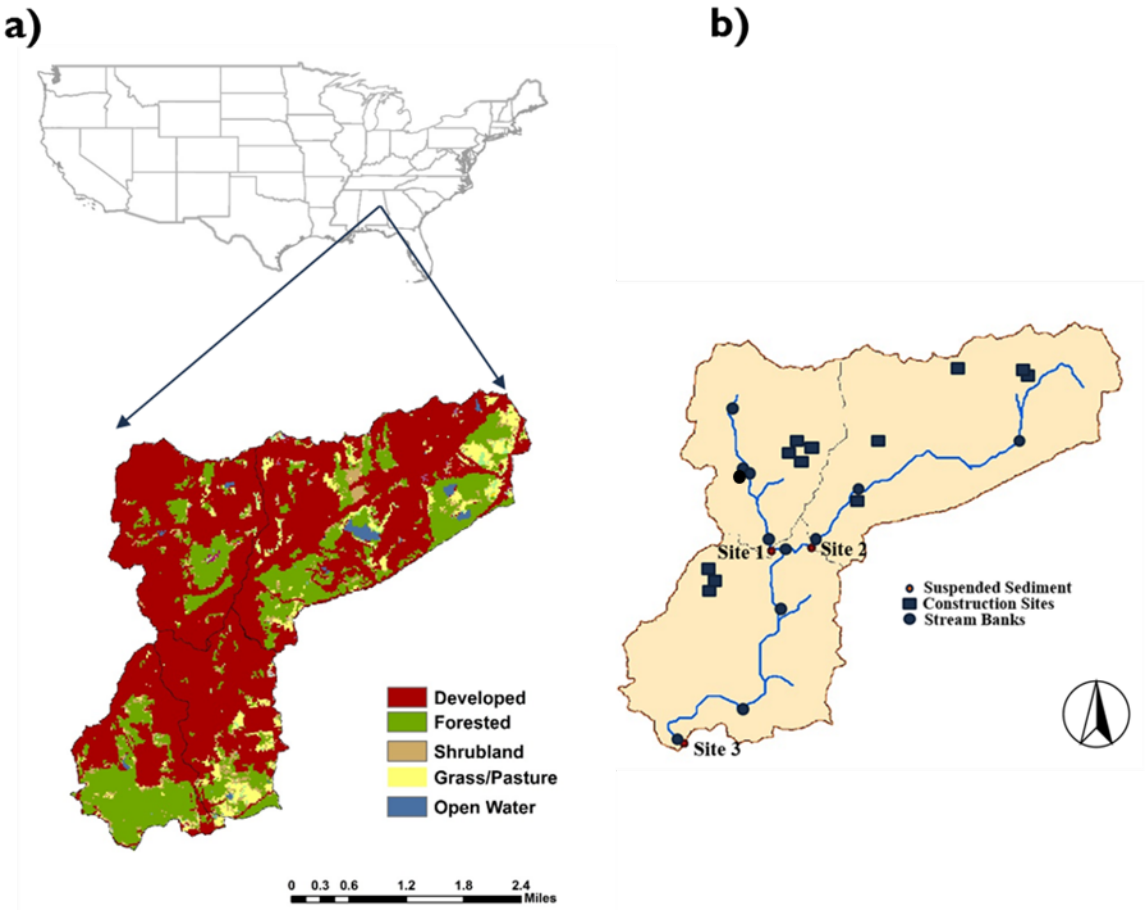

Fig. 3.1. a) Land use distribution in the Moore's Mill Creek watershed and b) Location of suspended sediment, stream banks and construction sampling sites

a)

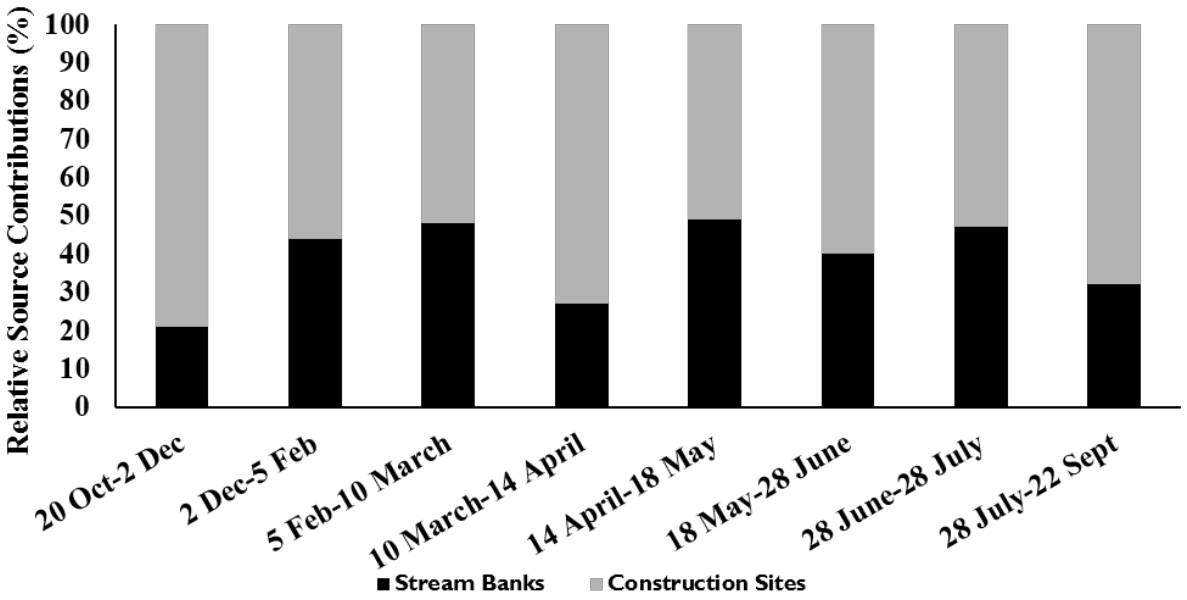
Relative Source Contributions (%)
100
90
80
70
60
50
40
30
20
10
0
20 Oct-2 Dec
2 Dec-5 Feb
5 Feb-10 March
10 March-14 April
14 April-18 May
18 May-28 June
28 June-28 July
28 July-22 Sept
Stream Banks
Construction Sites

b)

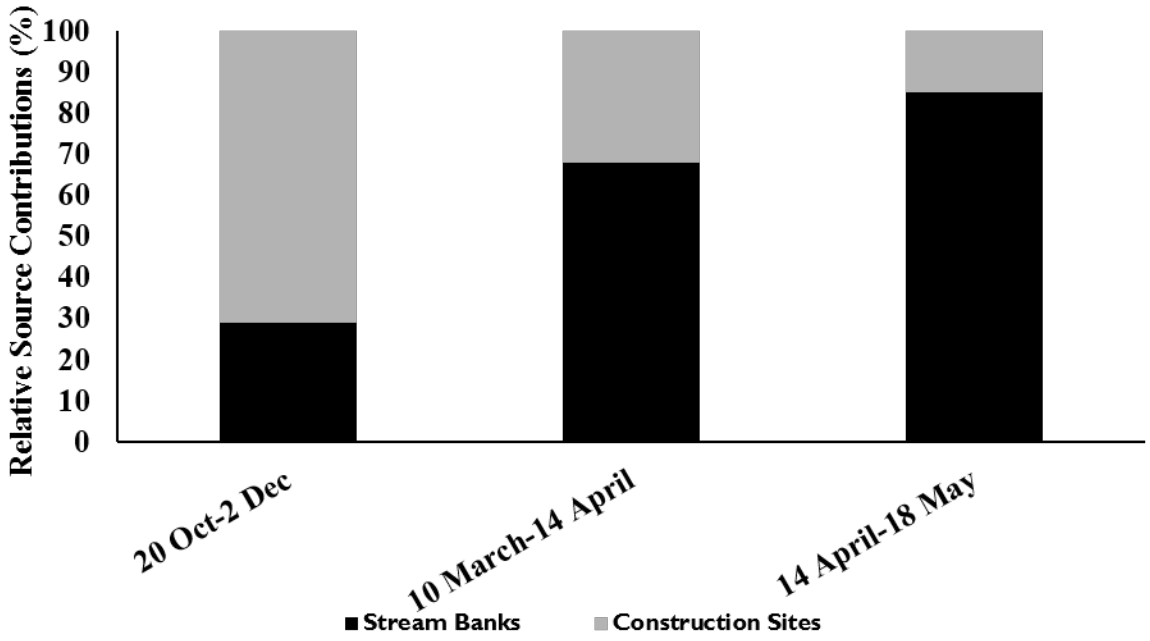
Relative Source Contributions (%)
100
90
80
70
60
50
40
30
20
10
0
20 Oct-2 Dec
10 March-14 April
14 April-18 May
Stream Banks
Construction Sites

c)

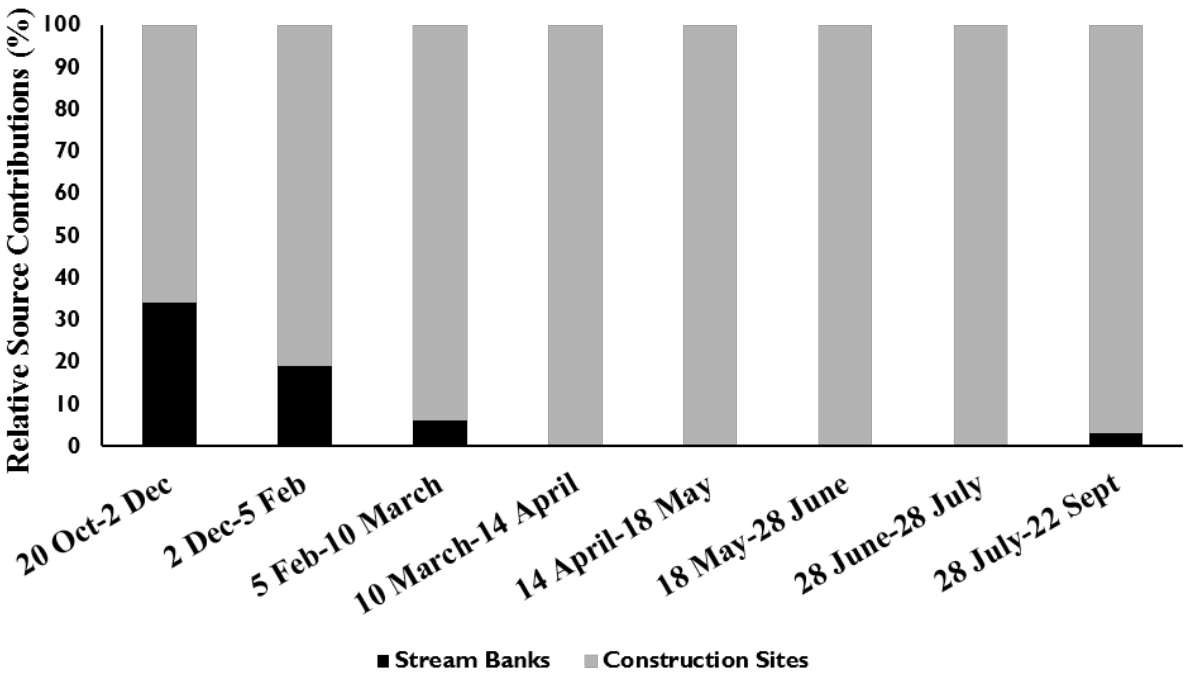

Fig. 3.2. Relative source contribution (%) to suspended sediment (for particle size 63-212 μm) from stream banks and construction sites at: (a) site 1, (b) site 2, and (c) site 3

a)

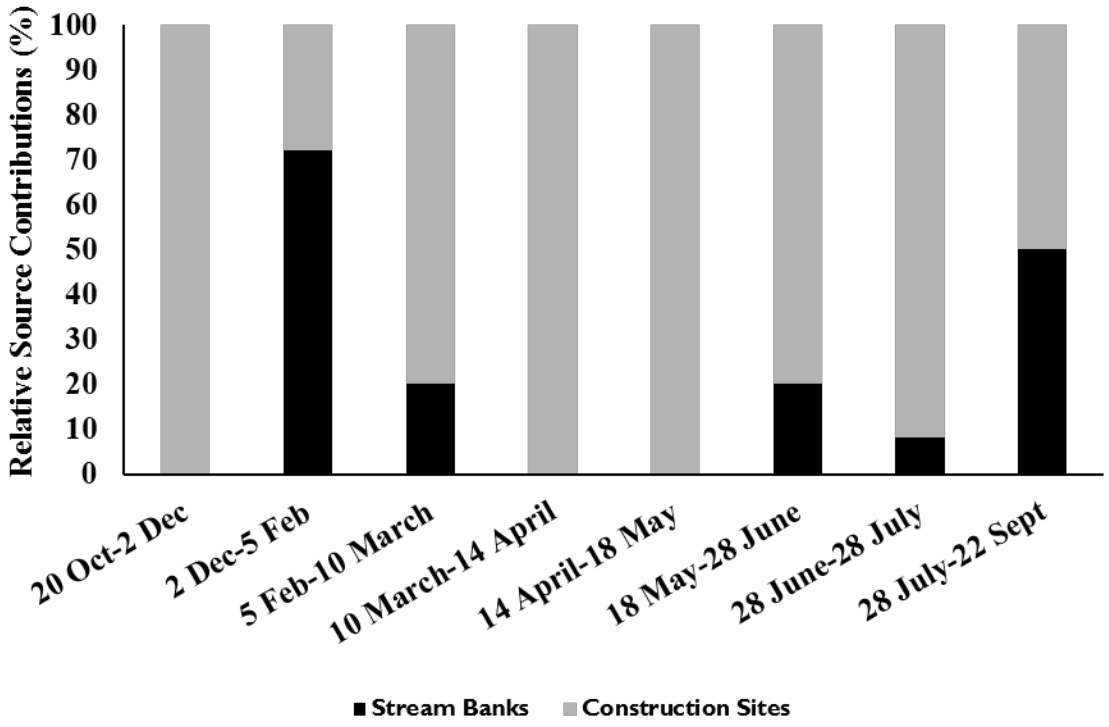
Relative Source Contributions (%)
100
90
80
70
60
50
40
30
20
10
0
20 Oct-2 Dec
2 Dec-5 Feb
5 Feb-10 March
10 March-14 April
14 April-18 May
18 May-28 June
28 June-28 July
28 July-22 Sept
Stream Banks
Construction Sites

b)

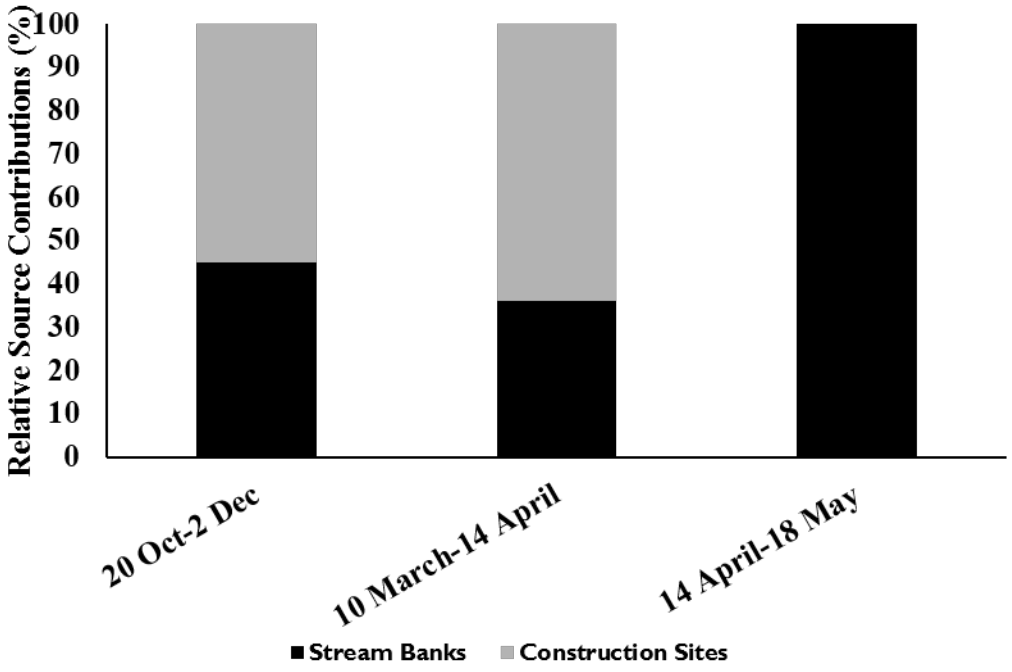
Relative Source Contributions (%)
100
90
80
70
60
50
40
30
20
10
0
20 Oct-2 Dec
10 March-14 April
14 April-18 May
Stream Banks
Construction Sites

c)

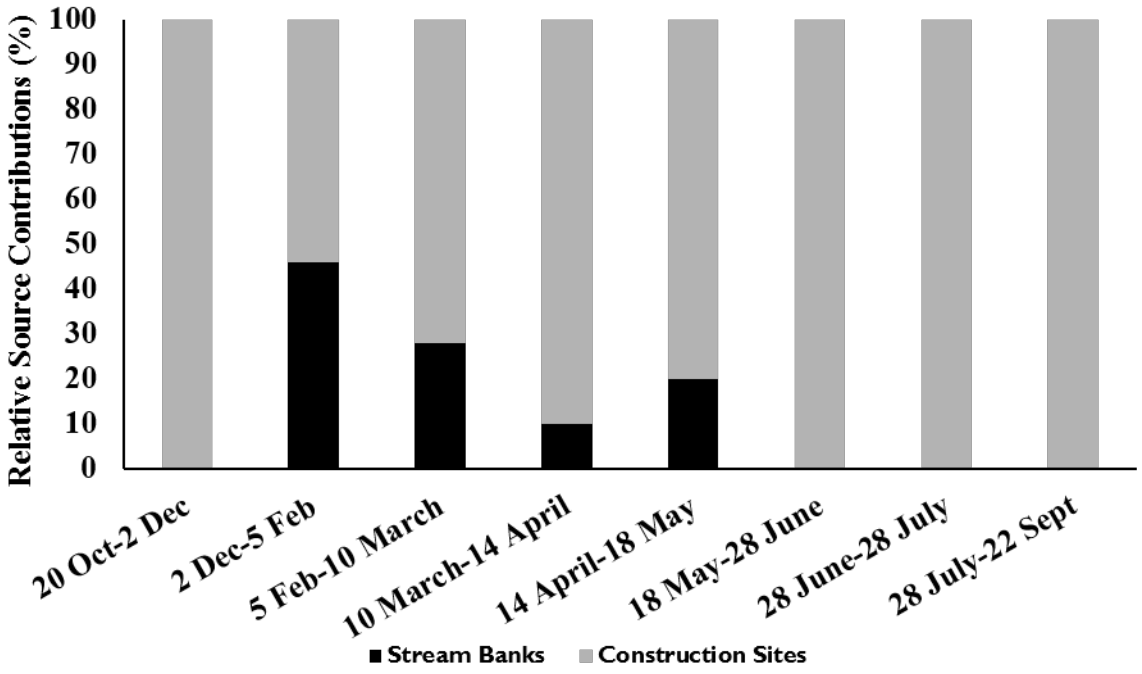

Fig. 3.3. Relative source contribution (%) to suspended sediment (for particle size <63 μm) from stream banks and construction sites at: (a) site 1, (b) site 2, and (c) site 3

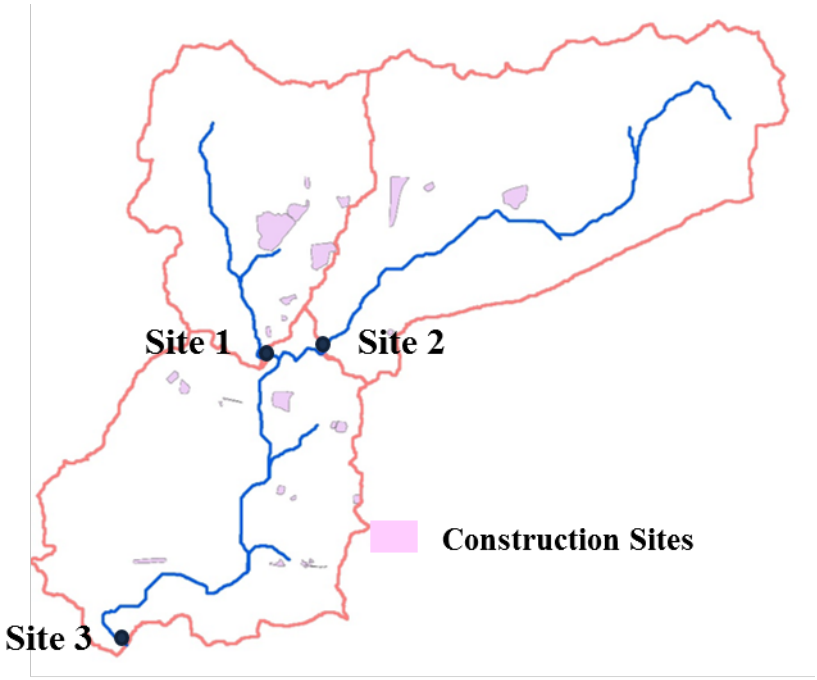

Fig. 3.4. Active construction sites in the watershed in the year 2017

a)

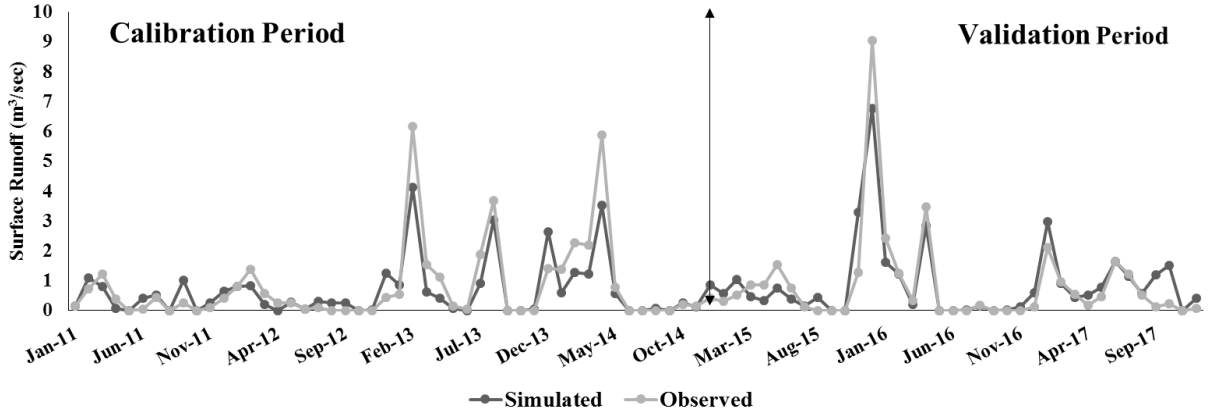
Calibration Period
Validation Period
Surface Runoff (m³/sec)
10
9
8
7
6
5
4
3
2
1
0
Jan-11
Jun-11
Nov-11
Apr-12
Sep-12
Feb-13
Jul-13
Dec-13
May-14
Oct-14
Mar-15
Aug-15
Jan-16
Jun-16
Nov-16
Apr-17
Sep-17
Simulated
Observed

b)

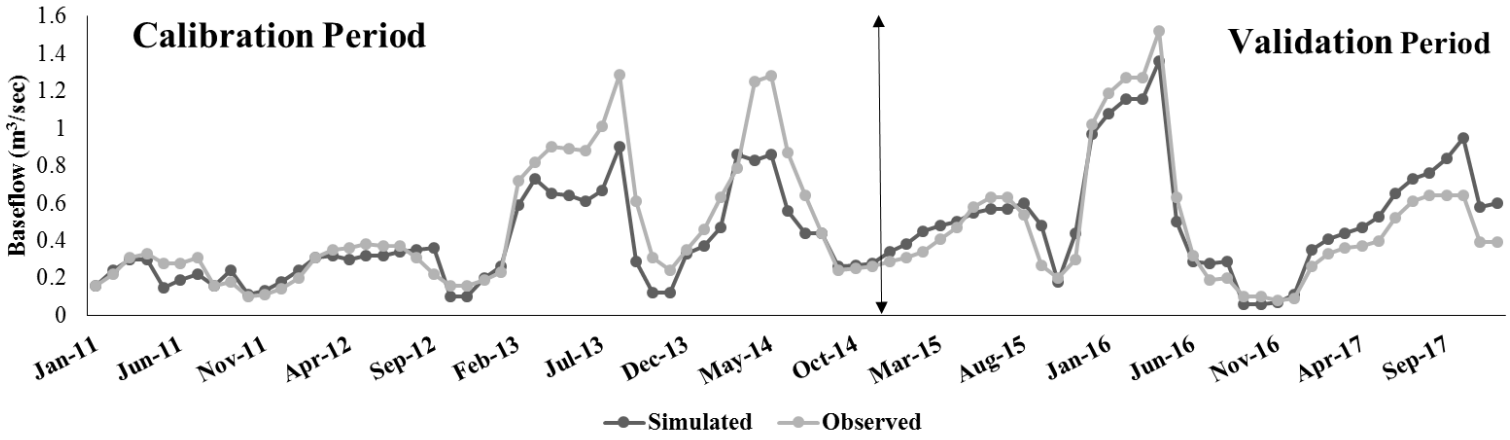
Calibration Period
Validation Period
Baseflow (m3/sec)
1.6
1.4
1.2
1
0.8
0.6
0.4
0.2
0
Jan-11
Jun-11
Nov-11
Apr-12
Sep-12
Feb-13
Jul-13
Dec-13
May-14
Oct-14
Mar-15
Aug-15
Jan-16
Jun-16
Nov-16
Apr-17
Sep-17
Simulated
Observed

c)

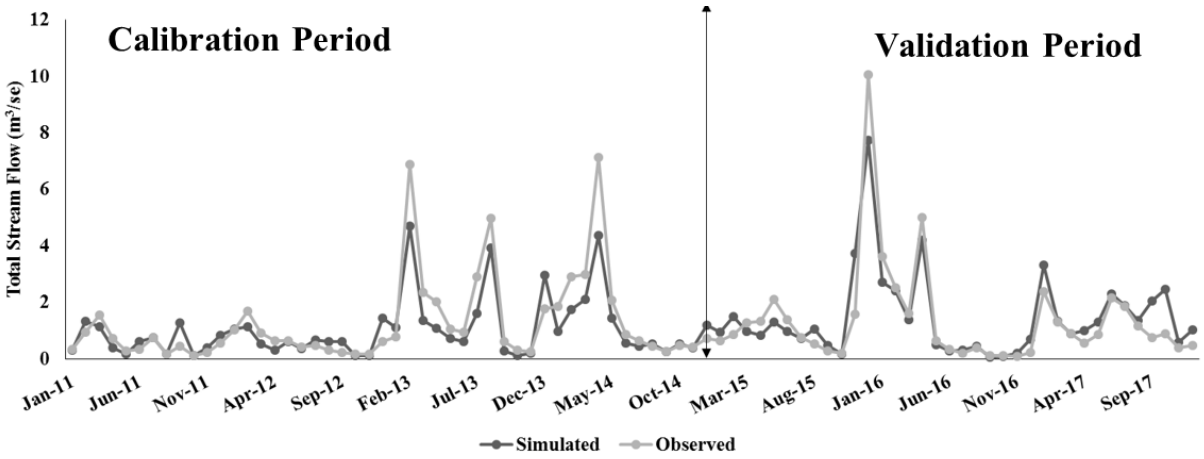

Fig. 3.5. Observed and SWAT-simulated average monthly: (a) surface runoff (m^3/sec), (b) baseflows (m^3/sec), and (c) total flow (m^3/sec) rates for the calibration (January 2011–December2014) and validation periods (January 2015- December 2017*)*

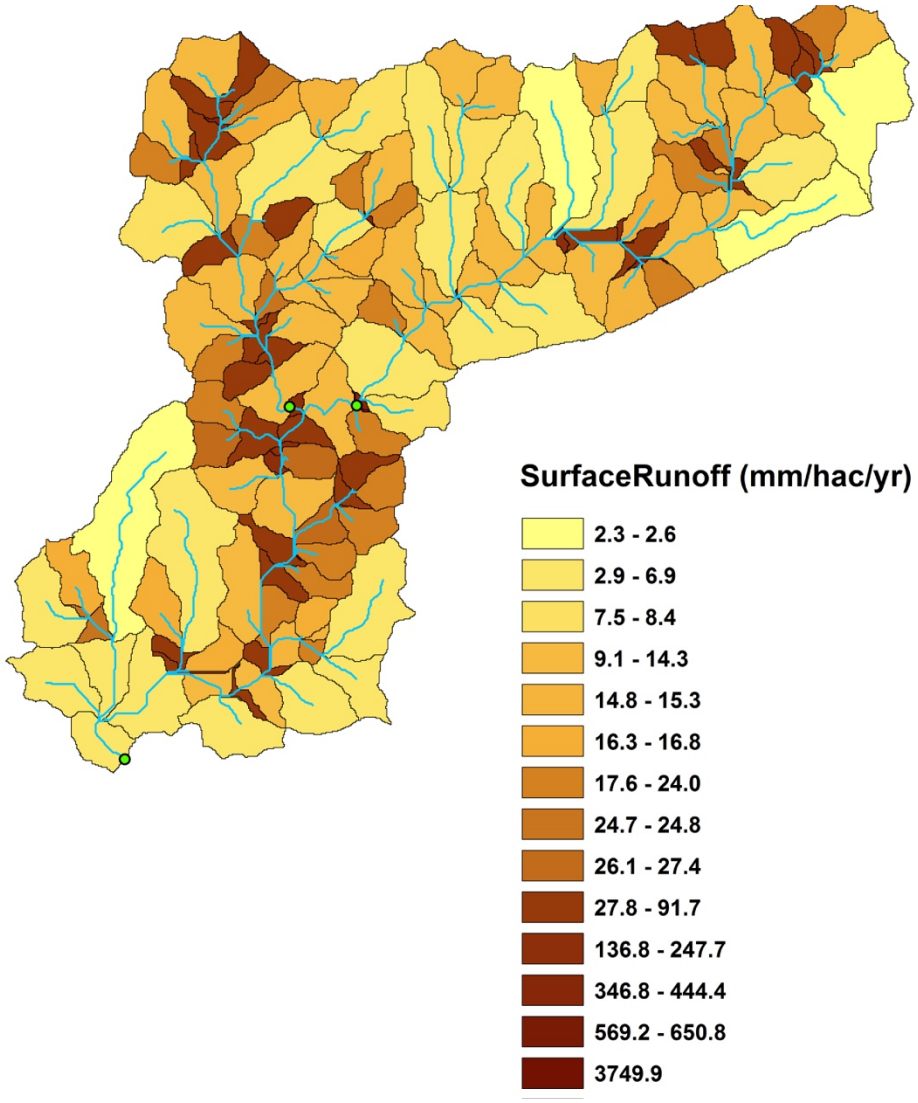

Fig. 3.6. Average annual surface runoff (mm/ha/yr) generated in each subwatershed

REFERENCES

Alabama Department of Environmental Management 303 (d) list, 2016 ADEM 303 (d) (http://www.adem.state.al.us/programs/water/wquality/2016AL303dList.pdf (accessed 17 June, 2017).

Barthod, Louise R. M., Kui Liu, David A. Lobb, et al. (2015). Selecting Color-Based Tracers and Classifying Sediment Sources in the Assessment of Sediment Dynamics Using Sediment Source Fingerprinting. Journal of Environmental Quality 44(5): 1605–1616.

Bini, Claudio, Giacomo Sartori, Mohammad Wahsha, and Silvia Fontana. (2011). Background Levels of Trace Elements and Soil Geochemistry at Regional Level in NE Italy. Journal of Geochemical Exploration 109(1). Pedogeochemical Mapping of Potentially Toxic Elements: 125–133.

Bledsoe, Brian P., and Chester C. Watson. (2001). Effects of Urbanization on Channel Instability1. JAWRA Journal of the American Water Resources Association 37(2): 255–270.

Cempel, M, and G Nikel. (2006). Nickel: A Review of Its Sources and Environmental Toxicology: 8.

Chanasyk, D.S, E Mapfumo, and W Willms. (2003). Quantification and Simulation of Surface Runoff from Fescue Grassland Watersheds. Agricultural Water Management 59(2): 137–153.

Cheng, Hefa, and Yuanan Hu. (2010). Lead (Pb) Isotopic Fingerprinting and Its Applications in Lead Pollution Studies in China: A Review. Environmental Pollution 158(5): 1134–1146.

Collins, A. L., S. Pulley, I. D. L. Foster, et al. (2017). Sediment Source Fingerprinting as an Aid to Catchment Management: A Review of the Current State of Knowledge and a Methodological Decision-Tree for End-Users. Journal of Environmental Management 194(Supplement C): 86–108.

Collins, A. L, and D. E Walling. (2002). Selecting Fingerprint Properties for Discriminating Potential Suspended Sediment Sources in River Basins. Journal of Hydrology 261(1–4): 218–244.

Collins, A. L., D. E. Walling, and G. J. L. Leeks. (1997). Source Type Ascription for Fluvial Suspended Sediment Based on a Quantitative Composite Fingerprinting Technique. CATENA 29(1): 1–27.

Collins, A. L., D. E. Walling, L. Webb, and P. King. (2010). Apportioning Catchment Scale Sediment Sources Using a Modified Composite Fingerprinting Technique Incorporating Property Weightings and Prior Information. Geoderma 155(3–4): 249–261.

Collins, A. L., Y. Zhang, D. McChesney, et al. (2012). Sediment Source Tracing in a Lowland Agricultural Catchment in Southern England Using a Modified Procedure Combining Statistical Analysis and Numerical Modelling. Science of The Total Environment 414(Supplement C).

City of Auburn (2011). Natural Systems. https://www.auburnalabama.org/CompPlan2030/4.0%20Natural%20Systems.pdf. Accessed June 17, 2017.

Davis, C M, and J F Fox. (2009). Sediment Fingerprinting: Review of the Method and Future Improvements for Allocating Nonpoint Source Pollution. Journal of Environmental Engineering 135(7): 490–504.

Deasy, C., R. E. Brazier, A. L. Heathwaite, and R. Hodgkinson. (2009). Pathways of Runoff and Sediment Transfer in Small Agricultural Catchments. Hydrological Processes 23(9): 1349–1358.

Douglas-Mankin, K. R., Srinivasan, R., & Arnold, J. G. (2010). Soil and Water Assessment Tool (SWAT) model: Current developments and applications. Transactions of the ASABE, 53(5), 1423–1431.

Easton, Zachary M., Daniel R. Fuka, M. Todd Walter, et al. (2008). Re-Conceptualizing the Soil and Water Assessment Tool (SWAT) Model to Predict Runoff from Variable Source Areas. Journal of Hydrology 348(3–4): 279–291.

Fang, Xing, Wesley C. Zech, and Christopher P. Logan. (2015) Stormwater Field Evaluation and Its Challenges of a Sediment Basin with Skimmer and Baffles at a Highway Construction Site. Water 7(7): 3407–3430.

Foucher, Anthony, Patrick J. Laceby, Sébastien Salvador-Blanes, et al. (2015). Quantifying the Dominant Sources of Sediment in a Drained Lowland Agricultural Catchment: The Application of a Thorium-Based Particle Size Correction in Sediment Fingerprinting. Geomorphology 250: 271–281.

Fox, James F., and Athanasios N. Papanicolaou. (2007). The Use of Carbon and Nitrogen Isotopes to Study Watershed Erosion Processes1. JAWRA Journal of the American Water Resources Association 43(4): 1047–1064.

Franz, C., F. Makeschin, H. Weiß, and C. Lorz. (2014). Sediments in Urban River Basins: Identification of Sediment Sources within the Lago Paranoá Catchment, Brasilia DF, Brazil - Using the Fingerprint Approach. The Science of the Total Environment 466–467: 513–523.

Fu, Baihua, John B Field, and Lachlan T Newham (2006). Tracing The Source Of Sediment In Australian Coastal Catchments: 6.

Gellis, Allen C., and Gregory B. Noe. (2013). Sediment Source Analysis in the Linganore Creek Watershed, Maryland, USA, Using the Sediment Fingerprinting Approach: 2008 to 2010. Journal of Soils and Sediments 13(10): 1735–1753.

George H. Hargreaves, and Zohrab A. Samani. (1985). Reference Crop Evapotranspiration from Temperature. Applied Engineering in Agriculture 1(2): 96–99.

Gholami, Leila, Seyed Hamidreza Sadeghi, and Mehdi Homaee. (2013). Straw Mulching Effect on Splash Erosion, Runoff, and Sediment Yield from Eroded Plots. Soil Science Society of America Journal 77: 268–278.

Harbor, Jon. (1999).Engineering Geomorphology at the Cutting Edge of Land Disturbance: Erosion and Sediment Control on Construction Sites. Geomorphology 31(1): 247–263.

Hooda, Peter. (2010). Trace Elements in Soils. John Wiley & Sons.

Huisman, Natalie L. H., K. G. Karthikeyan, Jasmeet Lamba, Anita M. Thompson, and Graham Peaslee. (2013). Quantification of Seasonal Sediment and Phosphorus Transport Dynamics in an Agricultural Watershed Using Radiometric Fingerprinting Techniques. Journal of Soils and Sediments 13(10): 1724–1734.

Kemp Paul, Sear David, Collins Adrian, Naden Pamela, and Jones Iwan. (2011). The Impacts of Fine Sediment on Riverine Fish. Hydrological Processes 25(11): 1800–1821.

Koiter, A. J., P. N. Owens, E. L. Petticrew, and D. A. Lobb. (2013).The Behavioural Characteristics of Sediment Properties and Their Implications for Sediment Fingerprinting as an Approach for Identifying Sediment Sources in River Basins. Earth-Science Reviews 125(Supplement C): 24–42.

Koiter, Alexander J., David A. Lobb, Philip N. Owens, et al. (2013). Investigating the Role of Connectivity and Scale in Assessing the Sources of Sediment in an Agricultural Watershed in the Canadian Prairies Using Sediment Source Fingerprinting. Journal of Soils and Sediments 13(10): 1676–1691.

Koiter, Alexander J., Philip N. Owens, Ellen L. Petticrew, and David A. Lobb. (2015). The Role of Gravel Channel Beds on the Particle Size and Organic Matter Selectivity of Transported Fine-Grained Sediment: Implications for Sediment Fingerprinting and Biogeochemical Flux Research. Journal of Soils and Sediments 15(10): 2174–2188.

Kraushaar, Sabine, Thomas Schumann, Gregor Ollesch, et al. (2015). Sediment Fingerprinting in Northern Jordan: Element-Specific Correction Factors in a Carbonatic Setting. Journal of Soils and Sediments 15(10): 2155–2173.

Laceby, J. Patrick, Olivier Evrard, Hugh G. Smith, et al. (2017). The Challenges and Opportunities of Addressing Particle Size Effects in Sediment Source Fingerprinting: A Review. Earth-Science Reviews 169: 85–103.

Lamba, Jasmeet, K. G. Karthikeyan, and A. M. Thompson. (2015). Apportionment of Suspended Sediment Sources in an Agricultural Watershed Using Sediment Fingerprinting. Geoderma 239–240: 25–33.

Lim, Kyoung Jae, Bernard A. Engel, Joongdae Choi, et al. Automated Web Gis Based Hydrograph Analysis Tool, What1 - Lim - 2005 - JAWRA Journal of the American Water Resources Association - Wiley Online Library. https://onlinelibrary.wiley.com/doi/full/10.1111/j.1752-1688.2005.tb03808.x, accessed May 8, 2018.

Liu, Bing, Daniel E. Storm, Xunchang J. Zhang, Wenhong Cao, and Xingwu Duan. (2016).A New Method for Fingerprinting Sediment Source Contributions Using Distances from Discriminant Function Analysis. CATENA 147: 32–39.

Liu, Kui, David A. Lobb, Jim J. Miller, Philip N. Owens, and Melody E.G. Caron. (2017).Determining Sources of Fine-Grained Sediment for a Reach of the Lower Little Bow River, Alberta, Using a Colour-Based Sediment Fingerprinting Approach. Canadian Journal of Soil Science 98(1): 55–69.

Martínez-Carreras, Núria, Andreas Krein, Francesc Gallart, et al. (20100. Assessment of Different Colour Parameters for Discriminating Potential Suspended Sediment Sources and Provenance: A Multi-Scale Study in Luxembourg. Geomorphology 118(1): 118–129.

Martínez-Carreras, Núria, Andreas Krein, Thomas Udelhoven, et al. (2010). A Rapid Spectral-Reflectance-Based Fingerprinting Approach for Documenting Suspended Sediment Sources during Storm Runoff Events. Journal of Soils and Sediments 10(3): 400–413.

McCarney-Castle, Kerry, Tristan M. Childress, and Christian R. Heaton. (2017). Sediment Source Identification and Load Prediction in a Mixed-Use Piedmont Watershed, South Carolina. Journal of Environmental Management 185(Supplement C): 60–69.

Miller, Jerry R., Mark Lord, Steven Yurkovich, Gail Mackin, And Lawrence Kolenbrander (2005). Historical Trends In Sedimentation Rates And Sediment Provenance, Fairfield Lake, Western North Carolina1. Jawra Journal Of The American Water Resources Association 41(5): 1053–1075.

Mishra, Surendra Kumar, and Vijay P. Singh. (2003). SCS-CN Method. *In* Soil Conservation Service Curve Number (SCS-CN) Methodology Pp. 84–146. Water Science and Technology Library. Springer, Dordrecht.

Moriasi, D. N., J. G. Arnold, M. W. Van Liew, et al. (2007). Model Evaluation Guidelines for Systematic Quantification of Accuracy in Watershed Simulations.

Mukundan, R., D. E. Radcliffe, J. C. Ritchie, L. M. Risse, and R. A. McKinley. (2010).Sediment Fingerprinting to Determine the Source of Suspended Sediment in a Southern Piedmont Stream. Journal of Environmental Quality 39(4): 1328–1337.

Mzuza, Maureen Kapute, Zhang Weiguo, Lostina S. Chapola, Mavuto Tembo, and Fanuel Kapute. (2017). Determining Sources of Sediments at Nkula Dam in the Middle Shire River, Malawi, Using Mineral Magnetic Approach. Journal of African Earth Sciences 126: 23–32.

Neitsch, S L, J G Arnold, J R Kiniry, And J R Williams. (2005). Soil And Water Assessment Tool Theoretical Documentation: 494.

National Oceanic and Atmospheric Administration (NOAA). National Climatic Data Center (https://www.ncdc.noaa.gov/cdo-web/).

Nosrati, Kazem, Gerard Govers, Brice X. Semmens, and Eric J. Ward. (2014). A Mixing Model to Incorporate Uncertainty in Sediment Fingerprinting. Geoderma 217–218: 173–180.

Owens, P. N., A. Koiter, E. L. Petticrew, and D. A. Lobb. (2015). The Preferential Transport of Sediment and Its Implications for Sediment Fingerprinting: A Flume Simulation. AGU Fall Meeting Abstracts 21: EP21C-0914.

Palazón, L., L. Gaspar, B. Latorre, W. H. Blake, and A. Navas. (2014). Evaluating the Importance of Surface Soil Contributions to Reservoir Sediment in Alpine Environments: A Combined Modelling and Fingerprinting Approach in the Posets-Maladeta Natural Park. Solid Earth; Gottingen 5(2): 963–978.

Palazón, Leticia, Leticia Gaspar, Borja Latorre, William H. Blake, and Ana Navas (2015). Identifying Sediment Sources by Applying a Fingerprinting Mixing Model in a Pyrenean Drainage Catchment. Journal of Soils and Sediments 15(10): 2067–2085.

Palazón, Leticia, Borja Latorre, Leticia Gaspar, et al. (2016). Combining Catchment Modelling and Sediment Fingerprinting to Assess Sediment Dynamics in a Spanish Pyrenean River System. Science of The Total Environment 569–570: 1136–1148.

Phillips, J. M., M. A. Russell, and D. E. Walling. (2000). Time-integrated Sampling of Fluvial Suspended Sediment: A Simple Methodology for Small Catchments. Hydrological Processes 14(14): 2589–2602.

Pitt, Robert, Shirley E. Clark, and Donald W. Lake. (2007) Construction Site Erosion and Sediment Controls: Planning, Design and Performance. DEStech Publications, Inc.

Pulley, Simon, Ian Foster, and Paula Antunes. (2015). The Uncertainties Associated with Sediment Fingerprinting Suspended and Recently Deposited Fluvial Sediment in the Nene River Basin. Geomorphology 228: 303–319.

Pulley, Simon, Ian Foster, and Adrian L. Collins. (2017). The Impact of Catchment Source Group Classification on the Accuracy of Sediment Fingerprinting Outputs. Journal of Environmental Management 194(Supplement C): 16–26.

Rhoton, F. E., W. E. Emmerich, D. A. DiCarlo, et al. (2008). Identification of Suspended Sediment Sources Using Soil Characteristics in a Semiarid Watershed. Soil Science Society of America Journal 72(4): 1102.

Rossi, Luca, Nathalie Chèvre, Rolf Fankhauser, et al. (2013). Sediment Contamination Assessment in Urban Areas Based on Total Suspended Solids. Water Research 47(1): 339–350.

Rostamian, Rokhsare, Aazam Jaleh, Majid Afyuni, et al. (2008). Application of a SWAT Model for Estimating Runoff and Sediment in Two Mountainous Basins in Central Iran. Hydrological Sciences Journal 53(5): 977–988.

Russell, Kathryn L., Geoff J. Vietz, and Tim D. Fletcher. (2017). Global Sediment Yields from Urban and Urbanizing Watersheds. Earth-Science Reviews 168: 73–80.

Schmalz, B., Q. Zhang, M. Kuemmerlen, et al. (2015). Modelling Spatial Distribution of Surface Runoff and Sediment Yield in a Chinese River Basin without Continuous Sediment Monitoring. Hydrological Sciences Journal: 1–24.

Smith, Hugh G., and William H. Blake. (2014). Sediment Fingerprinting in Agricultural Catchments: A Critical Re-Examination of Source Discrimination and Data Corrections. Geomorphology 204(Supplement C): 177–191.

The World Bank. (2014). World Bank Open Data: Urban Population (% of Total) and Urban Population Growth (Annual %).

Tyler, Germund. (2004). Rare Earth Elements in Soil and Plant Systems - A Review. Plant and Soil 267(1–2): 191–206.

USDA-NRCS.Soil Survey Geographic (SSURGO) database for Lee County, Alabama.

USEPA. (1996). Microwave assisted acid digestion of siliceous and organically based matrices. OHW, Method, *3052*.

USEPA. (2017). National Summary of State Information. https://ofmpub.epa.gov/waters10/attains_nation_cy.control#STREAM/CREEK/RIVER. Accessed 9 December 2017.

Vercruysse, Kim, Robert C. Grabowski, and R. J. Rickson. (2017). Suspended Sediment Transport Dynamics in Rivers: Multi-Scale Drivers of Temporal Variation. Earth-Science Reviews 166: 38–52.

Walling, D. E. (2005).Tracing Suspended Sediment Sources in Catchments and River Systems. Science of The Total Environment 344(1–3): 159–184.

Walling, D. E., A. L. Collins, and R. W. Stroud. (2008). Tracing Suspended Sediment and Particulate Phosphorus Sources in Catchments. Journal of Hydrology 350(3). Characterization and Apportionment of Nutrient and Sediment Sources in Catchments: 274–289.

Walling, Desmond E., Philip N. Owens, and Graham J. L. Leeks. (1999). Fingerprinting Suspended Sediment Sources in the Catchment of the River Ouse, Yorkshire, UK. Hydrological Processes 13(7): 955–975.

Walsh, Christopher J., Tim D. Fletcher, and Anthony R. Ladson. (2005). Stream Restoration in Urban Catchments through Redesigning Stormwater Systems: Looking to the Catchment to Save the Stream. Journal of the North American Benthological Society 24(3): 690–705.

Wilkinson, Scott N., Gary J. Hancock, Rebecca Bartley, Aaron A. Hawdon, and Rex J. Keen (2013). Using Sediment Tracing to Assess Processes and Spatial Patterns of Erosion in Grazed Rangelands, Burdekin River Basin, Australia. Agriculture, Ecosystems & Environment 180(Supplement C): 90–102.

Wilson, C. G., R. A. Kuhnle, D. D. Bosch, et al. (2008). Quantifying Relative Contributions from Sediment Sources in Conservation Effects Assessment Project Watersheds. Journal of Soil and Water Conservation 63(6): 523–532.

Yahaya Ahmed Iyaka. (2011). Nickel in Soils: A Review of Its Distribution and Impacts. Scientific Research and Essays 6(33).

Yu, Mingjing, and Bruce L. Rhoads. (2018). Floodplains as a Source of Fine Sediment in Grazed Landscapes: Tracing the Source of Suspended Sediment in the Headwaters of an Intensively Managed Agricultural Landscape. Geomorphology.

CHAPTER 4

FINGERPRINTING THE DOMINANT SOURCES OF IN-STREAM SEDIMENT USING DISTANCES FROM DISCRIMINANT FUNCTION ANALYSIS (DFA)

4.1 Introduction

Sediment is one of the major non-point source pollutants causing impairment of surface waters. To develop effective and efficient watershed-level management plans aimed at mitigating excessive delivery of sediment to streams, it is important to identify the dominant sources of sediment within a watershed. Sediment fingerprinting techniques are being increasingly used to identify sediment sources. These techniques help in development of watershed management strategies aimed at reducing sediment loadings and restoring aquatic ecosystem health (Rose et al., 2018; Smith & Blake, 2014). Sediment fingerprinting method involves comparison of physical or geochemical properties of sediment in the potential sources to the corresponding properties in the in-stream sediment (suspended or bed sediment) to quantify relative contributions of the potential sources to in-stream sediment (Juracek & Ziegler, 2009). The fingerprinting properties may include, but are not limited to, geochemical, radionuclide, mineral magnetic, stable isotopes, organic constituents or color properties (Smith & Blake, 2014).

Studies conducted using sediment fingerprinting techniques to apportion the contribution of different sources to in-stream sediment can be traced back to the 1970s (Rummery et al.,1979;

Wall & Wilding, 1976; Wood, 1978). Since then, sediment source fingerprinting applications have expanded greatly and substantial research efforts have been made to evaluate and improve fingerprinting methods (Palazón et al., 2015; Smith et al., 2015). Over the past few years, research has been conducted to evaluate uncertainties associated with the sediment fingerprinting methods (Pulley et al., 2015; Sherriff et al., 2015; Smith & Blake, 2014). The various sources of uncertainty include errors related to sampling methods, intra-versus inter-source variability in fingerprinting properties, fingerprinting property selection, and mixing models (Barthod et al., 2015; Smith & Blake, 2014; Stewart et al., 2015).

To reduce the uncertainty in the sediment fingerprinting procedures, statistical methods are used to select composite of conservative fingerprinting properties that could best discriminate among the sources (Collins & Walling, 2002; Liu et al., 2016). First, a range test is performed to select fingerprinting properties that are conservative (Collins et al., 2012). Following the range test, the fingerprinting properties that pass this test are subjected to a two-step statistical procedure (Collins et al., 1997). In the first step, Kruskal-Wallis H-test is used to determine the uniqueness of the sediment sources based on the fingerprinting property signatures. The Kruskal-Wallis H test is commonly used because fingerprinting property data sets are rarely normally distributed and most often have unequal variances (Collins & Walling, 2002). This test is followed by a stepwise discriminant function analysis (DFA) to select the optimum combination of fingerprinting properties needed to represent the largest proportion of variance. The DFA estimates discriminant function coefficients, which indicate the explanatory power of individual fingerprint properties (Collins et al., 2010; Davis & Fox, 2009). Subsequently, a multivariate mixing model is used to estimate the relative contribution of the potential sources to in-stream sediment (Carter et al., 2003; Collins et al., 1998).

Depending on the statistical methods employed to quantify relative source contribution from different sources to in-stream sediment, differences/similarities in sediment source apportionment results have been reported. For example, Nosrati et al. (2018) showed the importance of statistical procedures employed in fingerprinting studies by reporting statistical significant differences in the predicted source contributions generated using three different combinations of statistical tests. Also, Palazón et al. (2015) reported different source contribution estimates using different set of statistical methods . However, limited work has been done to assess the sensitivity of source apportionments results to statistical methods (Nosrati et al., 2018; Liu et al., 2016). Therefore, the overall goal of this study was to test if the outputs from DFA alone can be used to apportion the contribution of sources to in-stream sediment without the use of a mixing model. The specific objectives of this study were to: a) compare the source contributions to stream bed sediment estimated by Collins mixing model and the DFA for two particle size ranges (63-212 μm and <63 μm) and b) compare the source apportionment results determined using Collins mixing model and the DFA for suspended sediment for the two particle size ranges (63-212 μm and <63 μm).

4.2 MATERIALS AND METHODS

4.2.1 Study Area

The sediment source samples were sampled from a 31-km^2 Moore's Mill Creek watershed, located in the eastern part of Alabama, USA (Fig. 4.1.a). Lying within the Southern Piedmont physiographic province, this watershed is a part of the lower Tallapoosa River Basin with sandy loam and sandy clay as the dominant soil textures. Based on the Cropland Data Layer (2017) developed by USDA-NASS (https://www.nass.usda.gov/Research_and_Science/Cropland/

SARS1a.php), land use in this watershed is predominantly developed (66%) with areas of forested (23%), pasture (5%), and shrubland (4%) landcover (Fig. 4.1.a). This basin has an average annual rainfall of 1430 mm (1997-2017) and average annual high and low temperatures of 25º C and 11º C, respectively (1997-2017). The catchment is based of bedrock lithology ranging from Schist, Gneiss, Mylonite, Quartzite to Sandstone.

4.2.2 Surface Soil Sampling and In-Stream Sediment Collection

The potential sources of sediment considered in this study included construction sites and stream banks. Source sampling was done based on the general criteria of (i) accessibility, (ii) potential connectivity or proximity of sampling locations to stormwater drains/streams and (iii) presence of exposed actively eroding stream banks. Thirteen different construction sites were sampled within this watershed and stream bank sampling involved collection of soil samples from 17 different sites within this watershed (Fig. 4.1.b; Appendix A. Fig. A1 and A2). The source sample collection procedure is discussed in detail in the section 2.2.2 of chapter 2. Also, the stream bed and suspended sediment sample collection procedure is discussed in detail in section 2.2.2 of chapter 2 and section 3.2.2 of chapter 3 respectively (Appendix A Fig. A3 and A4).

4.2.3 Soil Analysis

Following the oven drying at 60° C and subsequent disaggregation using pestle and mortar, the soil and sediment samples were dry-sieved to two particle size fractions, namely, 63-212 μm (fine sand) and <63 μm (silt and clay). At the Wisconsin State Laboratory of Hygiene, Madison, Wisconsin, USA, samples were analyzed for Li, Be, B, Mg, Na, Al, P, S, K, Ca, Sc, Ti, V, Cr, Mn, Fe, Co, Ni, Cu, Zn, Ga, As, Se, Rb, Sr, Y, Zr, Nb, Rh, Pd, Ag, Mo, Cd, Sn, Sb, Cs, Ba, La, Ce, Pr, Nd, Sm, Eu, Gd, Dy, Ho, Yb, Lu, Hf, Ta, W, Ir, Pt, Hg, Tl, Pb, Bi, Th, and U using ICP-MS

microwave-aided digestion procedure based on United States Environmental Protection Agency Method 3052 (USEPA, 1996).

4.2.4 Statistical Analysis

All the measured fingerprinting property concentrations were subjected to a range test. This test determines if the values of all fingerprinting property concentrations measured in the in-stream sediment samples fall within the observed range of values obtained from the source sediment samples (Franz et al., 2014; Gellis & Noe, 2013). A two-fold statistical selection procedure was used to test the discriminatory power of the fingerprinting properties to discriminate among the source groups. Firstly, Kruskal-Wallis H-test (α= 0.05) was used to select the tracers which can discriminate between the source categories namely, construction sites and stream banks. The fingerprinting properties that passed the Kruskal-Wallis H-test were included in the stage two, which involved the use of stepwise DFA. The DFA output provided composite fingerprint (optimum or smallest combination of fingerprinting properties) capable of providing maximum discrimination between the sources.

4.2.5 Multivariate Mixing Model

Relative source contributions from construction sites and stream banks to in-stream sediment at each site were calculated using the Collins mixing model based on the minimization of the objective function i.e. sum of squares of the weighted relative errors (Collins et al., 2012). The mixing model equation is described as follows:

$$\sum_{j=1}^{p}\left(\frac{\mathrm{C_{ssj}}-\sum_{i=1}^{m}\mathrm{C_{sj}P_i}}{\mathrm{C_{ssj}}}\right)^2 W_i$$

where p is the number of fingerprinting properties in the composite fingerprint; m is the number of source groups; C_{ssj} is the concentration of the fingerprinting property (j) in the in-stream sediment sample; Cs_j is the mean concentration of the fingerprinting property (j) in the source group; P_i is the relative contribution from source group (i); and W_i is the fingerprinting property discriminatory weighting factor. The fingerprinting property discriminatory weighting factor (W_i) was used to ensure that the fingerprinting property with the greatest discriminatory power exerts the greatest influence on the solutions of the mixing model (Collins et al., 2010). Two linear boundary conditions must be satisfied by the multivariate mixing model to ensure that the relative source contributions from each source group to in-stream sediment must lie between 0 and 1, and the sum of the relative source contributions from all the source groups is unity:

$$\sum_{i=1}^{m} P_i = 1$$

$$0 \leq P_i \leq 1$$

4.2.6 Identifying In-Stream Sediment Sources Using DFA

The method to determine source contrbutions to in-stream sediment using DFA alone was adopted from Liu et al. (2016). Stepwise DFA was used to select the composite of fingerprinting properties that provided best discrimination among the sources and subsequently the source contributions were calculated using the following equations:

$$D_m = \sum_{i=1}^{n} \frac{\acute{\rho}}{100} |F_i(source_m) - F_i(sediment_i)| \quad (1)$$

$$W_m = \frac{1}{D_m} \quad (2)$$

$$W = \sum_{i=1}^{m} \frac{1}{D_m} \quad (3)$$

$$P_m = \frac{W_m}{W} * 100 \quad (4)$$

Where, D_m is the distance from source m; ρ is the percentage at which function i correctly classified the groups; W_m is the weighting for source m; W is the total weighting, P_m is the contribution from source m (%); m is the number of sources; n is the number of functions used to classify the groups; $F_{i(source)}$ is the centre of source; and $F_{i(sediment)}$ is the center of sediment. The mixing model outputs were compared with the outputs of DFA alone for each subwatershed for both the particle sizes.

4.3 RESULTS AND DISCUSSIONS

4.3.1 Statistical Discrimination of Fingerprinting Properties

The fingerprinting properties that passed the range test and Kruskal Wallis H-test for 63-212 μm and <63 μm at each site for stream bed and suspended sediment are included in Tables 4.2 to 4.5. The number and combination of the fingerprinting properties selected by stepwise DFA varied among different subwatersheds and the results are included in Tables from 4.6 to 4.9. The optimum set of fingerprinting properties selected by the stepwise DFA for stream bed sediment classified 100 % of the sources correctly at each site for both the particle size fractions. The percentage of sources classified currently by the optimum set of fingerprinting properties selected by DFA for suspended sediment varied from 96.7 to 100% for 63-212 μm among three sites. Whereas for < 63 μm, optimum number of fingerprinting properties classified 100% of the source samples correctly at each site. Overall, results of the stepwise DFA test show that optimum number of fingerprinting properties selected for both particle size fractions provided strong discrimination between construction sites and stream banks.

4.3.2 Estimation of Source Contributions by Collins Mixing Model

Relative source contributions to stream bed and suspended sediment based on the Collins mixing model are discussed in detail in chapter 2 and 3. Briefly, for site 1, stream banks were the

dominant sources of stream bed sediment for both the particle size fractions. Land use in this subwatershed is mainly developed (91 %, Cropland Data Layer, 2017). The increase in urbanization results in increase of stormwater runoff and hence increased risk of channel instability (Bledsoe & Watson, 2001). Also, the temporal variability in the stream bed sediment sources likely depended on the phase of construction activities from commencement to completion during the time of sampling. Erosion rates vary at construction sites depending upon the activities conducted at the site. Major activities that result in significant disturbance of soils include clearing, grubbing, excavating, soil stockpiling, and utilities and infrastructure installation (Pitt et al., 2007)

At site 2, stream banks were the dominant sources of the stream bed sediment for both the particle size fractions. This subwatershed is also mainly urbanized and as indicated earlier, urbanization of a watershed results in alteration of river channels owing to increased surface runoff and increased hydraulic stress on the stream banks. For site 3, the dominant sources of stream bed sediment for both the particle sizes were construction sites. High contribution from construction sites was likely because of the existence of areas of active construction in close proximity to the creek without enough riparian buffers (Chapter 3).

The construction sites were the dominant contributors of suspended sediment for both the particle size fractions at all the sites. The rates of erosion from construction sites are considerably higher than those from areas under undisturbed vegetation (Mukundan et al., 2010), which likely resulted in greater contribution from construction sites to suspended sediment. Also, increase in surface runoff due to increased development leads to excessive delivery of sediment from construction sites to surface waters. Sediment yield tends to be larger in urban areas than

unurbanized areas even if only small areas of unprotected or exposed soil are there (Leopold & Pecora, 1968).

Moreover, the suspended sediment had greater specific surface area or was finer in size (average specific surface area was 132.3±8.7 $m^2 kg^{-1}$ and 170.6±9.1 $m^2 kg^{-1}$ for particle size 63-212 μm and <63 μm, respectively) compared to stream bed sediment (average specific surface area was 60±4.2 $m^2 kg^{-1}$ and 120.6±5.9 $m^2 kg^{-1}$ for particle size 63-212 μm and <63 μm, respectively). Also, the sediment from construction sites were finer (average specific surface area was 129.91±9.6 $m^2 kg^{-1}$ and 291.26±24.5 $m^2 kg^{-1}$ for the particle size 63-212 μm and <63μm, respectively) compared to sediment from stream banks (average specific surface area was 114.35±6.4 $m^2 kg^{-1}$ and 212.7±9.5 $m^2 kg^{-1}$ for the particle size 63-212 μm and <63μm, respectively). Therefore, as indicated by the specific surface area values, construction sites consisted of finer particles compared to stream banks and therefore were the dominant sources of suspended sediment. The stream bank particles could be present in the stream as aggregates (because of mass wasting or bank failure) or individual particles depending upon the hydraulic forces exerted during flow events (Lamba et al., 2015). But the aggregates are more likely to deposit on the stream bed as compared to fine particles eroded from construction sites, which are more likely to remain in suspension due to greater specific surface area. As a result, stream banks were the dominant sources of sediment deposited on the stream bed and construction sites were the dominant sources of suspended sediment.

4.3.3 Comparison of the Source Contributions Estimated by Collins Mixing Model and DFA

The results obtained by using DFA and Collins mixing model for site 1 are given in table 4.10. For 63-212 μm particle size fraction, both the methods showed that stream banks were the dominant sources of stream bed sediment. Therefore, both the methods provided similar source apportionment results. For <63 μm particle size fraction, DFA indicated that for majority (73 %) of the sampling period, construction sites were the dominant sources, whereas the mixing model showed that for 46% of the samples collected, construction sites were the dominant sources of stream bed sediment. Therefore, the dominant sources of stream bed sediment determined using both methods for <63 μm particle size fraction varied. In site 2 subwatershed for 63-212 μm and <63 μm, both the methods predicted that for majority of the sampling period, stream banks had greater contribution to the stream bed sediment (Table 4.11). For site 3 subwatershed, both the methods indicated that construction sites were the dominant sources of stream bed sediment for 63-212 μm particle size fraction (Table 4.12). However, for <63 μm particle size fraction, both the methods did not return similar results. The mixing model indicated partial contribution from both the construction sites and stream banks to the stream bed sediment, whereas the DFA indicated that for 100 % of the samples collected, stream banks were the dominant sources of stream bed sediment. In case of suspended sediment sources, both mixing model and DFA predicted similar dominant sources for majority of the sampling period for both the particle size fractions at all sites (Table 4.13- 4.15).

Overall, comparisons of two methods show that DFA and mixing model predicted similar dominant sources of in-stream sediment for both the particle size fractions for majority of our sampling period. However, dominant sources of in-stream sediment determined using both the methods were not similar every time. Similar results were reported by Liu et al. (2016). Different factors, such as, number of sources considered, sample size and conservative/non-conservative

behavior of fingerprinting properties can affect source apportionment results predicted by two methods (Liu et al., 2016). For example, a small sample size for each subwatershed could affect source group centroids, which are used to determine relative source contributions in DFA method. Tests on synthetic sediment mixtures which can help to improve parametrization of the DFA model and characterizing source groups' centroids accurately can help to improve the accuracy of the DFA method to quantify contribution to in-stream sediment from different sources (Liu et al., 2016). Further research is needed to understand the role of statistical procedures for fingerprinting properties selection as it is fundamental to obtain reliable source contribution results.

4.4 Conclusions

Sediment source contributions were predicted for the Moore's Mill Creek watershed, Alabama, US. Stream bank and construction sites samples were collected across the whole watershed, and in-stream sediment (suspended and stream bed) samples were collected at the outlets of two subwatersheds as well the whole watershed outlet. Two methods were used to determine relative contribution from different sources to suspended and stream bed sediment, the Collins mixing model and DFA. Both the methods identified similar dominant sources for stream bed as well as for suspended sediment at all sites for both the particle size fractions for majority of the sampling period. However, the method of calculating the source contributions using distances from DFA requires further research because the sediment source apportionment results predicted by mixing model and DFA were not always similar. The results determined by using DFA alone method largely depends on the sample size for each subwatershed and the optimum set of fingerprinting properties used. Therefore, care must be taken while selecting the most appropriate set of properties for the success of this method.

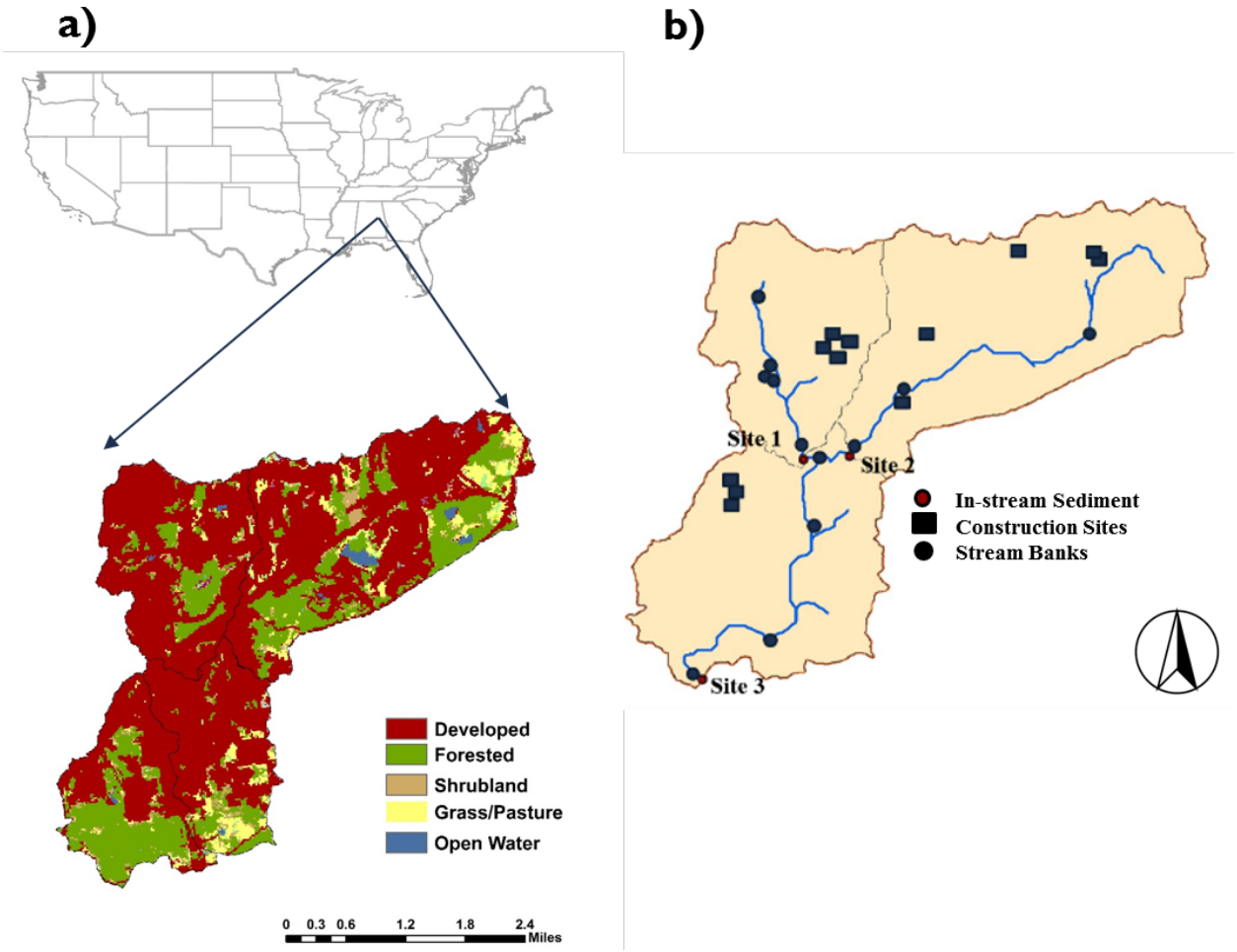

Fig. 4.1. a) Land use distribution in the Moore's Mill Creek watershed and b) Location of in-stream sediment, stream banks and construction sampling sites.

Table 4.1. Individual stream bed depth intervals at each site and the dates of in-stream sediment sample collection throughout the sampling period

Sites	Depth Intervals of the soil cores for the first month of sampling period	Stream Bed Sample Collection Dates	Suspended Sediment Sample Collection Dates
Site 1	0-5 cm, 5-10 cm, 10-15 cm, and 15-20 cm	December 2, February 5, March 10, April 14, May 18, June 28, July 28, September 22	December 2, February 5, March 10, April 14, May 18, June 28, July 28, September 22
Site 2	0-5 cm, 5-10 cm, 10-15 cm	_*	December 2, April 14, May 18**
Site 3	0-5 cm, 5-10 cm	_*	December 2, February 5, March 10, April 14, May 18, June 28, July 28, September 22

*Sampling dates were same for all sites

**Samplers were lost for the rest of the sampling period

Table 4.2. Fingerprinting properties that satisfied the range test and the Kruskal-Wallis H-test (p=0.05) criteria for stream bed sediment at each site for particle size 63-212 μm

Range test

Sites	Fingerprinting Properties														
1	Li	Be	Na	P	K	Ca	V	Cr	Mn	Co	Ni	Cu	Zn	Rb	Nb
	Ag	Cd	Cs	Ba	Nd	Sm	Eu	Gd	Dy	Ho	Yb	Lu	Tl	Pb	Th
	U														
2	Be	B	Na	P	K	Ca	Mn	Co	As	Rb	Y	Zr	Rh	Ag	Sr
	Sb	Cs	Ba	Pr	Nd	Sm	Eu	Gd	Dy	Ho	Yb	Lu	Hg	Tl	Pb
3	Li	Be	Na	P	K	Ca	Sc	Ti	V	Cr	Mn	Fe	Co	Ni	Zn
	Ga	As	Rb	Y	Zr	Nb	Mo	Ag	Sr	Sb	Cs	Ba	La	Ce	Pr
	Nd	Sm	Eu	Gd	Dy	Ho	Yb	Lu	Hf	Ta	Tl	Pb	U		

Kruskal-Wallis H-test

Sites	Fingerprinting Properties														
1	Be	V	Cr	Nb	Ag	Pb	Th								
2	Be	B	Zr	Ag	Pb										
3	Li	Be	Sc	V	Cr	Fe	Ni	Ga	As	Y	Zr	Nb	Mo	Ag	Pr
	Nd	Sm	Ho	Hf	Ta	Pb	U								

Table 4.3. Fingerprinting properties that satisfied the range test and the Kruskal-Wallis H-test (p=0.05) criteria for stream bed sediment at each site for particle size <63 μm

Range test

Sites	Fingerprinting Properties														
1	Li	Be	B	Na	Al	S	Ca	Sc	Cr	Mn	Co	Ni	Ga	As	Rb
	Sr	Zr	Mo	Cd	Cs	Ba	Pr	Nd	Sm	Eu	Gd	Dy	Ho	Yb	Lu
	Hf	Pt	Tl	Pb											
2	Li	Be	B	Al	P	S	Ca	Sc	V	Cr	Mn	Fe	Co	Ni	Zn
	Ga	As	Y	Zr	Mo	Pd	Cd	Sn	Sb	Cs	La	Pr	Nd	Sm	Eu
	Gd	Dy	Ho	Yb	Lu	Hf	W	Hg	Tl	Pb	U				
3	Li	Be	B	Na	Al	P	S	Ca	Sc	V	Cr	Fe	Co	Ni	Zn
	Ga	As	Rb	Sr	Y	Zr	Mo	Pd	Cd	Sb	Cs	La	Pr	Eu	Gd
	Dy	Yb	Lu	Hf	Hg	Tl	Pb	U							

Kruskal-Wallis H-test

Sites	Fingerprinting Properties														
1	Be	Sc	Mn	Co	Ga	As	Rb	Cd	Ba	Pr	Nd	Sm	Eu	Gd	Dy
	Ho	Yb	Lu	Pt	Pb										
2	Be	B	V	Cr	Fe	Ni	Ga	Zr	Cd	Hf	U				
3	Be	B	V	Cr	Fe	Co	Ni	Ga	Rb	Sr	Y	Zr	Pd	Cd	La
	Pr	Eu	Gd	Dy	Yb	Lu	Hf	Pb	U						

Table 4.4. Fingerprinting properties that satisfied the range test and the Kruskal-Wallis H-test (p=0.05) criteria for suspended sediment at each site for particle size <63 μm

Range test															
Sites	**Fingerprinting properties**														
1	Li	Be	B	Na	P	K	Sc	Ti	V	Cr	Fe	Co	Ni	Ga	As
	Rb	Zr	Nb	Mo	Cd	Cs	Ba	Pr	Eu	Gd	Ta	W	Ir	Pt	Hg
	Tl	Pb	Bi	U											
2	Li	Be	Mg	Al	K	Sc	V	Cr	Fe	Co	Ni	Zn	Ga	As	Zr
	Nb	Cd	Cs	Ba	Nd	Lu	Hf	Ta	W	Ir	Pt	Tl	Pb	Bi	U
3	Li	Be	B	Na	Al	K	Sc	V	Cr	Fe	Co	Ni	Ga	As	Rb
	Zr	Nb	Cd	Sb	Cs	Ba	Pr	Eu	Hf	Ta	W	Ir	Pt	Hg	Tl
	Pb	Bi	U												
Kruskal-Wallis H-test															
Sites	**Fingerprinting properties**														
1	Be	Sc	V	Co	Ga	As	Rb	Nb	Cd	Ba	Pr	Eu	Gd	Ta	Ir
	Pt	Pb	Bi												
2	Be	V	Cr	Fe	Ni	Ga	Zr	Cd	Hf	Ir	Pt	Bi	U		
3	Be	B	V	Cr	Fe	Co	Ni	Ga	Rb	Zr	Cd	Ba	Pr	Eu	Hf
	Ta	Ir	Pt	Pb	Bi	U									

Table 4.5. Fingerprinting properties that satisfied the range test and the Kruskal-Wallis H-test (p=0.05) criteria for suspended sediment at each site for particle size 63-212 μm

Range test

Sites	Fingerprinting properties														
1	B	Na	K	Ti	V	Cr	Ga	Rb	Y	Zr	Nb	Sr	Cs	Ba	Sm
	Dy	Lu	Hf	Ta	W	Ir	Pt	Tl	Pb	Bi	U				
2	Li	Be	B	Na	Mg	Al	P	K	Ca	Sc	Ti	V	Fe	Co	Cu
	Zn	Ga	Rb	Y	Zr	Nb	Ag	Cs	Ba	Sm	Eu	Gd	Dy	Ho	Yb
	Lu	Hf	Ta	Tl	Pb	Bi	Th	U							
3	Li	Be	B	Na	K	Al	Sc	Ti	V	Fe	Co	Ni	Ga	Se	Rb
	Zr	Nb	Ag	Cs	Ba	Eu	Lu	Hf	Ta	W	Ir	Pt	Hg	Tl	Pb
	Bi	U													

Kruskal-Wallis H-test

Sites	Fingerprinting properties														
Site 1	V	Cr	Ga	Zr	Nb	Ta	W	Pb	Bi						
Site 2	Be	B	Al	Sc	V	Fe	Ga	Zr	Nb	Ag	Hf	Ta	Pb	Bi	Th
Site 3	Li	Be	B	Al	Sc	V	Fe	Ga	Ni	Se	Zr	Nb	Hf	Ag	Ta
	W	Pb	Bi	U											

Table 4.6. Results of stepwise DFA for stream bed sediment at each site for particle size 63-212 μm

Site	Fingerprinting property	Wilks' lambda	Percentage source samples classified correctly	Cumulative percentage source samples classified correctly	Fingerprinting property discriminatory weighting
1	V	0.258	100	100	1.08
	Nb	0.134	92.3	100	1
2	Ag	0.078	100	100	1.25
	Be	0.057	80	100	1
3	V	0.286	96.7	96.7	1.53
	Sm	0.262	70	93.33	1.1
	Y	0.162	73.33	96.7	1.16
	Fe	0.113	86.7	96.7	1.37
	Zr	0.099	80	96.7	1.26
	Ta	0.087	76.7	96.7	1.21
	Ho	0.077	63.33	100	1

Table 4.7. Results of stepwise DFA for stream bed sediment at each site for particle size <63 μm

Site	Fingerprinting property	Wilks' lambda	Percentage source samples classified correctly	Cumulative percentage source samples classified correctly	Tracer discriminatory weighting
1	Mn	0.218	100	100	1.3
	Be	0.116	76.9	100	1
	Co	0.035	100	100	1.3
	Rb	0.023	76.9	100	1
	Ba	0.005	76.9	100	1
	As	0.002	92.3	100	1.2
	Sc	0.0006	84.6	100	1.1
	Pt	0.0002	76.9	100	1
2	Ga	0.198	100	100	1.25
	Ni	0.152	80	100	1
3	Cd	0.468	90	90	1.23
	Rb	0.313	76.7	86.7	1.04
	Ga	0.181	93.3	96.7	1.27
	Sr	0.108	73.3	100	1
	La	0.092	80	100	1.09

Table 4.8. Results of stepwise DFA for suspended sediment at each site for particle size 63-212 μm

Site	Fingerprinting property	Wilks' lambda	Percentage source samples classified correctly	Cumulative percentage source samples classified correctly	Tracer discriminatory weighting
1	Bi	0.151	100	100	1.18
	Ga	0.101	84.6	100	1.00
	Pb	0.074	84.6	100	1.00
	Ta	0.040	84.6	100	1.00
2	V	0.055	100	100	1.10
	Pb	0.037	100	100	1.10
	Bi	0.022	90	100	1.00
3	V	0.286	96.7	96.7	1.38
	Ag	0.259	86.67	93.3	1.24
	Pb	0.229	80.00	93.3	1.14
	Se	0.181	70.00	96.7	1.00
	Nb	0.153	80.00	96.7	1.14

Table 4.9. Results of stepwise DFA for suspended sediment at each site for particle size <63 μm

Site	Fingerprinting property	Wilks' lambda	Percentage source samples classified correctly	Cumulative percentage source samples classified correctly	Tracer discriminatory weighting
1	Bi	0.049	100	100	1.3
	Ir	0.032	84.6	100	1.1
	Ba	0.025	76.9	100	1.0
2	Ga	0.198	100	100	1.25
	Ni	0.152	80	100	1
	Bi	0.107	80	100	1
3	Rb	0.152	76.67	76.67	1.04
	U	0.122	73.33	86.7	1.00
	Zr	0.091	86.67	100	1.18
	Pr	0.070	80	100	1.09
	Eu	0.064	76.67	100	1.04
	Ni	0.038	80	100	1.09

Table 4.10 Comparison of results from the DFA and mixing model for stream bed sediment for sit

	63-212 µm				<63 µm				Are the dominant sources of stream bed sediment similar as indicated by DFA and mixing model?	
	Using DFA		Using Mixing Model		Using DFA		Using Mixing Model			
Months	Stream Banks	Construction Sites	Stream Banks	Construction Sites	Stream Banks	Construction Sites	Stream Banks	Construction Sites	63-212 µm	<63 µm
Dec (core 1)	94.8	5.2	100	0	47.2	52.7	48	52	Yes	Yes
Dec (core 2)	94.1	5.9	100	0	44.6	55.4	37	63	Yes	Yes
Dec (core 3)	96.4	3.6	100	0	60.3	39.6	54	46	Yes	Yes
Dec (core 4)	90.2	9.8	100	0	36	63.9	36	64	Yes	Yes
2 Dec-5 Feb	84.5	15.5	100	0	45.5	54.5	84	16	Yes	No
5 Feb-10 March	83.9	16.1	100	0	84	15.9	100	0	Yes	Yes
10 March-14 April	93.6	6.4	100	0	73.7	26.3	100	0	Yes	Yes
14 April-18 May	83.6	16.4	100	0	43.9	56.0	72	28	Yes	No
18 May-28 June	69.5	30.5	88	12	38.8	61.2	55	45	Yes	No
28 June-28 July	79.9	20.1	100	0	26.1	73.8	0	100	Yes	Yes
28 July-22 Sept	90.3	9.7	100	0	32.1	67.9	0	100	Yes	Yes

Table 4.11 Comparison of results from the DFA and mixing model for stream bed sediment for site 2

	63-212 µm				<63 µm				Are the dominant sources of stream bed sediment similar as indicated by DFA and mixing model?	
	Using DFA		Using Mixing Model		Using DFA		Using Mixing Model			
Months	Stream banks	construction sites	stream banks	construction sites	stream banks	construction sites	stream banks	construction sites	63-212 µm	<63 µm
2 Dec (core 1)	99.8	0.2	100	0	93.1	6.9	97	3	Yes	Yes
2 Dec (core 2)	44.8	55.2	100	0	98.4	1.6	74	26	No	Yes
2 Dec (core 3)	42.1	57.9	100	0	96.6	3.4	72	28	No	Yes
2 Dec-5 Feb	68.4	31.6	100	0	98.6	1.4	82	18	Yes	Yes
5 Feb-10 March	56.9	43.1	99	1	87.3	12.7	76	24	Yes	Yes
10 March-14 April	60.5	39.5	97	3	92.8	7.2	93	7	Yes	Yes
14 April-18 May	68.2	31.8	100	0	99.3	0.7	95	5	Yes	Yes
18 May-28 June	92.5	7.5	100	0	89.3	10.7	100	0	Yes	Yes
28 June-28 July	74.8	25.2	100	0	87.8	12.2	100	0	Yes	Yes
28 July-22 Sept	69.8	30.2	100	0	85.7	14.3	100	0	Yes	Yes

Table 4.12. Comparison of results from the DFA and mixing model for stream bed sediment for site 3

	63-212 µm				<63 µm				Are the dominant sources of stream bed sediment similar as indicated by DFA and mixing model?	
	Using DFA		Using Mixing Model		Using DFA		Using Mixing Model			
Months	Stream banks	construction sites	stream banks	construction sites	stream banks	construction sites	stream banks	construction sites	63-212 µm	<63 µm
2 Dec (core 1)	46.9	53.1	20	80	93.4	6.6	46	54	Yes	No
2 Dec (core 2)	59	41	57	43	91.8	8.2	45	55	Yes	No
2 Dec-5 Feb	15.8	84.2	9	91	98.6	1.4	44	56	Yes	No
5 Feb-10 March	22.1	77.9	28	72	87.1	12.9	42	58	Yes	No
10 March-14 April	60.0	40.0	59	41	80.8	19.2	42	58	Yes	No
14 April-18 May	30.4	69.6	23	77	78.1	21.9	0	100	Yes	No
18 May-28 June	14.5	85.5	90	10	60.0	40.0	47	53	No	No
28 June-28 July	18.8	81.2	70	30	50.4	49.6	0	100	No	No
28 July-22 Sept	40.0	60.0	46	54	58.1	41.9	0	100	Yes	No

Table 4.13. Comparison of results from the DFA and mixing model for suspended sediment for site 1

	63-212 µm				<63 µm				Are the dominant sources of suspended sediment similar as indicated by DFA and mixing model?	
	Using DFA		Using Mixing Model		Using DFA		Using Mixing Model			
Month	Stream banks	construction sites	stream banks	construction sites	stream banks	construction sites	stream banks	construction sites	63-212 µm	<63 µm
20 October-2 Dec	14.7	85.3	21	79	37.0	63.0	0	100	Yes	Yes
2 Dec-5 Feb	74.6	25.4	44	56	33.3	66.7	72	28	No	Yes
5 Feb- 10 March	7.5	92.5	48	52	14.0	86.0	20	80	Yes	Yes
10 March-14 April	26.4	73.6	27	73	6.7	93.3	0	100	Yes	Yes
14 April- 18 May	1.6	98.4	49	51	25.2	74.8	0	100	Yes	Yes
18 May-28 June	28.6	71.4	40	60	62.1	37.9	20	80	Yes	No
28 June-28 July	4.6	95.4	47	53	78.1	21.9	8	92	Yes	No
28 July- 22 Sept	40.2	59.8	32	68	67.0	33.0	50	50	Yes	No

Table 4.14. Comparison of results from the DFA and mixing model for suspended sediment for site 2

	63-212 µm				<63 µm				Are the dominant sources of suspended sediment similar as indicated by DFA and mixing model?	
	Using DFA		Using Mixing Model		Using DFA		Using Mixing Model			
Months	Stream banks	construction sites	stream banks	construction sites	stream banks	construction sites	stream banks	construction sites	63-212 µm	<63 µm
20 October-2 Dec	75.2	24.8	29	71	31.9	68.1	45	55	No	Yes
10 March-14 April	91.7	8.3	68	32	37.6	62.4	36	64	Yes	Yes
14 April- 18 May	74.5	25.5	85	15	98.3	1.7	100	0	Yes	Yes

Table 4.15. Comparison of results from the DFA and mixing model for suspended sediment for site 3

	63-212 µm				<63 µm				Are the dominant sources of suspended sediment similar as indicated by DFA and mixing model?	
	Using DFA		Using Mixing Model		Using DFA		Using Mixing Model			
Months	Stream banks	construction sites	stream banks	construction sites	stream banks	construction sites	stream banks	construction sites	63-212 µm	<63 µm
20 October-2 Dec	94.1	5.9	34	66	28.9	71.1	0	100	No	Yes
2 Dec-5 Feb	30.5	69.5	19	81	86.0	14.0	46	54	Yes	No
5 Feb- 10 March	99.5	0.5	6	94	89.2	10.8	28	72	No	No
10 March-14 April	63.7	36.3	0	100	17.5	82.5	10	90	No	Yes
14 April- 18 May	42.9	57.1	0	100	62.3	37.7	20	80	Yes	No
18 May-28 June	14.4	85.6	0	100	20.0	80.0	0	100	Yes	Yes
28 June-28 July	4.5	95.5	0	100	24.5	75.5	0	100	Yes	Yes
28 July- 22 Sept	22.3	77.7	3	97	16.4	83.6	0	100	Yes	Yes

REFERENCES

Barthod, L. R. M., Liu, K., Lobb, D. A., Owens, P. N., Martínez-Carreras, N., Koiter, A. J., Gaspar, L. (2015). Selecting Color-based Tracers and Classifying Sediment Sources in the Assessment of Sediment Dynamics Using Sediment Source Fingerprinting. Journal of Environmental Quality, 44(5), 1605–1616. https://doi.org/10.2134/jeq2015.01.0043

Bledsoe, B. P., & Watson, C. C. (2001). Effects of Urbanization on Channel Instability1. JAWRA Journal of the American Water Resources Association, 37(2), 255–270. https://doi.org/10.1111/j.1752-1688.2001.tb00966.x

Carter, J., Owens, P. N., Walling, D. E., & Leeks, G. J. L. (2003). Fingerprinting suspended sediment sources in a large urban river system. Science of The Total Environment, 314–316, 513–534. https://doi.org/10.1016/S0048-9697(03)00071-8

Collins, A. L, & Walling, D. E. (2002). Selecting fingerprint properties for discriminating potential suspended sediment sources in river basins. Journal of Hydrology, 261(1–4), 218–244. https://doi.org/10.1016/S0022-1694(02)00011-2

Collins, A. L., Walling, D. E., & Leeks, G. J. L. (1997). Source type ascription for fluvial suspended sediment based on a quantitative composite fingerprinting technique. CATENA, 29(1), 1–27. https://doi.org/10.1016/S0341-8162(96)00064-1

Collins, A. L., Walling, D. E., Webb, L., & King, P. (2010). Apportioning catchment scale sediment sources using a modified composite fingerprinting technique incorporating property weightings and prior information. Geoderma, 155(3–4), 249–261. https://doi.org/10.1016/j.geoderma.2009.12.008

Collins, A. L., Zhang, Y., McChesney, D., Walling, D. E., Haley, S. M., & Smith, P. (2012). Sediment source tracing in a lowland agricultural catchment in southern England using a modified procedure combining statistical analysis and numerical modelling. Science of The Total Environment, 414(Supplement C), 301–317. https://doi.org/10.1016/j.scitotenv.2011.10.062

Collins, Adrian L., Walling, D. E., & Leeks, G. J. L. (1998). Fingerprinting the Origin of Fluvial Suspended Sediment in Larger River Basins: Combining Assessment of Spatial Provenance and Source Type. Geografiska Annaler: Series A, Physical Geography, 79(4), 239–254. https://doi.org/10.1111/j.0435-3676.1997.00020.x

Davis, C. M., & Fox, J. F. (2009). Sediment Fingerprinting: Review of the Method and Future Improvements for Allocating Nonpoint Source Pollution. Journal of Environmental Engineering, 135(7), 490–504. http://dx.doi.org/10.1061/(ASCE)0733-9372(2009)135:7(409)

Franz, C., Makeschin, F., Weiß, H., & Lorz, C. (2014). Sediments in urban river basins: identification of sediment sources within the Lago Paranoá catchment, Brasilia DF, Brazil - using the fingerprint approach. The Science of the Total Environment, 466–467, 513–523. https://doi.org/10.1016/j.scitotenv.2013.07.056

Gellis, A. C., & Noe, G. B. (2013). Sediment source analysis in the Linganore Creek watershed, Maryland, USA, using the sediment fingerprinting approach: 2008 to 2010. Journal of Soils and Sediments, 13(10), 1735–1753. https://doi.org/10.1007/s11368-013-0771-6

Juracek, K. E., & Ziegler, A. C. (2009). Estimation of sediment sources using selected chemical tracers in the Perry lake basin, Kansas, USA. International Journal of Sediment Research, 24(1), 108–125. https://doi.org/10.1016/S1001-6279(09)60020-2

Lamba, J., Karthikeyan, K. G., & Thompson, A. M. (2015). Apportionment of suspended sediment sources in an agricultural watershed using sediment fingerprinting. Geoderma, 239–240, 25–33. https://doi.org/10.1016/j.geoderma.2014.09.024

Leopold, B., & Pecora, W. T. (1968). Hydrology for Urban Land Planning- A Guidebook on the Hydrologic Effects of Urban Land Use.

Liu, B., Storm, D. E., Zhang, X. J., Cao, W., & Duan, X. (2016). A new method for fingerprinting sediment source contributions using distances from discriminant function analysis. CATENA, 147, 32–39. https://doi.org/10.1016/j.catena.2016.06.039

Mukundan, R., Radcliffe, D. E., Ritchie, J. C., Risse, L. M., & McKinley, R. A. (2010). Sediment Fingerprinting to Determine the Source of Suspended Sediment in a Southern Piedmont Stream. Journal of Environmental Quality, 39(4), 1328–1337. https://doi.org/10.2134/jeq2009.0405

Nosrati, K., Collins, A. L., & Madankan, M. (2018). Fingerprinting sub-basin spatial sediment sources using different multivariate statistical techniques and the Modified MixSIR model. CATENA, 164, 32–43. https://doi.org/10.1016/j.catena.2018.01.003

Palazón, L., Latorre, B., Gaspar, L., Blake, W. H., Smith, H. G., & Navas, A. (2015). Comparing catchment sediment fingerprinting procedures using an auto-evaluation approach with virtual sample mixtures. Science of The Total Environment, 532, 456–466. https://doi.org/10.1016/j.scitotenv.2015.05.003

Phillips, J. M., Russell, M. A., & Walling, D. E. (2000). Time-integrated sampling of fluvial suspended sediment: a simple methodology for small catchments. Hydrological Processes, 14(14), 2589–2602.

Pitt, R., Clark, S. E., & Lake, D. W. (2007). Construction Site Erosion and Sediment Controls: Planning, Design and Performance. DEStech Publications, Inc.

Pulley, S., Foster, I., & Antunes, P. (2015). The uncertainties associated with sediment fingerprinting suspended and recently deposited fluvial sediment in the Nene river basin. Geomorphology, 228, 303–319. https://doi.org/10.1016/j.geomorph.2014.09.016

Rose L. A., Karwan D. L., & Aufdenkampe A. K. (2018). Sediment Fingerprinting Suggests Differential Suspended Particulate Matter Formation and Transport Processes Across Hydrologic Regimes. Journal of Geophysical Research: Biogeosciences, 0(0). https://doi.org/10.1002/2017JG004210

Rummery, T. A., Oldfield, F., Thompson, R., & Walling, D. E. (1979). Identification of suspended sediment sources by means of magnetic measurements: Some preliminary results. Water Resources Research, 15(2), 211–218. https://doi.org/10.1029/WR015i002p00211

Sherriff, S. C., Franks, S. W., Rowan, J. S., Fenton, O., & Ó'hUallacháin, D. (2015). Uncertainty-based assessment of tracer selection, tracer non-conservativeness and multiple solutions in sediment fingerprinting using synthetic and field data. Journal of Soils and Sediments, 15(10), 2101–2116. https://doi.org/10.1007/s11368-015-1123-5

Smith, H. G., & Blake, W. H. (2014). Sediment fingerprinting in agricultural catchments: A critical re-examination of source discrimination and data corrections. Geomorphology, 204(Supplement C), 177–191. https://doi.org/10.1016/j.geomorph.2013.08.003

Smith, H. G., Evrard, O., Blake, W. H., & Owens, P. N. (2015). Preface—Addressing challenges to advance sediment fingerprinting research. Journal of Soils and Sediments, 15(10), 2033–2037. https://doi.org/10.1007/s11368-015-1231-2

Stewart, H. A., Massoudieh, A., & Gellis, A. (2015). Sediment source apportionment in Laurel Hill Creek, PA, using Bayesian chemical mass balance and isotope fingerprinting. Hydrological Processes, 29(11), 2545–2560. https://doi.org/10.1002/hyp.10364

USEPA. (1996). Microwave assisted acid digestion of siliceous and organically based matrices. OHW, Method, *3052*.

Wall, G. J., & Wilding, L. P. (1976). Mineralogy and Related Parameters of Fluvial Suspended Sediments in Northwestern Ohio 1. Journal of Environmental Quality, 5(2), 168–173. https://doi.org/10.2134/jeq1976.00472425000500020012x

Wood, P. A. (1978). Fine-sediment mineralogy of source rocks and suspended sediment, rother catchment, West Sussex. Earth Surface Processes, 3(3), 255–263. https://doi.org/10.1002/esp.3290030305

CHAPTER 5

CONCLUSIONS

The major conclusions of this study were: (a) the relative importance of different sources contributing to in-stream sediment (suspended and stream bed) change spatially and temporally within a watershed, therefore, identification of sediment sources only at the watershed outlet and only for few storm events might not be sufficient to target sources for best management practices (BMPs), (b) sediment particle size (63-212 μm and <63 μm) has a significant effect on the relative contributions from different sources to in-stream sediment at a subwatershed level, and (c) relative source contributions might vary depending upon the statistical procedures employed in the fingerprinting studies.

Based on the individual chapters, the following conclusions were made:

Sources of sediment deposited on the stream bed in this watershed varied temporally and spatially (Chapter 2). Results of this study show that both construction sites and stream banks were important sources of stream bed sediment. The contribution from construction sites and stream banks to stream bed sediment within this watershed ranged from 0 to 100% and 0 to 100%, respectively. Extent of an impervious area and riparian land use within a subwatershed affected the relative contributions from construction sites and stream banks to stream bed sediment at each site. The relative contributions to stream bed sediment from construction sites were greater in the subwatershed with active construction activities in proximity to the stream.

The results of this study also show that generally the construction sites were the dominant sources of suspended sediment for both the particle sizes at all the sites (Chapter 3). The

contribution from construction sites to suspended sediment ranged from 0 to 100%, varying temporally. The rapid urbanization in this watershed has increased the amount of surface runoff generated within this watershed which has increased the entrainment of sediment from construction sites in the runoff and hence the sediment delivery into the stream.

Apart from Collins mixing model, another method was also used to quantify the relative source contributions from construction sites and stream banks using distances from DFA (Chapter 4). The method of calculating the source contributions using distances from DFA requires further research because the sediment source apportionment results predicted by mixing model and DFA were not always similar. The results determined by using DFA alone method largely depends on the sample size for each subwatershed and the optimum set of fingerprinting properties used. Therefore, care must be taken while selecting the most appropriate set of properties for the success of this method.

Targeting BMPs on constructions sites within this watershed can significantly reduce the sediment loadings to the streams. To minimize stream bank erosion, techniques for stream bank stabilization should be recommended. The riparian areas should be restored and managed as they perform an important function of trapping sediment. SWAT model can be used to identify subwatersheds contributing disproportionately high amounts of surface runoff and water yield per unit area to streams. The subwatersheds generating significant amount of surface runoff and water yield have potential to contribute disproportionately high amount of sediment to streams. Therefore, BMPs targeted in these areas can significantly reduce the sediment loadings to the streams.

Future research should focus on determination of erosion rates from construction sites during different phases to better understand the linkage between the phase of construction activities

and the corresponding sediment erosion rates. In addition, quantification of effectiveness of BMPs to reduce sediment loading with the use of watershed-scale modeling could be done. Also, fallout radionuclides could be used to determine sediment residence time in streams and estimate the age and percent new sediment in stream bed and suspended sediment samples.

Appendix A

Fig. A1. Construction sites within the Moore's Mill Creek watershed

Fig. A2. Stream banks within the Moore's Mill Creek watershed

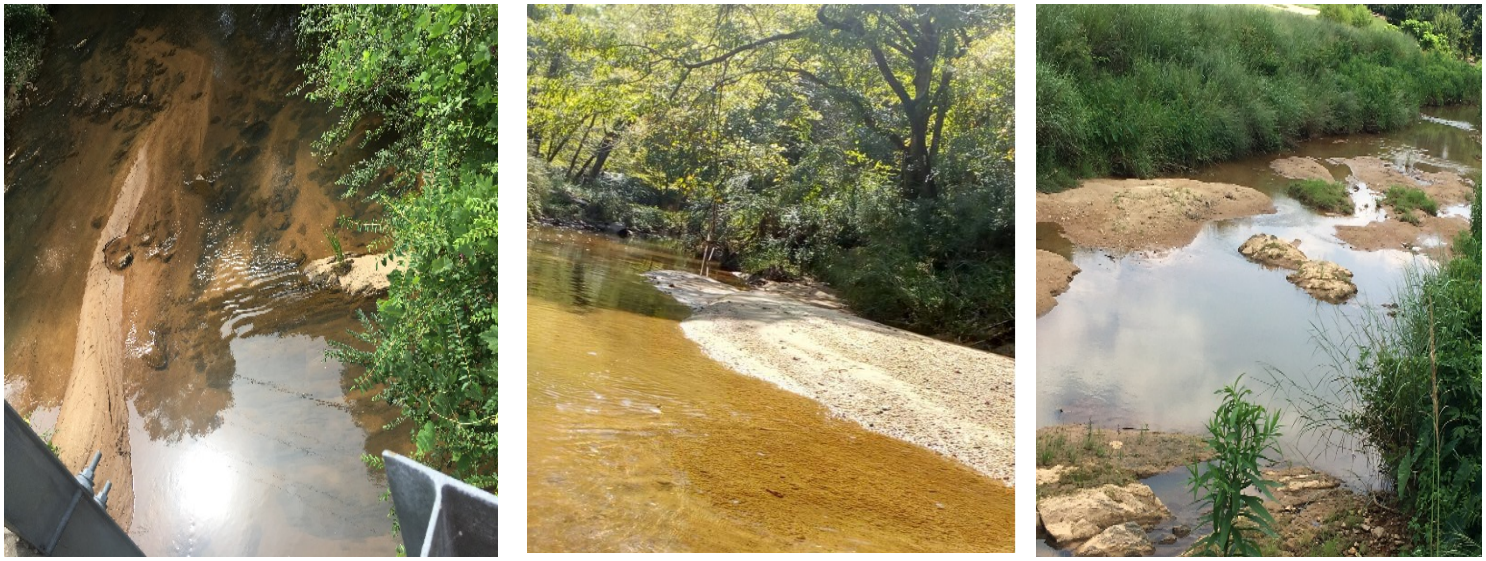

Fig. A3. Stream beds at different locations within the Moore's Mill Creek watershed

Fig. A4. Time integrated in-situ suspended sediment collection samplers

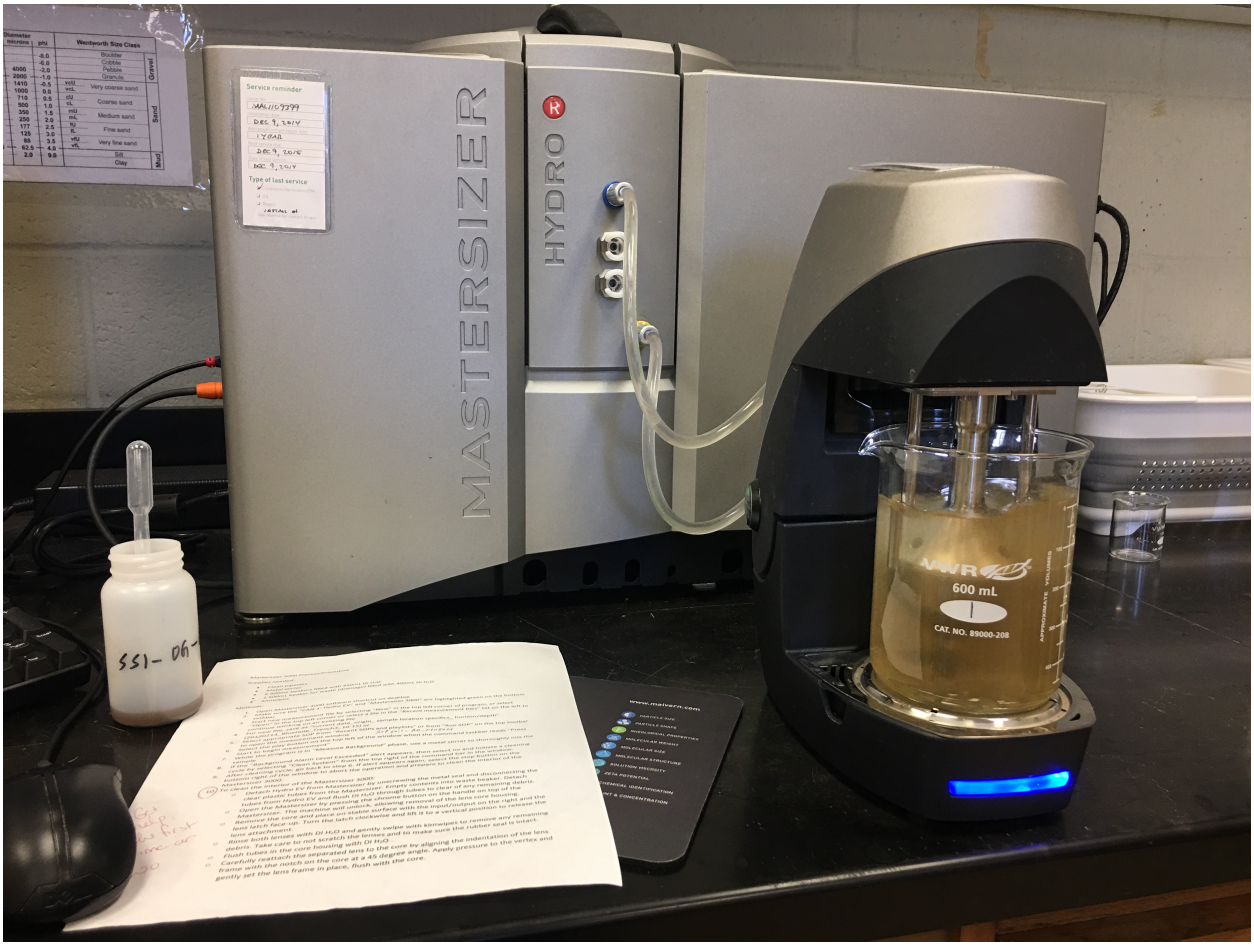

Fig. A5. Particle size analysis using Malvern Mastersizer